

9-30-1989

Agitation requirements for complete drawdown of floating solids in stirred tanks

Joseph Philemon Mmbaga
New Jersey Institute of Technology

Follow this and additional works at: <https://digitalcommons.njit.edu/theses>



Part of the [Chemical Engineering Commons](#)

Recommended Citation

Mmbaga, Joseph Philemon, "Agitation requirements for complete drawdown of floating solids in stirred tanks" (1989). *Theses*. 1960.

<https://digitalcommons.njit.edu/theses/1960>

This Thesis is brought to you for free and open access by the Electronic Theses and Dissertations at Digital Commons @ NJIT. It has been accepted for inclusion in Theses by an authorized administrator of Digital Commons @ NJIT. For more information, please contact digitalcommons@njit.edu.

Copyright Warning & Restrictions

The copyright law of the United States (Title 17, United States Code) governs the making of photocopies or other reproductions of copyrighted material.

Under certain conditions specified in the law, libraries and archives are authorized to furnish a photocopy or other reproduction. One of these specified conditions is that the photocopy or reproduction is not to be “used for any purpose other than private study, scholarship, or research.” If a user makes a request for, or later uses, a photocopy or reproduction for purposes in excess of “fair use” that user may be liable for copyright infringement,

This institution reserves the right to refuse to accept a copying order if, in its judgment, fulfillment of the order would involve violation of copyright law.

Please Note: The author retains the copyright while the New Jersey Institute of Technology reserves the right to distribute this thesis or dissertation

Printing note: If you do not wish to print this page, then select “Pages from: first page # to: last page #” on the print dialog screen

The Van Houten library has removed some of the personal information and all signatures from the approval page and biographical sketches of theses and dissertations in order to protect the identity of NJIT graduates and faculty.

ABSTRACT

Title of Thesis: **AGITATION REQUIREMENTS FOR COMPLETE
DRAWDOWN OF FLOATING SOLIDS IN STIRRED
TANKS**

Joseph P. Mmbaga, Master of Science in Chemical
Engineering, 1989

Thesis directed by Dr. Piero Armenante

The agitation requirements for complete drawdown of floating solids in mechanically agitated tank vessels has been studied both theoretically and experimentally.

A semi-theoretical equation has been derived on the basis of Kolmogoroff's theory of isotropic turbulence to determine the minimum impeller speed required for drawdown. The equation contains one adjustable parameter which has been found to be a function of the impeller type and position in the tank vessel.

The equation was tested using various vessels and impeller configurations. The solid phase consisted of high density polyethylene (density = 897kg/m^3), low density polyethylene (density = 840kg/m^3) and cork material (density = 510kg/m^3) with particle sizes ranging from $300\mu\text{m}$ to $2200\mu\text{m}$. The liquid phase consisted of water and aqueous solutions of zinc chloride in different concentrations so that the liquid density could be varied in the range 996kg/m^3 - 1180kg/m^3 .

The effect of impeller position and pumping direction has been extensively examined, as well as the use of non-conventional baffling systems to facilitate the drawdown of floating particles into the liquid.

It was concluded that impeller clearance and pumping direction have a considerable influence over the minimum drawdown speed and its corresponding power consumption. A partial baffling system consisting of four half baffles has been found to have the lowest power requirements.

Noticeable similarities exist between settling solids suspensions and floating solids drawdown, particularly for floating particles which, at rest, are almost completely immersed in the liquid. For cases different from this, the suspension of floating solids becomes a three phase system with entrapped air playing a significant role in particle drawdown. The proposed model works well within the experimental range covered (i.e. small density difference ($<340\text{kg/m}^3$) and medium particle size (300 - 2500 μm)) and can be used to predict the performance of floating solid-liquid systems.

AGITATION REQUIREMENTS
FOR
COMPLETE DRAWDOWN OF FLOATING SOLIDS
IN STIRRED TANKS

by

Joseph P. Mmbaga

Thesis submitted to the Faculty of the Graduate School of
the New Jersey Institute of Technology in partial
fulfillment of the requirements for the degree of
Master of Science in Chemical Engineering
1989

APPROVAL SHEET

Title of Thesis: Agitation requirements for complete
drawdown of floating solids in stirred
tanks

Name of Candidate: Joseph Philemon Mmbaga
Master of Science in Chemical
Engineering 1989

Thesis and Abstract

Approved:

.....
Dr. Piero M. Armenante
Assistant Professor
Dept. of Chemical Engineering,
Chemistry and Environmental Science

Sept. 7, 1989
Date

.....
Dr. Henry Shaw
Professor
Dept. of Chemical Engineering,
Chemistry and Environmental Science

Sept. 11, 1989
Date

.....
Dr. Dana Knox
Associate Professor
Dept. of Chemical Engineering,
Chemistry and Environmental Science

Sept 8, 1989
Date

V I T A

Name: Joseph Philemon Mmbaga

Permanent Adress:

Degree and date to be conferred: Master of Science in
Chemical Engineering, 1989.

Date of birth:

Place of birth:

Secondary education: Azania High School, Dar es Salaam
Tanzania, 1980.

Collegiate institutions attended:	Dates	Degree	Date of Degre
N. J. Institute of Technology	1987-1989	M.S.	1989
University of Dar es Salaam	1982-1986	B.S.	1986

Major: Chemical Engineering

Minor: Computer Science

Positions held: Assistant Lecturer,
Chemical & Process Engineering Dept.,
University of Dar es Salaam
Tanzania

Teaching Assistant,
Educational Opportunity Program
NJIT, Newark , NJ, U.S.A.

Research Assistant,
Chemical Engineering Dept.,
NJIT, Newark, NJ, U.S.A.

Teaching Assistant,
Articulation Program,
NJIT, Newark, NJ, U.S.A.

Dedication

This work is dedicated to my mother, Salome Petro for her love and care for me.

ACKNOWLEDGEMENT

Sincere acknowledgements to my supervisor, Dr. Piero Armenante for his continual guidance throughout the whole period of my research and his interest in my work.

Not to be forgotten are all my fellow Graduate Students at NJIT, especially my running mates, Fortune S. Mhlanga and Abubakar Ibrahim for their material and moral support.

Last but not least, members of my thesis committee, Dr. Dana Knox and Dr. Henry Shaw for their support and constructive criticism.

TABLE OF CONTENTS

<u>CONTENT</u>	<u>page</u>
Approval sheet	
Vita	
Abstract	
Dedication	i
Acknowledgments	ii
Table of Contents	iii
List of Tables	vii
List of Figures	viii
1 INTRODUCTION	1
1.1 Mixing Processes	1
1.2 Processing Pairs Description	1
1.3 Liquid-Solid Contacting	4
1.4 Objectives of Present Work	6
2 PRELIMINARY CONSIDERATIONS AND LITERATURE SURVEY	7
2.1 Theoretical Considerations	7
2.1.1 Turbulent Flow	7
2.1.2 Types of Turbulent Flow	8
2.1.3 Kolmogoroff's Theory and Isotropic turbulence	9
2.1.4 Power Requirements in Stirred Tanks	11
2.1.5 Some useful Formulae	11
2.1.6 Effect of Vessel Geometry on Mixing Process	12

2.1.6.1	Shape of the Vessel	12
2.1.6.2	Effect of Baffles	13
2.1.6.3	Tank Size and Configuration	15
2.1.7	Effect of Impeller	15
2.1.7.1	Impeller Type and Design	15
2.1.7.2	Impeller Position (Clearance)	17
2.1.8	Process Definitions and States of Suspension	21
2.1.8.1	Complete Drawdown of Floating Solids	21
2.1.8.2	Homogeneous Suspension	21
2.1.8.3	Complete On-Surface Motion of all Particles	21
2.1.9	The Just Suspended Criteria Applied to Floating Solids	21
2.2	Previous Studies in Floating Solids	23
3	MODEL DEVELOPMENT	27
3.1	Minimum Drawdown Speed	27
3.2	Model for ϕ and Proposed Drawdown Mechanism	33
3.2.1	First Approach	33
3.2.2	Second Approach	35
3.3.3	Modification in Macroscopic Flow Paths For Pitched Blade Turbines	35
4	EXPERIMENTAL PROGRAMS TO TEST THE VALIDITY OF THE PROPOSED EQUATION	39
4.1	Effect of Impeller Size	39
4.2	Effect of Particle Size	39
4.3	Effect of Density Difference	40

4.4	Effect of Impeller Type	40
4.5	Effect of Clearance Ratio (C/D).....	41
4.6	Effect of Size Ratio (T/D).....	41
4.7	Clearance Effects	41
5	EXPERIMENTAL SYSTEM AND METHODS	43
5.1.1	Experimental Set-up	43
5.1.2	Motor and motor Controller	43
5.1.3	Impellers used in this Work	43
5.1.4	Tank Vessels used in this Work	46
5.2	Measurement of System Properties	46
5.2.1	Floating Solids Density and Particle Size ..	46
5.2.2	Liquid Density	48
5.3	Speed Measurement	49
5.4	Power Measurement	49
6	RESULTS AND DISCUSSION	
6.1	Effect of Impeller Size on N_{js}	51
6.2	Effect of Particle Size on N_{js}	56
6.3	Effect of Density Difference on N_{js}	60
6.4	Effect of Power Number on N_{js}	63
6.5	Effect of Tank Size on N_{js}	65
6.6	Effect of C/D Ratio on N_{js}	72
6.7	Power Consumption	77
6.7.1	Effect of Impeller Size on Power Consumption	77
6.7.2	Effect of Impeller Clearance on Power Consumption	83
6.8	The use of Different Baffling Systems	87

6.9	The Proportionality Parameter Φ	93
6.10	Effect of Changing Liquid Level	105
6.11	Comparison of Open and Closed Tanks	107
7	CONCLUSIONS AND RECOMMENDATIONS	
7.1	Conclusions	117
7.2	Recommendations for Future Work	120
8	NOMENCLATURE	121
APPENDIX A-1	States of Suspension	124
APPENDIX A-2	Data Bank #1	137
APPENDIX A-3	Data Bank #2	146
APPENDIX A-4	Data Bank #3	174
REFERENCES	182

LIST OF TABLES

1	Mixing Processes	2
5.1	Impellers used in this Work	45
5.2	Tanks used in this Work	45
5.4	Solid Particles used and their Densities	48
6.3	Liquids used in this Work and their Densities .	49
6.1	Index on D at Constant $C = 1/2T$ and $C = 1/3T$..	51
6.2	Index on D at Constant C/D ratio	55
6.3	Index on dp at Constant $C/D = 1$	56
6.4	Index on Density Difference	60
6.5	Index on Power Number (P_o)	63
6.6	Index on T	65
6.7	Baffling Notation	87
6.8	Constants for Φ using Exponential Function	93
6.9	Constants for Φ using Power Function	99
6.10	Macroscopic Flow Path Functions	102

LIST OF FIGURES

FIGURE	page
1.1 Standard Vessel with Baffles and Impeller	14
2.1 Disk Turbine Impeller	16
2.2 45° Pitched Blade Impeller	16
2.3 Turbulent Flow Pattern with 45° Pitched Blade Impeller	19
2.4 Turbulent Flow Pattern With Disk Turbine	20
3.1 Forces Acting on a Particle	27
3.2 Particle Attack by Eddies	28
3.3 Macroscopic Flow Path for Disk Turbine	34
3.4 Macroscopic Flow Path for Pitched Blade Turbine	35
3.5 Macroscopic Flow Path for Pitched Blade Impeller Pumping Upwards (modified approach)	37
3.6 Macroscopic Flow Path for Pitched Blade Impeller Pumping Downwards (modified approach)	38
5.1 Experimental Arrangement	44
6.1.1 Effect of Impeller Size on N_{js} for $C/D = 1$	52
6.1.2 Effect of Impeller Size on N_{js} at const. $C = 1/3T$	53
6.1.3 Effect of Impeller Size on N_{js} at const. $C = 1/2T$	54
6.2.1 Effect of Particle Size on N_{js} (disk turbine) ...	57
6.2.2 Effect of Particle Size on N_{js} (pitched blade turbine DP)	58
6.2.3 Effect of Particle Size on N_{js} (pitched blade turbine UP)	59
6.3.1 Density difference effect	

(C 1/3T, dp=2205microns)	61
6.3.2 Density Difference Effect	
(C 1/2T, dp=2205microns)	62
6.4 Effect of Po on Njs	64
6.5.1 Effect of Tank Size on Njs	66
6.5.2 Effect of Tank Size on Njs (pitched blade DP) ...	67
6.5.3 Effect of Scale up on Njs	69
6.5.4 Effect of T/D Ratio on Njs	70
6.5.5 Effect of C/T Ratio on Njs for C/D = 1	71
6.6.1 Effect of C/D Ratio on Njs	
(polypropylene, all impellers)	73
6.6.2 Effect of C/D Ratio on Njs	
(polypropylene, Pitched Blade Impeller UP & DP) .	74
6.6.3 Effect of C/D Ratio on Njs (HD polyethylene, disk	
turbine, pitched impeller UP & DP)	75
6.6.4 Effect of C/D Ratio on Njs (large tank)	76
6.7.0 Power Number Curve	78
6.7.1 Power Consumption Curve for Disk Turbine	79
6.7.2 Power Consumption Curve for Flat Blade Impeller .	80
6.7.3 Power Consumption Curve for Pitched Blade	
Impeller	81
6.7.4 Effect of Impeller Size on Power Consumption	82
6.7.5 Effect of C/D Ratio on Power Consumption at Njs...	84
6.7.6 Power Consumption for Pitched Blade Impellers ...	85
6.8.1 Effect of Number of Baffle on Power at Njs	88
6.8.2 Power Consumption for Different Baffling Systems	89

6.8.3	Njs for Different Baffling Systems	91
6.8.4	Effect of Number of Baffles on Njs	92
6.9.1	Predicted and Experimental Values for ϕ (Disk turbine, LD polyethylene).....	94
6.9.2	Predicted and Experimental Values for ϕ (Pitched Blade turbine, LD polyethylene).....	95
6.9.3	Predicted and Experimental Values for ϕ (Disk turbine, HD polyethylene)	96
6.9.4	Predicted and Experimental Values for ϕ (Pitched blade (DP), HD polyethylene).....	97
6.9.5	Predicted and Experimental Values for ϕ (Pitched blade (UP), HD polyethylene).....	98
6.9.6	Plot of x vs. ϕ	100
6.9.7	Plot of x vs. ϕ	103
6.9.8	Plot of x vs. ϕ	104
6.10.1	Effect of Vessel Draw-off on Njs	106
6.11.1	Comparison of Njs for Open and Closed Vessels (Disk turbine)	108
6.11.2	Comparison of Njs for Open and Closed Vessels (Pitched blade turbine (DP)).....	109
6.11.3	Comparison of Njs for Open and Closed Vessels (Pitched blade turbine (UP)).....	110
6.11.4	Plot of D vs. Njs for Open and Closed Vessels (Disk turbine)	111
6.11.5	Plot of D vs. Njs for Open and Closed Vessels (Pitched blade turbine (DP)).....	112
6.11.6	Plot of D vs. Njs for Open and Closed Vessels	

(pitched blade turbine UP).....	113
6.11.7 Plot of D vs. Njs for Open and Closed Vessels	
(disk turbine)	114
6.11.8 Plot of D vs. Njs for Open and Closed Vessels	
(pitched blade turbine (DP)).....	115

CHAPTER 1

INTRODUCTION

1.1 MIXING

Fluid mixing is one of the most important operations in many industrial chemical process. Petroleum refining, pharmaceuticals, pulp and paper, waste treatment , food processing and beverages are a few examples of industries where fluid mixing is widely applied.

Mechanical agitation, static mixing and jet mixing are examples of common ways to mix in an industrial scale.

We can classify multiphase fluid mixing according to five categories of processing pairs shown in Table 1. Each processing pair can further be subdivided into physical and chemical processing. The achievement of good results in mixing depends on the application class of the fluid system and the desired result.

1.2 PROCESSING PAIRS DESCRIPTION

1.2.1 Liquid-Solid Systems

Suspension:- Description and specification of suspension at various points in the mixing vessel can be measured by physical techniques such as visual observation, concentration gradient, etc.

Dissolution:- mass transfer process. Solids are actually dissolved from the solid into the liquid phase

Physical Processing	Application Class	Chemical Processing
Suspension	Liquid-Solid	Dissolution
Dispersion	Liquid-gas	Absorption
Emulsions	Liquid-Liquid (immiscible)	Extraction
Blending	Liquid-Liquid (miscible)	Reactions
Pumping	Fluid motion	Heat transfer

Table 1 Mixing Processes

1.2.2 Liquid-Gas Systems

Dispersion:- This refers to the physical distribution and dispersion of a gas in a liquid.

Absorption:- This refers to mass transfer processes such as the transfer of oxygen from air bubbles to the solution, as in the case of fermentation processes.

1.2.3 Liquid-Liquid (immiscible)

Emulsions:- Some products may be such that a stable emulsion is required. In this case, the physical description of the emulsion type and stability is entirely adequate and appropriate to define the ultimate goal.

Extraction:- In liquid-liquid extraction, an unstable emulsion is employed as a means for achieving

mass transfer. The dispersion is then allowed to settle and separate for subsequent processing. Thus, description of the emulsion characteristics is only appropriate with respect to the requirement is the mass transfer step.

1.2.4 Liquid-Liquid (miscible)

Blending:- Blending of miscible liquids is a very common process requirement and can be described by means of a physical specification of the final blend.

Reactions:- In chemical reactions, uniformity of the reactants is important since chemical kinetics usually requires a knowledge of the concentration of the various reactants in a quantitative description. This needs special consideration if we think in terms of macro-scale and micro-scale mixing concepts.

1.2.5 Fluid Motion

Pumping:- This is the category in which a description of the mixing requirement is given in terms of fluid motion and/or other fluid parameters. This may be the ultimate requirement in the mixing tank or it may be assumed that once this requirement is met, other parts of the process will also be satisfied. The knowledge of impeller pumping capacity and fluid discharge

behaviour is essential for this description, as well as other factors which affect motion like shape of the tank bottom, baffles, and geometrical characteristics of the system.

Heat transfer:- Agitators may also be used to provide flow across heat transfer surfaces which will in turn generate turbulence and enhance the heat transfer process.

It should be borne in mind that there are many other possible combinations of the basic application classes like gas-liquid-solid, liquid-liquid-solid-gas etc.

1.3 LIQUID-SOLID CONTACTING

Liquid-solid contacting is probably one of the most common application class in mixing technology. Mechanically agitated vessels, sometimes referred to as the stirred tanks, are most frequently used in chemical process industries to bring about economical liquid-solid contacting. The main goal in liquid-solid mixing is to provide intimate contact between the two phases in order for mass transfer, chemical reaction or biochemical reaction to take place. Sometimes contacting may be necessary in order to provide a uniform slurry to ease subsequent processing.

Liquid-Solid systems can further be subdivided into two major groups according to the density difference of the two phases present. If the solids are heavier than the liquid, we have a settling solids system, while if the

solids are lighter than the liquid we have a floating solids system. The suspension of settling solids has received much attention from many investigators such as Zwietering [1], Nienow [2], Oldshue [3], Baldi & Konti [8], Kolar [9], Etchells [11] and many correlations are available in the literature for the determination of the minimum speed of agitation required to achieve a desired degree of suspension. However, much less information is available in the literature on the dispersion of floating solids, which is also an important phenomena in industrial contacting processes. In this work the achievement of the complete drawdown state in a floating solid-liquid system will be studied from both a theoretical and experimental point of view.

1.4 OBJECTIVES OF PRESENT WORK

The objectives of present work are to :

- * Derive a model for floating solids suspension,
- * Validate the derived model experimentally,
- * Determine an optimum impeller type, baffling style and geometric parameters for minimum speed and power consumption in floating solids drawdown,
- * Compare the applicability of settling solids correlations to the case of floating solids drawdown, and
- * To investigate other parameters of importance in floating solids suspension and their applicability to industrial needs.

CHAPTER 2

PRELIMINARY CONSIDERATIONS AND LITERATURE SURVEY

2.1 THEORETICAL CONSIDERATIONS IN MIXING PROCESSES

Several basic considerations have to be made when studying a mixing process in a mechanically agitated vessel. In order to achieve the movement of fluid and particles in the process, external forces are required to overcome the resisting forces inherent in the fluid. The resisting forces in a fluid come from inertia of the fluid when there is a change in velocity of motion.

Shear and viscous drag forces also offer resistance to fluid movement depending on their relative magnitudes.

2.1.1 TURBULENT FLOW

Turbulent flow is characterized by chaotic unsteady movements of parts of the fluid. Such chaotic movements of the fluid elements are very complicated and can only be described in terms of average fluctuations. The result of these movements is a superposition of a spectrum of velocity fluctuations on an overall mean flow. Large eddies (primary eddies) produced in a turbulent flow correspond to the large velocity fluctuations of low frequency and are of the size comparable to the physical dimensions of the flow system. Smaller eddies of higher frequency are produced by the interaction of the large eddies with slow moving

streams.

In turbulent flow, transfer of momentum between neighboring pulses of fluid (inertial effects) are of primary importance. Therefore, the velocity and density of the fluid assumes a greater importance in analyzing and characterizing the flow [13].

For flow in agitated vessels, the Reynolds number, which is actually the ratio the inertia forces to the viscous forces can be defined as :

$$Re = \frac{\rho v^2}{\mu v/d} \quad (2.1)$$

Since turbulent flow is characterized by high Reynolds number, we can infer directly from equation 1.1 that the inertial effects becomes more important than viscous effects as flow changes flow laminar to turbulent [3].

2.1.1 TYPES OF TURBULENT FLOW

A measure of the intensity of turbulence in a given direction is given by the velocity fluctuation v'_i . The instantaneous velocity in a given direction consists of the time averaged velocity at any point in fluid and the instantaneous fluctuation velocity. Since the fluctuation velocity can be positive or negative, it is convenient to express its amplitude as the mean square of the fluctuation velocities, and then take the root of the mean of the squares to get a root mean square fluctuation velocity \hat{u}_i' whence

$$\hat{u}_i' = \sqrt{[(v'i)^2]} \quad (\text{always positive}) \quad (2.2)$$

These fluctuating velocities account for much of mass and heat transfer in turbulent fluids [13].

2.1.3 KOLMOGOROFF'S THEORY AND ISOTROPIC TURBULENCE

2.1.3.1 Isotropic Turbulence

When the mean squares of the fluctuation velocities in all directions are the same i.e.,

$$\hat{u}_x' = \hat{u}_y' = \hat{u}_z' \quad (2.3)$$

we have a condition of isotropic turbulence.

The mean fluctuating velocity alone does not completely define a turbulent fluid. We also have to consider the spectrum of eddy sizes:

- * **Large eddies** contain as much as about 20% of the total kinetic energy of isotropic turbulence
- * **Intermediate size eddies** which make the main contribution to the kinetic energy (thus commonly dubbed "energy-containing" eddies)
- * **Small eddies** which contains relatively small fraction of the energy, but are responsible energy for dissipation by viscous effects. While the total energy of these eddies is not great, they are continuously being re-energized by momentum transfer from the larger eddies.

2.1.3.2 KOLMOGOROFF'S THEORY

Kolmogoroff [6] contends that for large Reynolds numbers of flow, the smaller eddies are independent of the

bulk motion of flow and are isotropic. The properties of these eddies are a function of the energy dissipation rate per unit mass, ϵ . Thus, although most of the kinetic energy of the flow is contained in the larger eddies, nearly all the dissipation occurs in the smallest eddies, even for the large spectrum of intermediate eddies which contain and dissipate but a little of the total energy.

Kolmogoroff's theory can be formalized as:

" At sufficiently high Reynolds numbers there is a range of high wave-numbers where the turbulence is statistically in equilibrium and uniquely determined by the parameters ϵ and ν . This state of equilibrium is universal" [9].

From dimensional reasoning, a Kolmogoroff length scale can be defined as :

$$\eta = \left(\frac{\nu^3}{\epsilon} \right)^{1/4} . \quad (2.4)$$

Similarly, a velocity scale can be defined as:

$$v = (\nu \cdot \epsilon)^{1/4} . \quad (2.5)$$

According to this theory, if distances and velocities are referred to these scales, a universal function β exists such that

$$\frac{u}{v} = \beta \left(\frac{d}{\eta} \right) \quad (2.6)$$

where u is the root mean square (r.m.s.) relative velocity between two points in the fluid at a distance d apart.

At the high Reynolds numbers then, an "inertial sub-

range" exists in which the viscous dissipation is not important. In this region,

$$u \propto (\epsilon \cdot d)^{1/3} \quad n \ll d \ll L \quad (2.7)$$

which is equivalent to

$$\beta \left(\frac{d}{n} \right) \propto \left(\frac{d}{n} \right)^{1/3} \quad (2.8)$$

For very short distances, the viscous forces cannot be neglected and the velocity gradient is constant i.e.:

$$\beta \left(\frac{d}{n} \right) \propto \frac{d}{n} \quad (2.9)$$

and

$$u \propto d(\epsilon)^{1/2} \quad d \ll n \quad (2.10)$$

Equation (7) compares with Taylors [13] expression for isotropic turbulence

$$\left(\frac{\delta u_d}{\delta d} \right)^2 = 1 \left(\frac{\delta u_n}{\delta d} \right)^2 = \frac{\epsilon}{15\nu} \quad (2.11)$$

where u_d and u_n are the velocities in the direction of d and normal to d respectively.

2.1.4 POWER REQUIREMENTS IN STIRRED TANKS.

When an impeller blade is rotated rapidly in a tank of liquid, turbulence arises from the sharp velocity discontinuities adjacent to the liquid streams discharged from the impeller blades. The external power required to rotate the impeller against the aforementioned forces is by

no doubt an important criteria in judging the performance of a mixing process. Terms affecting this criteria are the type and size of impeller employed, the size and shape of the mixing vessel, geometry and number of baffles employed and also the physical properties of the fluid in question.

2.1.5 SOME USEFUL FORMULAE

Reynolds number

$$Re \text{ or } Nre = D^2N/v = D^2Nr/\mu \quad (2.12)$$

Froude number

$$Fr \text{ or } Nfr = DN^2/g \quad (2.13)$$

Power number

$$Po \text{ (or } Np) = P/(rN^3D^5) \quad (2.14)$$

2.1.6 EFFECT OF VESSEL GEOMETRY ON THE MIXING PROCESS

2.1.6.1 Shape of Vessel

The shape of a vessel has considerable effects on the overall fluid mechanics in the vessel. Vertical cylindrical vessels are most commonly used and are the ones for which most investigations and correlations for mixing have been developed and tested. However, there are other applications which require special consideration for solid suspension with regard to flow pattern and other processing requirements. In this case, other tank geometries are usually used e.g. square, spherical and even hemispherical tanks. Flat bottomed cylindrical tank will be regarded as

standard shape in this investigation and is the only shape to be used in experiment and analysis. Figure 2 shows the standard vessel and its design parameters.

It is normally considered that the effects of flat bottoms, ASME dish bottoms, or shallow cone tanks are essentially equivalent [2]. This is not necessarily true for all solid suspension applications and peculiar cases may have to be treated individually.

2.1.6.2 Effect of Baffles

Baffles are usually installed in a vessel in order to eliminate the formation of vortices and promote a top down flow which is conducive to good mixing, rather than the swirling motion, typical of unbaffled tanks. The standard baffle configuration includes four baffles in a vertical tank, with width varying from one twelfth to one tenth of the tank diameter, extending slightly over the liquid free surface as shown in Figure 1.2. This optimum baffle width has been arrived at experimentally by varying the baffle width and measuring the increase in power consumption [3]. It has been observed that power consumption reaches a maximum between these two widths and that increase of width beyond this range does not effect power appreciably.

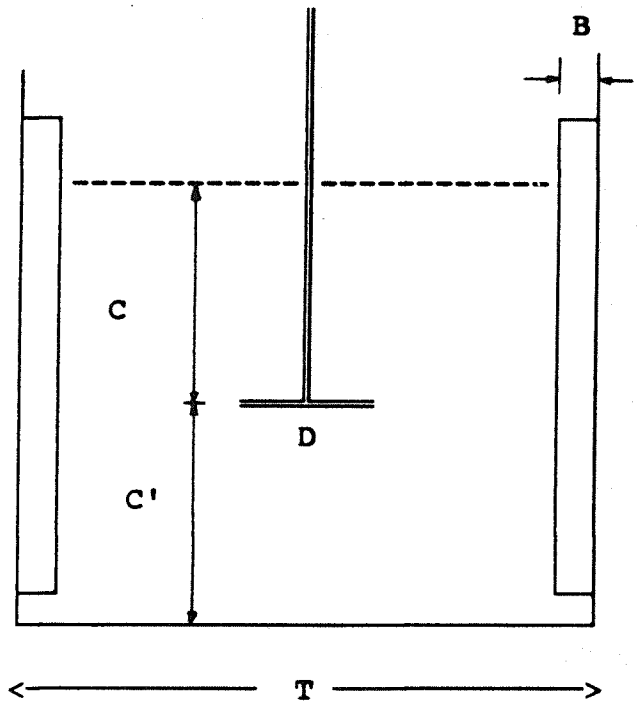


Figure 1.2 Standard vessel with impeller and baffles

- D impeller $D = 1/3T$
- T tank diameter
- C impeller clearance (floating solids)
- C' impeller clearance (settling solids)
- B baffles width = $1/12T \dots 1/10T$

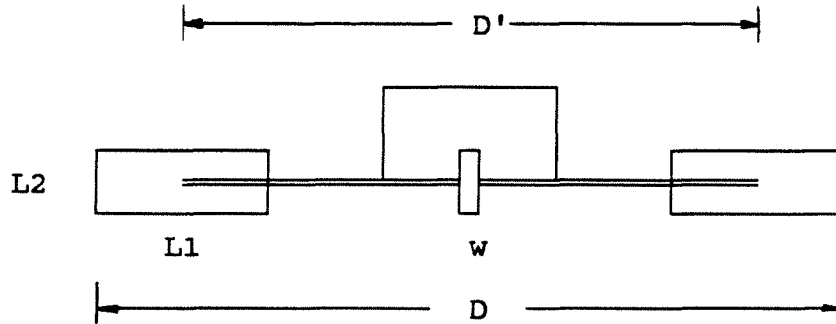
2.1.6.3 Tank Size and Configuration

The configuration of a tank in this context will refer to relative baffle size and positioning, draw-off position and other devices which may be attached to the tank wall and will have an effect to the mixing process. The effect of tank size will be discussed in Chapter 8.

2.1.7 EFFECTS OF IMPELLER

2.1.7.1 Impeller Type and Design

Impellers can be classified into two general types: axial flow impellers and radial flow impellers. An axial flow impeller is one in which the principal locus of flow occurs along the axis of the impeller while a radial-flow impeller is one which discharges along the impeller radius. Figures 2.3 and 2.4 shows representative impellers in the two categories and their typical design parameters. The difference in flow pattern due to impeller type can be seen in figures 2.5 and 2.6



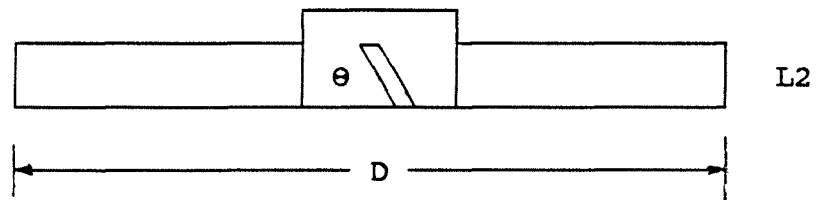
Impeller diameter = D

Blade height $L1 = D/4$

Blade length $L2 = D/5$

Disc diameter $D' = \frac{3D}{4}$

Figure 2.3 Disk Turbine



$L2$ Projected (swept) height = $\frac{1D}{8}$ or $\frac{1D}{5}$

θ Blade angle = 45°

Figure 2.4 45° Pitched Blade Turbine

2.1.7.2 Impeller Position (Clearance)

The position of the impeller has an effect on the power consumption and the minimum speed required for agitation. This is due to the fact that the region around the impeller experiences the highest energy dissipation rate [3], and the turbulence intensity decreases as you move away from the impeller.

For settling solids, clearance is defined as the distance from the impeller to the tank's bottom. However, for floating solids, clearance in this work will be defined as the distance from the impeller's mid-plane to the liquid free surface. Figure 1.2 shows clearance as defined in this work (C) and clearance as conventionally defined for settling solids.

An impeller can usually operate at liquid coverages from $0.5D$ to $2D$ [3]. When there is a need for a coverage greater than this, the use of multiple impellers may be called for.

In practice, however, impeller position may be dictated by the requirements during emptying-off a vessel and whether or not the vessel is being operated continuously.

Figure 2.5 shows the turbulent flow pattern generated by an axial flow turbine at low impeller clearances.

Figure 2.6 shows the turbulent flow pattern generated by a radial flow turbine. It can be noted that for clearances less than $1/5D$, the lower section of the pattern

is almost clipped out [2]. This has a considerable effect in the rate at which the particles can be drawn down.

The choice of one impeller over another for a given task depends on the complete definition of the mixing requirement (process result) and the given application class.

This brings us to the task of defining process results and suspension criteria.

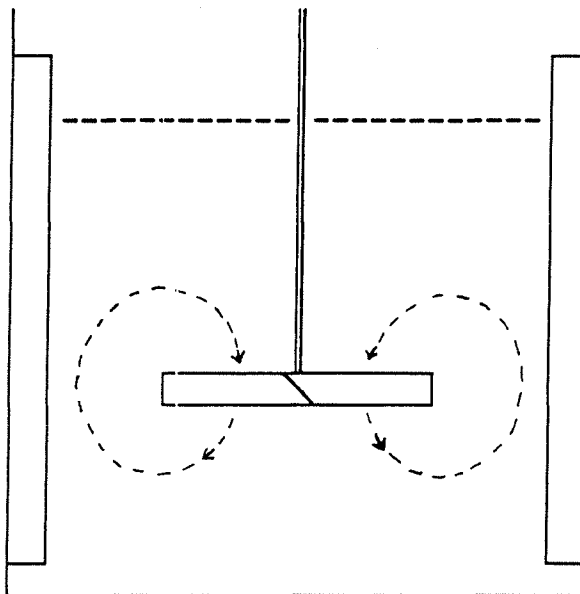


Figure 2.5 Turbulent flow pattern with a 45° Pitched blade Turbine

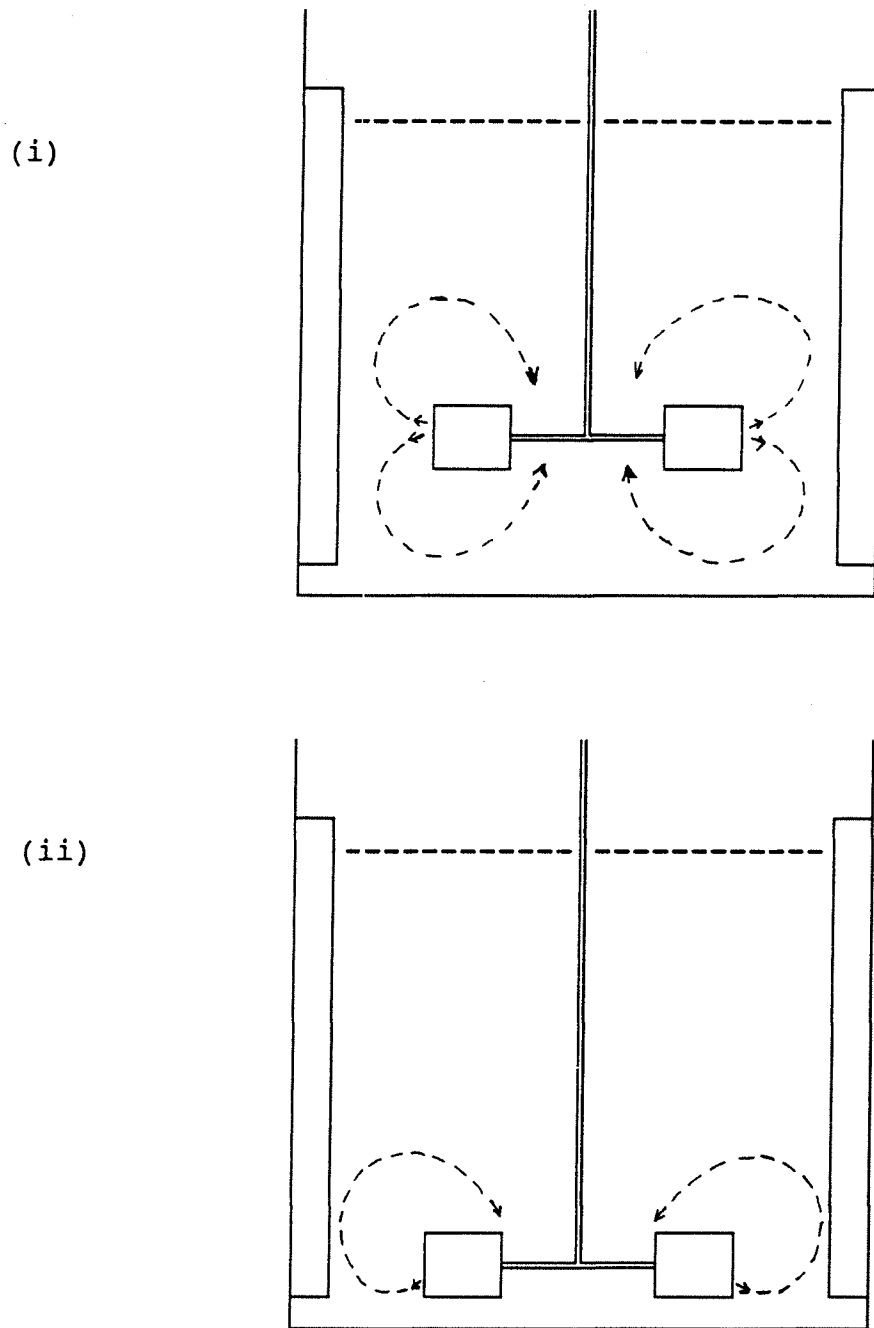


Figure 2.6 Turbulent flow pattern with a closed Disk

Turbine (i) $C > \frac{1}{5}D$ (ii) $C < \frac{1}{5}D$

2.1.8 PROCESS DEFINITIONS AND STATES OF SUSPENSION

2.1.8.2 Complete Drawdown of Floating Solids

Complete drawdown is achieved when most of the particles are drawn from the free surface and are in motion. No particle should remain at the surface for more than a few seconds. This definition is more or less analogous to the definition of complete suspension in settling solids systems [1,2].

2.1.8.3 Homogeneous Suspension (complete uniformity)

A homogeneous suspension exists when all the solid particles are uniformly distributed throughout the whole stirred vessel. The state of this suspension can be defined through measurements of local solids concentration at various points of the vessel.

2.1.8.4 Complete On-Surface Motion of All Particles

This is the condition where all particles, regardless of their size are moving are in motion in the tank. If there are stationary pools at the tank free surface they have to be identified and defined.

2.1.9 THE 'JUST SUSPENDED STATE' APPLIED TO FLOATING SOLIDS

The state where particles are 'just completely suspended' is very important in liquid-solid systems. This state represents the conditions whereby the entire surface area of the particles is available for processing. The impeller speed at this point is termed 'N_{js}' and is associated with the agitation speed below which the

effective area of the suspended particles is not yet utilized efficiently, and above which no significant change is observed in terms of mass transfer rates. Zwietering [1], was the first to apply the criteria of Just Completely Suspended state to settling solids suspension. Zwietering defined the just suspended state as the condition at which no particle was visually observed to remain at rest on a tank bottom for more than 2 seconds. He utilized dimensional analysis and experiments to determine the minimum impeller speed at which complete suspension is achieved. This point is therefore determined visually. With the aid of various devices, it is possible to determine the critical impeller speed with an accuracy of 2% to 5% for the same observer. The obvious advantage of this method is the fact that it can be performed without disturbance of the fluid flow or solids distribution. Furthermore, it is particularly suitable for systematic investigations since experimental effort is minimal and there is no difficulty in varying the experimental parameters over a wide range.

This very same criteria can be applied to floating solids system keeping in mind that particles which are stationary at the liquid surface are not considered to be suspended in this sense. This state will be defined as "Complete Drawdown" state in floating solid-liquid systems.

As stated earlier, there can be many more process definitions and criteria depending on what one is looking at. Several authors have given different definitions but

they all come down to the basic line that when the condition is reached, any further increase in agitator speed or power consumption will not effect the solids concentration profile. Gates et al. [11], classifies the degree of suspension using a scale from 1 to 10, with agitation scales 1-2 characterizing applications requiring minimal solids suspension levels to achieve process results, and agitation scales 9-10 characterizing applications where solid-suspension uniformity is required. This scale is widely used by Chemineer Inc., [11] as a method of determining agitation requirements for the mixing equipment they manufacture.

2.2 PREVIOUS WORK ON FLOATING SOLIDS DRAWDOWN

The literature on floating solid-liquid system is rather limited.

The work of Joosten, Schilder and Broere [7] can be considered as the first of the few articles on floating solids suspension. With the object of arriving at a less energy consuming agitator-baffle configuration for draw-down duty, they produced a correlation that predicts the minimum required stirrer speed for drawdown :

$$Fr_{\min} = c' (D/T)^p (\Delta r/r_1)^q \quad (2.1)$$

where Fr_{\min} is the Froude number at the minimum suspension speed and c' p and q constants to be determined experimentally.

For the optimal stirrer/baffle configuration that they proposed (one baffle $0.2 \times 0.3D$, four-bladed pitched blade paddle) the expression that fitted their results best was :

$$Fr_{\min} = 3.6 \times 10^{-2} (D/T)^{-3.65} (\Delta r/r_1)^{0.42} \quad (2.2)$$

The validity of this correlation was checked in the range:

$$0.27 \leq D \leq 1.8\text{m}; 0.29 \leq D/T \leq 0.6; 0.1 \leq \Delta r/r_1 \leq 0.76;$$

$$0.11 \leq H/T \leq 0.33; 2 \leq dp \leq 13\text{mm} \text{ and for } \mu = 10^{-3} \text{Ns/m}^2 \text{ and } r_1 = 1000\text{Kg/m}^3.$$

The same dependence of the Froude number was assumed to hold also for other types of impellers, and values for c' were calculated as shown in Table 1.1

Impeller	Constant c'
6-bladed inclined-blade paddle	3.3×10^{-2}
4-bladed inclined-blade paddle	3.6×10^{-2}
2-bladed inclined-blade paddle	7.4×10^{-2}
2-bladed marine propeller	19.6×10^{-2}

Table 2.1 Values of constant c' in Joosten Equation

Edwards and Ellis [4] have reported the critical impeller speeds required to draw down floating solids using a variety of impeller types and baffle configurations.

They concluded that:

- * The effect of particle concentration upon both the minimum drawdown speed and the associated power consumption is essentially insignificant (range of concentration covered 0.73-3.75% w/w)
- * The type of impeller used has a major effect on both minimum drawdown speed and the corresponding power consumption (impellers used were :- a six-bladed disk turbine, a three-bladed marine propeller (pumping downwards) and a simple flat paddle)
- * The baffle configuration has little or no effect on minimum drawdown speed
- * The position of the impeller above the base of the tank can significantly influence the power required for drawdown (clearances used : $1/3T$ and $2/3T$ measured from tank bottom).

Bruining and Frijlink [5] did a number of experiments with floating solids and concluded that the impeller pumping direction as well as the number of baffles is important. However, they did not produce any correlation.

Another significant work on floating solids drawdown is that of R. Hemrajani et al [6]. In this work, controlled vortex formation by using a "partial baffle mixing" (PBM) system is proposed as the key to homogeneous suspension of floating solids. The system consists of a

single 45° pitched blade impeller and four narrow baffles (1/50T) and has been arrived at through an extensive laboratory experimentation.

CHAPTER 3

MODEL DEVELOPMENT

We start our analysis by considering the case of a particle sitting at the liquid surface. The particle will be partially immersed shown in Figure 3.1. Using the nomenclature given in this figure, the forces acting to keep the particle in its present position are:

$$\text{weight of the particle} \quad mg = rs.Vs.g \quad (3.1)$$

$$\text{upthrust} \quad F_B = (V'l).rl.g \quad (3.2)$$

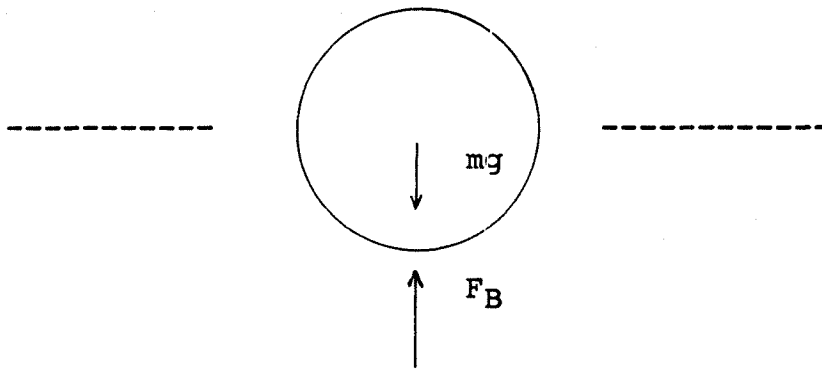


Figure 3.1 Forces acting on a particle

Since these two forces are acting in opposite directions, their net effect will determine whether a particle will sink or float. When the density of the liquid

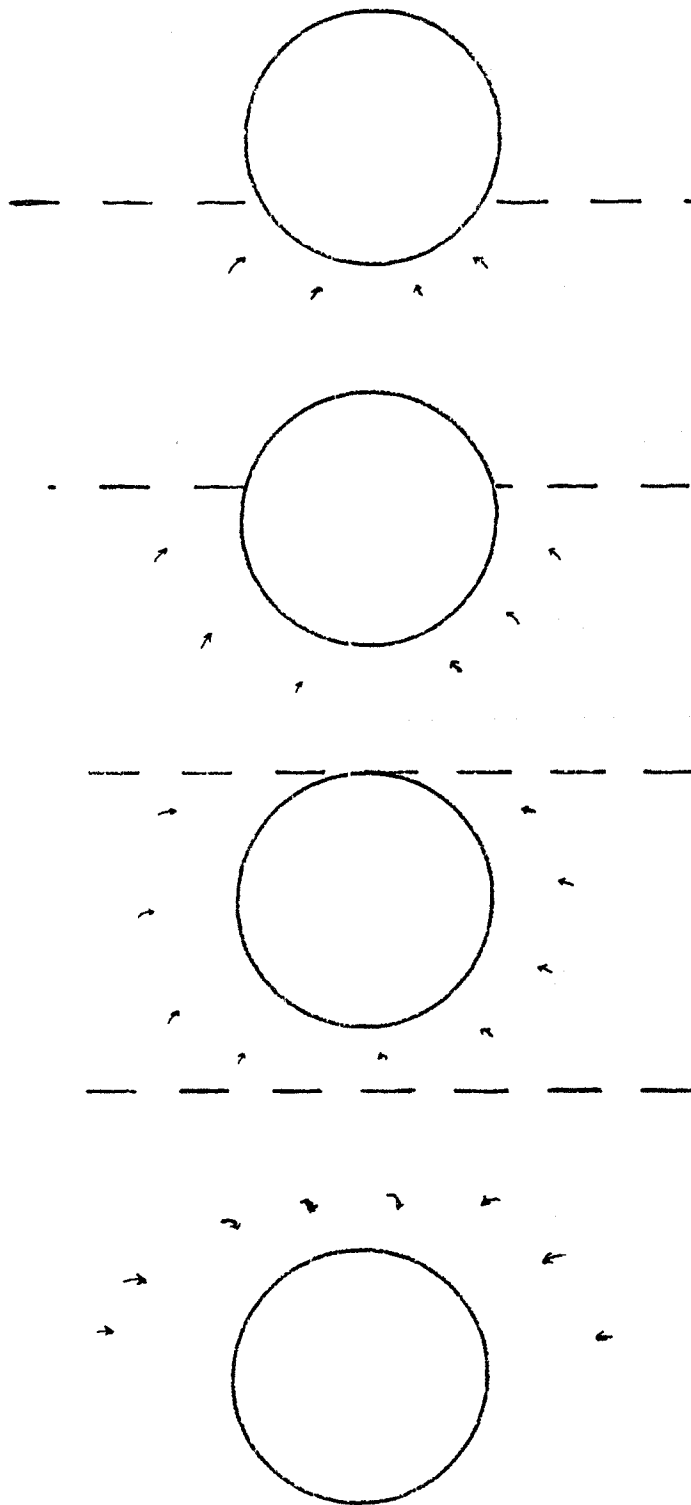


Figure 3.2 Particle attack by eddies

is lower than the density of the particle, the particle will obviously sink and we have a situation for settling solids. In this analysis however, we are interested in the case where the particle density is less than the liquid density.

In order to draw-down the particle, a force must be exerted by the turbulent eddies to move the particle a certain distance into the liquid which is sufficient for it to be entrapped and maintained in circulation by the large circulating currents in the main flow. The minimum distance assumed in this case is a distance equal to the particle diameter.

The force which has to be exerted by the turbulent eddy depends on how much area of the particle is available for the eddy to act upon.

In order for particle drawdown to occur, there must be sufficient energy from incoming eddies. Assuming that the flow conditions in the vessel (or at least at the top of the vessel) are such that sufficiently large Reynolds numbers have been reached, and that the turbulence is fully developed and isotropic (Kolmogoroff), we can estimate the eddy force as:

$$F_E = \tau \cdot A' \quad (3.3)$$

where A' is the area of the particle which is exposed to the eddy and τ is the shear stress associated with the eddy.

This force must be greater than the upthrust

$$F_E > Mg - F_B \quad (3.4a)$$

or

$$\tau.A' > r_l.V.s.g - rL.V'l.g \quad (3.4b)$$

Let's assume that τ can be expressed as:

$$\tau = r_l.u'^2 \quad (3.5)$$

where u' is the fluctuating velocity

then, from Kolmogoroff's (equation 2.7) it is

$$u \propto (\epsilon.d)^{1/3} \quad (3.6)$$

With the additional assumption that the distance d is of the same order of magnitude of the particle size and that the fluctuating velocity is proportional to the r.m.s. relative velocity u we can obtain:

$$u' \propto (\epsilon.dp)^{1/3} \quad (3.7)$$

Knowing that the mean energy dissipation rate in an agitated vessel is given by

$$\epsilon = \frac{P}{r_l.V} \quad (3.8)$$

and the power drawn by an impeller is given by

$$P = r_l P_o . N^3 . D^5 \quad (3.9)$$

we can express ϵ as

$$\epsilon = P_o . N^3 . D^5 \quad (3.10)$$

V

whence Equation (3.7) becomes

$$u' \propto \left(\frac{Po \cdot N^3 \cdot D^5 \cdot dp}{V} \right)^{1/3} \quad (3.11)$$

For a cylindrical vessel filled to a height H it is:

$$V = \frac{\pi \cdot T^2 \cdot H}{4}$$

thus

$$u' \propto \left(\frac{Po \cdot N^3 \cdot D^5 \cdot dp}{T^2 \cdot H} \right)^{1/3} \quad (3.12)$$

From Equation (3.5) it is

$$r \propto r_l \cdot \left(\frac{Po \cdot N^3 \cdot D^5 \cdot dp}{T^2 \cdot H} \right)^{2/3} \quad (3.13)$$

Then, using this with Equation (3.4c) it is:

$$F_E \propto r_l \cdot \left(\frac{Po \cdot N^3 \cdot D^5 \cdot dp}{T^2 \cdot H} \right)^{2/3} \cdot A' \quad (3.14)$$

or

$$F_E = \phi' \cdot r_l \cdot \left(\frac{Po \cdot N^3 \cdot D^5 \cdot dp}{T^2 \cdot H} \right)^{2/3} \cdot A' \quad (3.14a)$$

where ϕ' is a constant dependent on impeller type and position only.

For the eddy to be able to drawdown the particle, it must exert a force which is greater than $(mg - F_B)$

or

$$\phi' \cdot r_l \cdot A' \cdot \left(\frac{Po \cdot N^3 \cdot D^5 \cdot dp}{T^2 \cdot H} \right)^{2/3} > (rs \cdot Vs \cdot g - r_l \cdot V' \cdot l \cdot g) \quad (3.15)$$

Now, for conditions where the particle will be just suspended we can replace N by Njs and use the equality sign to get

$$\phi' \cdot r_l \cdot A' \cdot \left(\frac{\rho_o \cdot N^3 \cdot D^5 \cdot dp}{T^2 \cdot H} \right)^{2/3} = (r_s \cdot V_s \cdot g - r_l \cdot V' \cdot g) \quad (3.16)$$

Dividing equation by Vs we get:

$$\phi' \cdot r_l \cdot A' \cdot \left(\frac{\rho_o \cdot N^3 \cdot D^5 \cdot dp}{r_l} \right)^{2/3} = \left(\frac{r_s - r_l \cdot V' / V_s}{r_l} \right) \cdot g \cdot V_s \cdot T^2 \cdot H \quad (3.17)$$

which can be arranged to give critical speed (Njs) as

$$N_{js} = \phi \cdot \left(\frac{r_s - r_l \cdot V' / V_s}{r_l} \right) \cdot g^{1/2} \cdot \left(\frac{V_s}{A'} \right)^{1/2} \cdot \left(\frac{1}{\rho_o} \right)^{1/3} \cdot \left(\frac{T^2 \cdot H}{D^{5/3} \cdot dp^{1/3}} \right)^{1/3} \quad (3.18)$$

For a totally immersed spherical particle

$$\begin{aligned} A' &= 2 \cdot \pi \cdot R(2R) = 4\pi R^2 \\ V_s &= \frac{4 \cdot \pi \cdot R^3}{3} = V' \end{aligned} \quad (3.19)$$

Thus

$$A' / V_s = \frac{3}{2dp}$$

and $V' / V = 1$

Therefore

$$N_{js} = \phi \cdot \left(\frac{\Delta r}{r_l} \right) \cdot g^{1/2} \cdot \left(\frac{1}{\rho_o} \right)^{1/3} \cdot (T^2 \cdot H)^{1/3} \cdot (dp)^{1/6} \cdot D^{-5/3} \quad (3.20a)$$

and for a system where the vessel is filled to a height H equal to the vessel diameter it is:

$$N_{js} = \phi \cdot \left(\frac{\Delta r}{r_l} \right) \cdot g^{1/2} \cdot \left(\frac{1}{\rho_o} \right)^{1/3} \cdot (T) \cdot (dp)^{1/6} \cdot D^{-5/3} \quad (3.20b)$$

3.2 MODEL FOR Φ AND THE PROPOSED DRAWDOWN MECHANISM

From experimental and theoretical observations, the pseudo-constant Φ has been found to depend on impeller clearance, tank size and the impeller pumping characteristics. Two models will be proposed for this parameter.

3.2.1 First Approach

It is proposed to lump the parameters in the following exponential function:

$$\Phi = k_1 \cdot \exp(x \cdot k_2) \quad (3.21)$$

where x is the flow path function and k_1 and k_2 are constants to be determined experimentally and assigned to the corresponding impeller types.

With reference to Figures 3.3 and 3.4, the macroscopic flow path (x') can be approximated as follows depending on the type of impeller used:

* For disk turbine it is:

$$x' = C + T - D \quad (3.22)$$

* For pitched blade turbine pumping upwards it is:

$$x' = C + T/2 \quad (3.23)$$

* For pitched blade turbine pumping downwards:

$$x' = 3T - C \quad (3.24)$$

with $x = x'/D$

The constants, k_1 and k_2 can be determined experimentally from the following equation:

$$\ln(\Phi) = \ln(k_1) + k_2 \cdot x \quad (3.25)$$

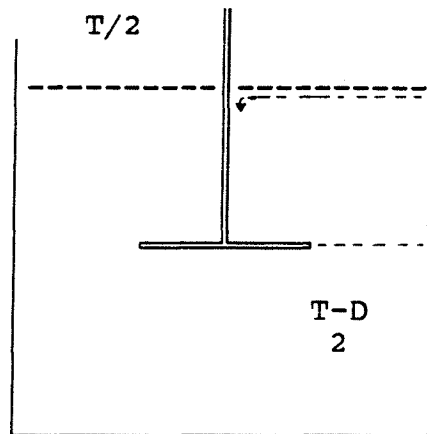


Figure 3.3 Macroscopic flow path for disk turbine

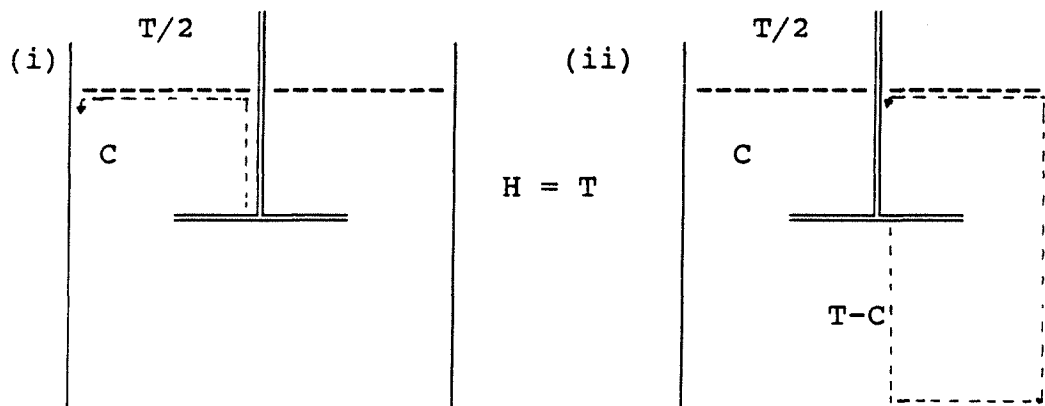


Figure 3.4 Macroscopic flow path for pitched blade turbine (i) Upward pumping (ii) Downward pumping

3.2.2 Second Approach

The second approach is to use a power function

$$\phi = k_1(x)^{k_2} \quad (3.26a)$$

From which the constants k_1 and k_2 may be obtained by regression of experimental data using equation:

$$\ln(\phi) = \ln(k_1) + k_2 \cdot \ln(x) \quad (3.26b)$$

3.2.3 Modification of the Macroscopic Flow Path for Pitched Blade Turbine

From experimental observations, the pitched blade turbine has been found to exhibit a mixed flow pattern and not a truly axial one. Therefore, the drawdown mechanism for this impeller changes depending on the C/T ratio employed. Working with settling solids, Susanto [23] observed a change in flow pattern at $C/T = 0.29$.

From Figure 3.5 the flow path function for pitched blade pumping upwards is calculated to be:

$$\bar{x} = \sqrt{2(T/(2D)-1/4)+(C/D-T/(2D)-1/4)+T/(2D)} \quad (3.27)$$

$$\text{for } C/T > 0.29$$

and

$$\bar{x} = \sqrt{2.C/D + (T/(2D)-C/D-1/4)} \quad (3.28)$$

$$\text{for } C/T < 0.29$$

Similarly, from Figure 3.6 the downward pumping flow path function is defined as:

$$\bar{x} = \sqrt{2(T/D-C/D) + (2T/D-1/4-C/D)} \quad (3.29)$$

$$\text{for } C/T > 0.71$$

and

$$\bar{x} = \sqrt{2(T/(2D)-1/4)} + (T/D+C/D) - 1/4 \quad (3.30)$$

for $C/T < 0.71$

A more appropriate definition of the flow path function for the pitched blade turbine can be given by removing the assumption that the flow pattern changes in correspondence of $C/T = 0.29$.

In this case we can introduce the flow path function x as:

$$\bar{\bar{x}} = \sqrt{2(T/(2D)-1/4)+(C/D-T/(2D)-1/4)+T/(2D)} \quad (3.31)$$

for $C/T > (C/T)_{crit. UP}$

$$\bar{\bar{x}} = \sqrt{2.C/D + (T/(2D)-C/D-1/4)} \quad (3.32)$$

for $C/T < (C/T)_{crit. UP}$

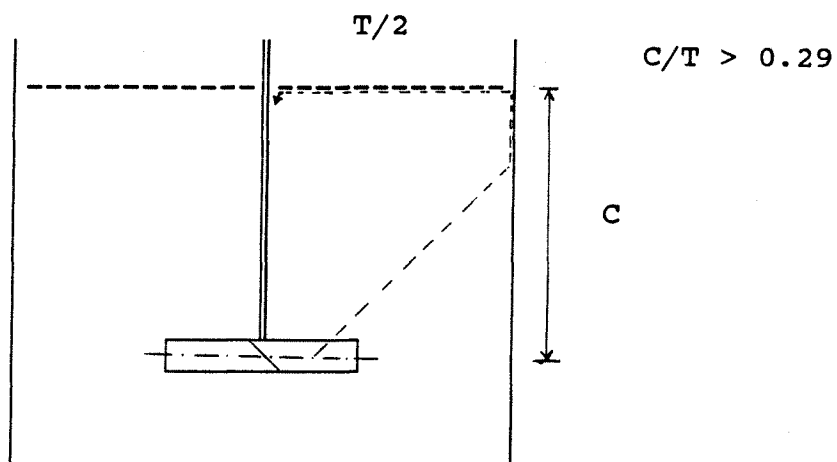
$$\bar{\bar{x}} = \sqrt{2(T/D-C/D) + (2T/D-1/4-C/D)} \quad (3.33)$$

for $C/T > (C/T)_{crit. DP}$

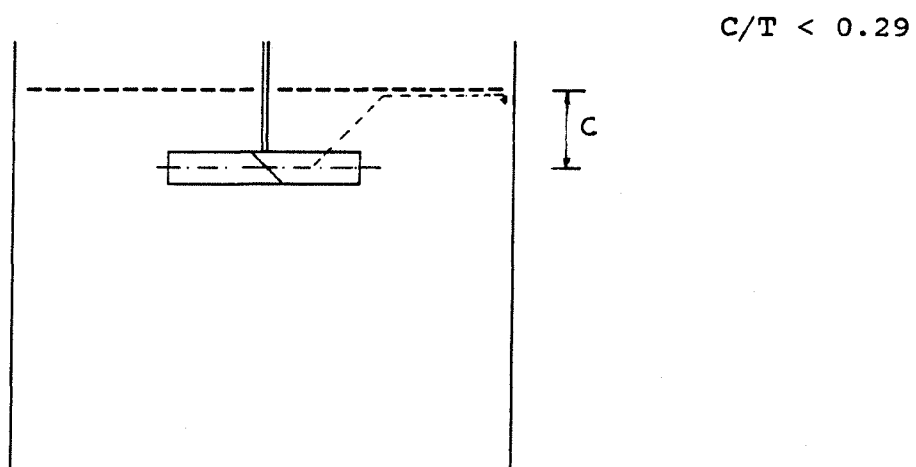
$$\bar{\bar{x}} = \sqrt{2(T/(2D)-1/4) + (T/D+C/D) - 1/4} \quad (3.33)$$

for $C/T < (C/T)_{crit. DP}$

where $(C/T)_{crit. UP}$ and $(C/T)_{crit. DP}$ is the critical C/T ratio where a transition in flow pattern is actually observed experimentally.

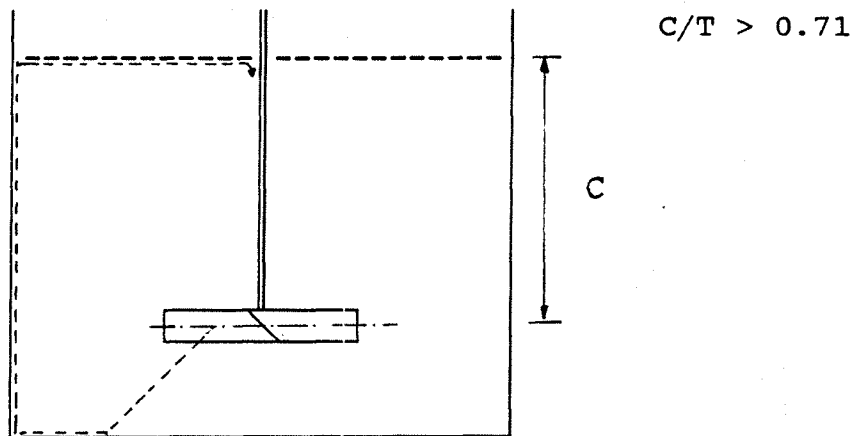


$$\bar{x}' = \sqrt{2}(T/2 - D/4) + (C - T/2 - D/4) + T/2$$

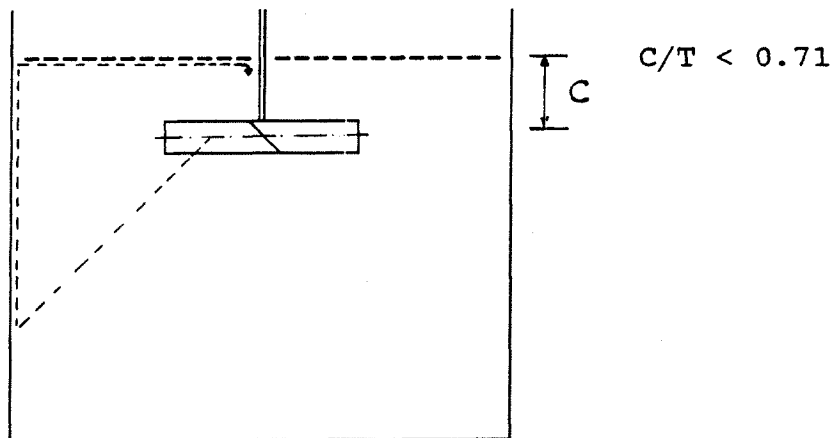


$$\bar{x}' = \sqrt{2} \cdot C + (T/2 - C - D/4)$$

Figure 3.5 Macroscopic flow path for pitched blade impeller pumping upwards



$$\bar{x}' = \sqrt{(T-C)} + (T/2 - D/4 - C) + T + T/2$$



$$\bar{x}' = \sqrt{2(T/2 - D/4)} + (T/2 - D/4) + C + T/2$$

Figure 3.6 Macroscopic flow path for pitched blade impeller pumping downwards

CHAPTER 4

EXPERIMENTAL PROGRAMS TO TEST THE VALIDITY OF THE PROPOSED EQUATION

Equation (3.20) can be written as:

$$N_{js} = \phi \cdot \Delta r^{c_1} \cdot P_o^{c_2} \cdot T^{c_3} \cdot d_p^{c_4} \cdot D^{c_5} \quad (4.1)$$

In order to test the validity of the proposed equation for minimum suspension speed, the following experiments have to be performed.

4.1 EFFECT OF IMPELLER SIZE

By keeping all parameters in equation (4.1) constant and changing only the size of the impeller used, the index c_5 may be obtained as

$$N_{js} = K_5 \cdot D^{c_5} \quad (4.2)$$

Taking logs:

$$\ln(N_{js}) = \ln(K_5) + c_5 \ln(D) \quad (4.3)$$

Thus, by using different impeller sizes of the same type and at clearances equal to the respective diameters and regressing the different values of $\ln(D)$ against $\ln(N_{js})$ the index c_5 can be obtained as coefficient for $\ln(D)$ and can be compared with the theoretically predicted value.

4.2 EFFECT OF PARTICLE SIZE (d_p)

Following the same approach as in 4.1 but varying the

particle size equation 4.1 can be written for this case as

$$\ln(Njs) = \ln(K4) + c4.\ln(dp) \quad (4.4)$$

By performing another set of experiments varying only the particle size the exponent $c4$ may be obtained. This experiment may be coupled with change in impeller diameter. The value of $c4$ can be obtained by linear regression for different impeller types and sizes.

4.3 THE EFFECT OF DENSITY DIFFERENCE $(r_l-r_s)/r_l$

Following the approach in section 4.1 but varying the density of the liquid r_l we equation (4.1) can be written after taking logs as

$$\ln(Njs) = \ln(K1) + c1.\ln(\Delta r/r_l) \quad (4.5)$$

Again the index $c1$ can be obtained by making different runs with same impeller type and size, clearance, particle size and density and regressing $\ln(\Delta r/r_l)$ against $\ln(Njs)$.

4.4 EFFECT OF IMPELLER TYPE (P_o)

Using the above approach the effect of different impeller types on Njs may be investigated. This may be done by performing experiments with same parameters but varying only the impeller type for each data set.

Equation (4.1) may be written for this case as

$$\ln(Njs) = \ln(K2) + c2.\ln(P_o) \quad (4.6)$$

Here again the index $c2$ may be obtained by regressing

the data obtained for different runs

4.5 The effect of clearance ratio (C/D)

The effect of clearance ratio may be studied experimentally by running same experiment but varying the position of the impeller

$$\ln(Njs) = \ln(K') + c'.\ln(C/D) \quad (4.7)$$

4.6 THE EFFECT OF SIZE RATIO (T/D)

The effect of size ratio may also be studied experimentally by running the same experiments but varying either the tank size or the impeller size.

$$\ln(Njs) = \ln(K'') + c''.\ln(T/D) \quad (4.8)$$

The constant may be obtained for comparison of different impeller type performances at different size ratios

4.7 CLEARANCE EFFECTS

Although clearance does not appear explicitly in the proposed model, it plays a significant role in the attainment of the desired process result. Determination of the optimum C/D ratio can be done by running a number of experiments at different clearances and determining the minimum speed required at each point. Then a comparison can be made based on power consumption to determine which

position is best and also which impeller will best suit a given process operation. Usually this is where empiricism enters our model development. The hydrodynamics involved are so complex that mere physical reasoning cannot lead to a meaningful modeling.

CHAPTER 5

EXPERIMENTAL SYSTEM AND METHODS

5.1 EXPERIMENTAL SETUP

Figure 5.1 shows the experimental setup used in this work. The various components of the setup are briefly described below.

5.1.1 Motor and motor Controller

The motor and motor controller which were used in the main part of the experimental investigation consists of a Cole Palmer unit, model number E650MG, with 45watts power rating, 3000rpm max. and a maximum torque of 0.8Nm. Other motors used were a 186watt Chemineer motor for calibration experiments and a 1.5kw G. K. Heller motor for experiments with large tanks.

5.1.2 Impellers used in this Work

The types of impellers used in this work are listed in Table 5.1. Since the pumping direction of pitched impellers affect the minimum drawdown speed, the 45° pitched blade turbine will be treated as two separate cases depending on the pumping direction. When the impeller rotation is such that the liquid is pushed upward (towards the floating solids), it will be denoted by UP, and when the direction is opposite it will be denoted by DP.

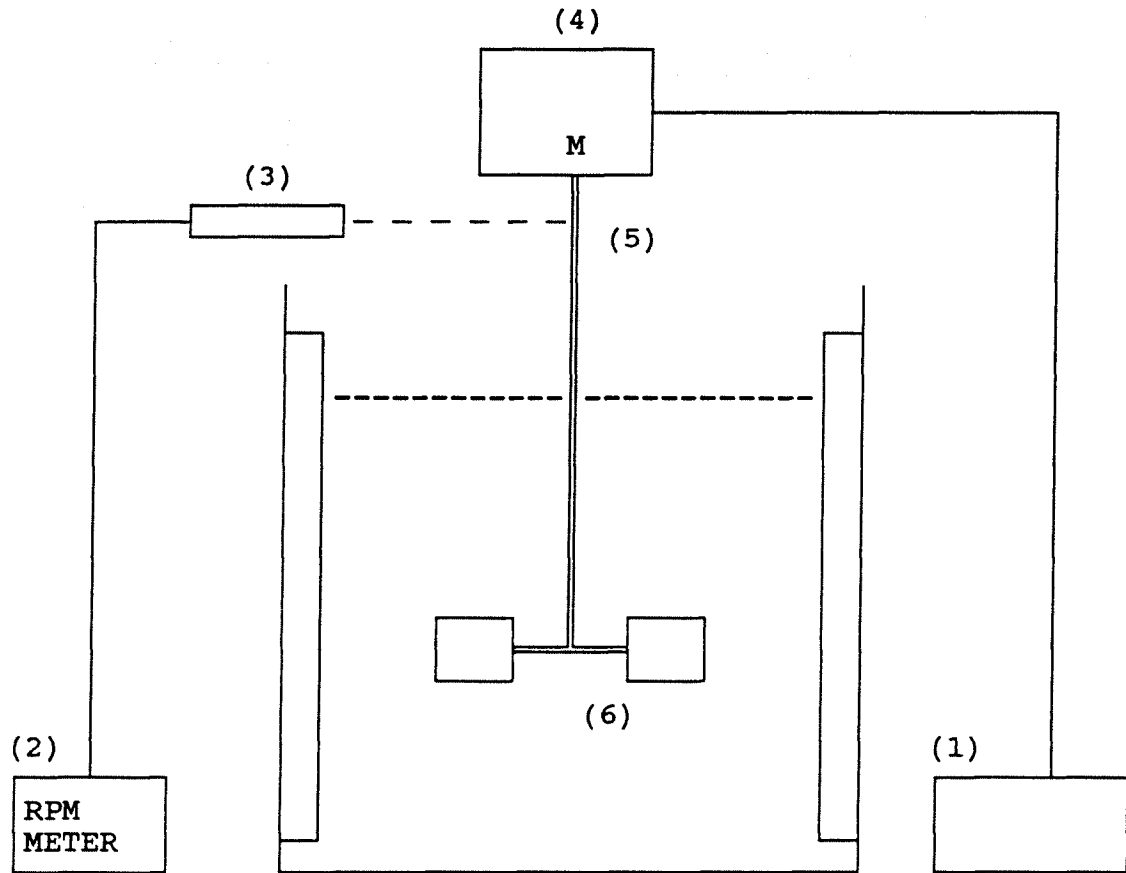


Figure 5.1 Experimental arrangement

- (1) Motor controller and speed measurement
- (2) Digital Speedometer (Cole Palmer)
- (3) Photo detector
- (4) Motor (Cole Palmer)
- (5) Reflective mark on motor shaft
- (6) Impeller

Impeller Type	Diameter (in)				Blades
Disk Turbine	2.5	3	4	8	6
Flat Blade Turbine	2.5	3	4	8	6
45 Pitched Blade Turbine	2.5	3	4	8	6

Table 5.1 Impellers used in this work

Vessel #	1	2	3	4	5
Internal diameter (mm)	200	250	290	290	585
Height (mm)	254	330	360	360	630
Wall thickness (mm)	6	6	6	6	6
Number of baffles	4F	4F	*	4H	4F
thickness (mm)	6	6	6	6	6
width (mm)	20	25	29	29	60

* removable baffles 4H, 3H, 2H, 1H

H half size

F full size

Table 5.2 Tanks used in this work

5.1.3 Tank Vessels used

Table 5.2 shows the size of the tanks used in this work. Vessel #2 is a special tank which can be fitted with a water-tight lid. This tank can be completely filled up with liquid, leaving no air-liquid interface. Using this tank enables one to carry out experiments with all floating particles completely immersed in the liquid. Vessel #3 has the same diameter as Vessel #2. In addition, baffles for Vessel #2 are removable. Each baffle can be slid into a groove at the bottom of the tank and screwed to the wall of the tank. This enables the experimentation with different baffling styles in order to come up with the best possible alternative.

5.2 MEASUREMENT OF SYSTEM PROPERTIES

5.2.1 Floating Solids Density

The density of the solids was measured using the following apparatus:

- * 25 cc. Pycnometric bottle
- * Constant temperature bath (Masterline 2090 Bath)
- * Mettler P1210 weighing scale
- * Low density liquid (n-hexane)

The following procedure was utilized:

- * The pycnometric bottle was weighed (obtaining it's mass = W_b)
- * A known mass of the solid particles was placed in the bottle (solid mass = W_s)

- * The bottle was filled with liquid of known density (water). The bottle was placed in water bath and kept for 30 minutes at 30°C in order to remove any dissolved gases in the bottle.
- * The weight of the bottle and it's contents is determined and recorded (total mass = Wt)
- * With the volume of bottle denoted as Vb (cm³) and density of known liquid as r_l (g/cm³), the density of the solid particles is obtained as:

$$r_s = \frac{W_s}{V_b - (W_t - W_b - W_s)/r_l} \quad \text{gm.cm}^{-3}$$

Table 5.3 shows the solid particles used and their densities.

Solid Particles	Density (kg/m ³)	Diameter (μm)
Polyethylene (HD)	897	2205
		2100
		1500
		640
		340
Polypropylene	720	2150
Cork	510	6200
Polyethylene (LD)	840	2200

Table 5.3 Solid particles used and their densities

5.2.2 Liquid Density

The same procedure is repeated above without the presence of solid particles.

The density of the liquid is obtained as

$$r_l = \frac{W_t - W_b}{V_b}$$

Table 5.4 shows the liquids used as their properties as measured using the procedure above

Liquid	Density kg/m ³ , 30°C
Pure distilled water	996.0
8% Zinc Chloride Soln.	1075.0
12% Zinc chloride Soln.	1146.1
14% Zinc Chloride Soln	1176.5

Table 5.4 Liquids used and their densities

5.3 SPEED MEASUREMENT

The impeller speed was read from motor rpm meter as shown in Figure 5.1. A stroboscope was used from time to time to verify the accuracy of the indicated speed on the rpm meter. For each data point the minimum drawdown speed was determined according to criteria given in Section 2.4.

5.4 POWER MEASUREMENT

The power consumption of the system was obtained by first measuring the electromotive force (emf) induced on the electromotor due to the torque applied on the impeller shaft. In order to relate the emf induced and the corresponding torque, a number of experiments were done using different impellers on a Chemineer Motor which was equipped with a dynamometer for the direct measurement of the force applied to the shaft. By running the same

experiments on the Cole Palmer Motor (same speed, impeller size and type, liquid, clearance, tank size, etc.) the corresponding emf could be obtained and using the two sets of data the relationship between emf and torque was established (see Appendix A-2). This relationship was then used in subsequent data evaluations to determine the power consumption.

CHAPTER 6

RESULTS AND DISCUSSION**6.1 EFFECT OF IMPELLER SIZE ON N_{js}**

Figure 6.1.1 and 6.1.2 shows plots of N_{js} vs. D for various impeller types at constant clearances and Figure 6.1.3 shows the same relationship at constant clearance ratio ($C/D = 1$). The notation UP (upward pumping) and DP (downward pumping) refers to the pumping direction of the pitched blade turbine. The indices for c_5 for the different lines are reported in Table 6.1 and 6.2 respectively.

Impeller type	index at $C=T/3$	$C = T/2$
Disk turbine	-2.00	-2.11
Flat Blade Turbine	-2.13	-2.19
Pitched Blade Turbine (UP)	-2.82	-1.49
Pitched Blade Turbine (DP)	-2.83	-2.82
Model prediction	-1.67	-1.67

Table 6.1 Index on D at constant $C = 1/3T$ and $C = 1/2T$

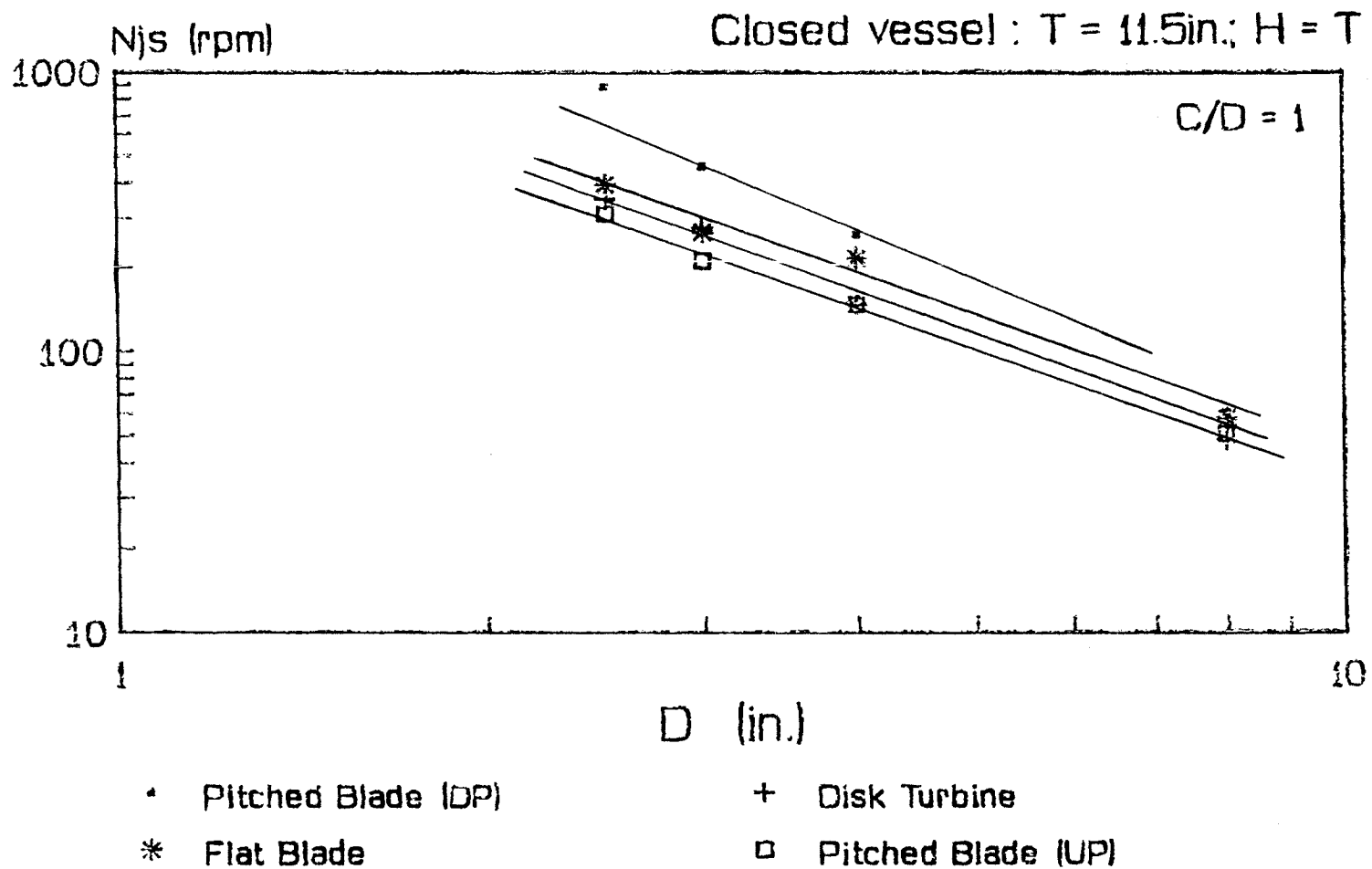


Figure 6.1.1 Effect of impeller size on N_{js}
 HD Polyethylene (897Kg/m³, d_p =2205microns) / Water (996Kg/m³)

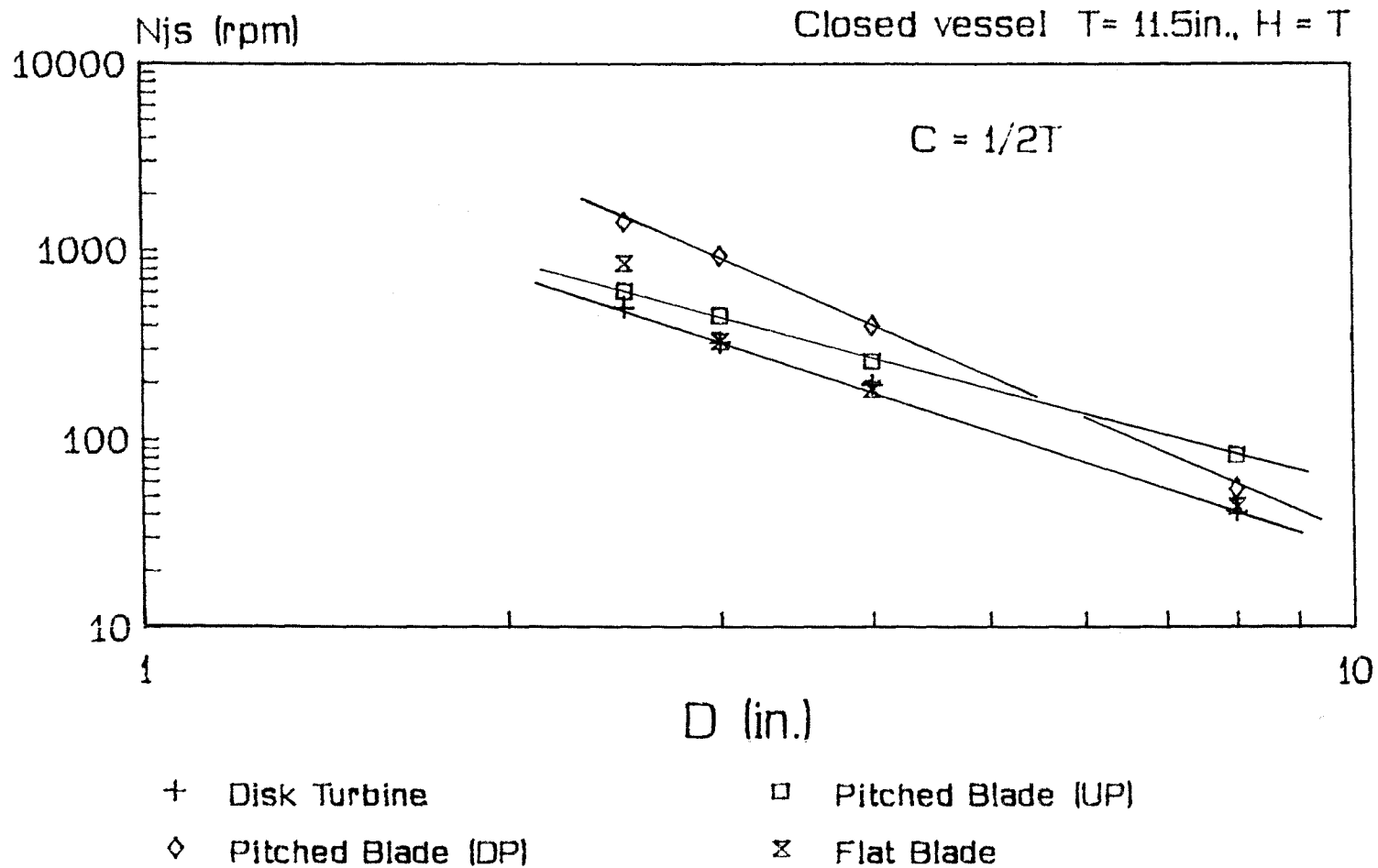


Figure 6.1.3 Effect of impeller size on N_{js} for const. C
 System: Polyethylene (897Kg/m³, $d_p=2205$ microns) / Water

Impeller type	index at C/D = 1
Disk turbine	-1.73
Flat Blade Turbine	-1.62
Pitched Blade Turbine (UP)	-1.65
Pitched Blade Turbine (DP)	-2.23
Model prediction	-1.67

Table 6.2 Index on D at constant C/D ratio

From the two tables and figures, it can be seen that the predicted relationship between impeller size and N_{js} holds for constant C/D ratios. It is also evident from the above table that the model predicts fairly well the dependence for the case of disk turbine, flat blade turbine and the pitched blade turbine pumping upwards. The pitched blade impeller pumping downwards (i.e. away from the solids) deviates from the rest of the impellers. This is probably due to the fact that the impeller pumps mainly axially downwards and so more agitation is needed for complete drawdown of the particles which are originally floating at the top surface.

6.2 EFFECT OF PARTICLE SIZE ON N_{js}

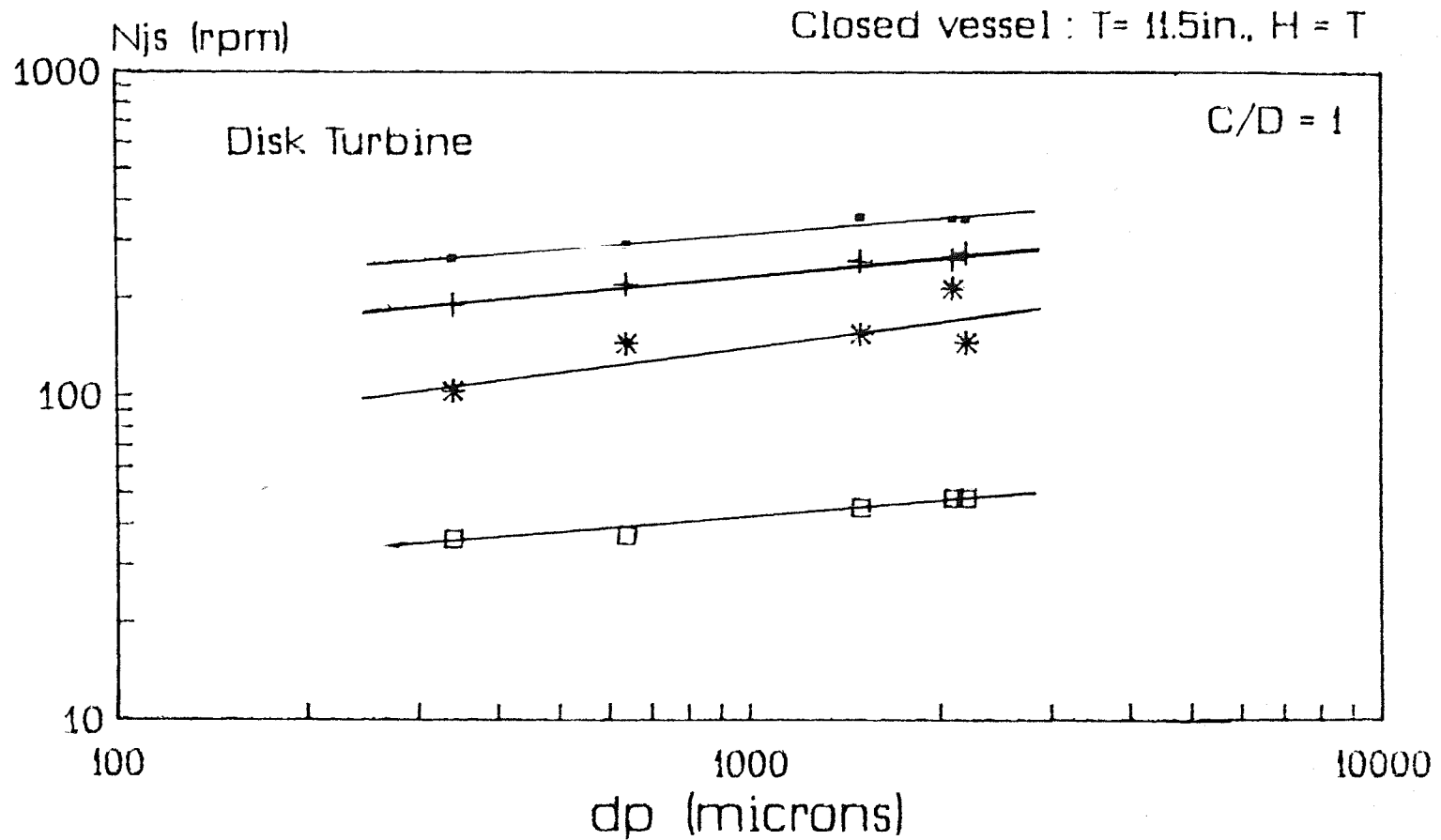
Figure 6.2.1 through 6.2.3 shows the graph of minimum suspension speed versus solid particle size. The index c_4 from linear regression for different impeller types and sizes is shown on Table 6.3

Impeller Type	Index on dp for			
	D=2.5	D=3in.	D=4in.	D=8in.
Disk turbine	0.161	0.189	0.165	0.168
Pitched Blade Turbine (UP)	0.161	0.131	0.153	0.152
Pitched Blade Turbine (DP)	0.149	0.152	0.147	0.137
Model prediction	0.167	0.167	0.167	0.167

Table 6.3 Index on dp for $C/D = 1$

On average, the experimentally obtained index for dp agrees very well for the value predicted by the model regardless of the impeller type or size.

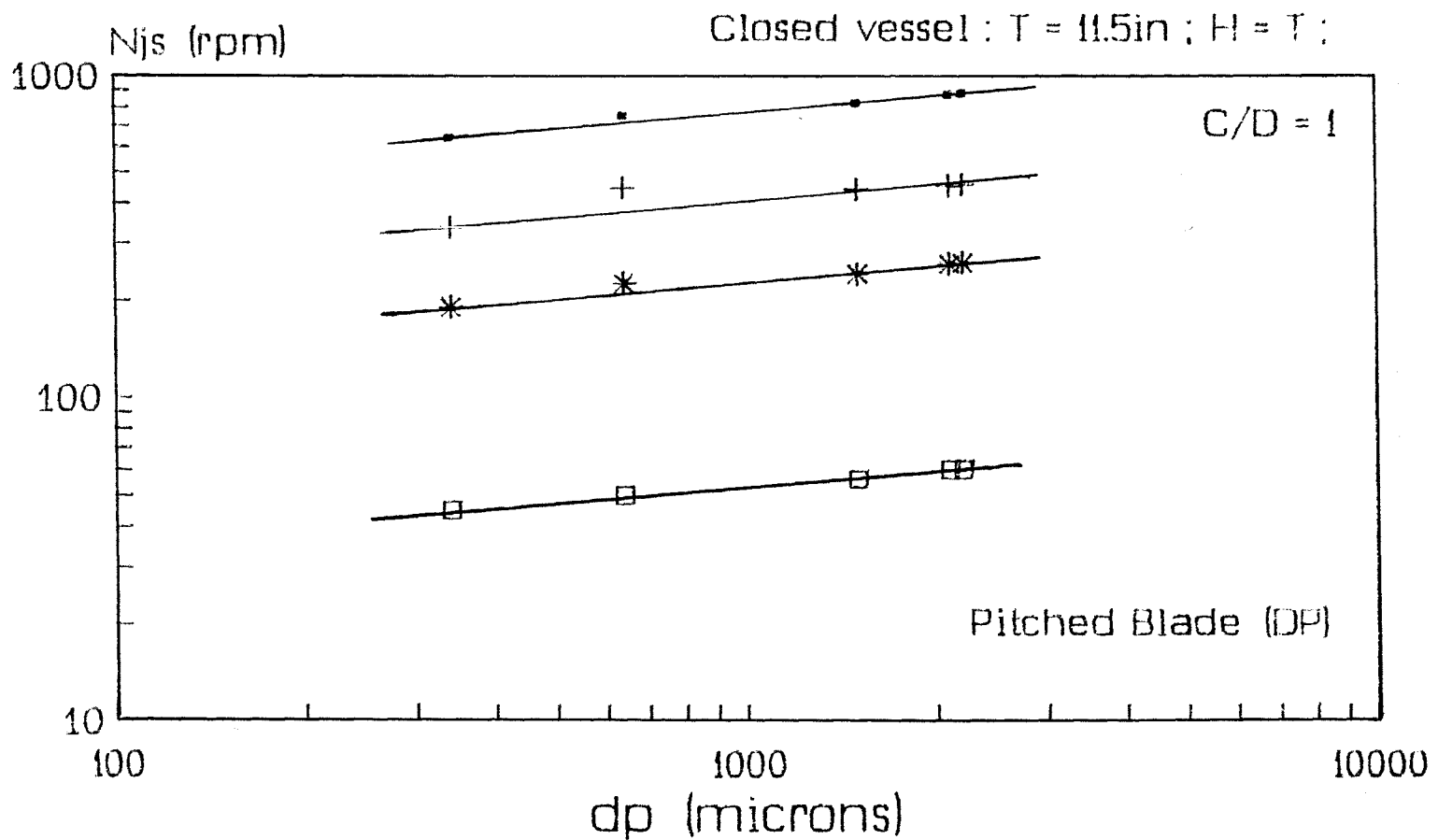
This is a good indication of the influence of particle size parameter on mixing operations. The impeller pumping direction in this case does not adversely influence N_{js} with respect to particle size.



• D = 2.5in. + D = 3in. * D = 4in. □ D = 8in.

Figure 6.2.1 Effect of particle size on Njs

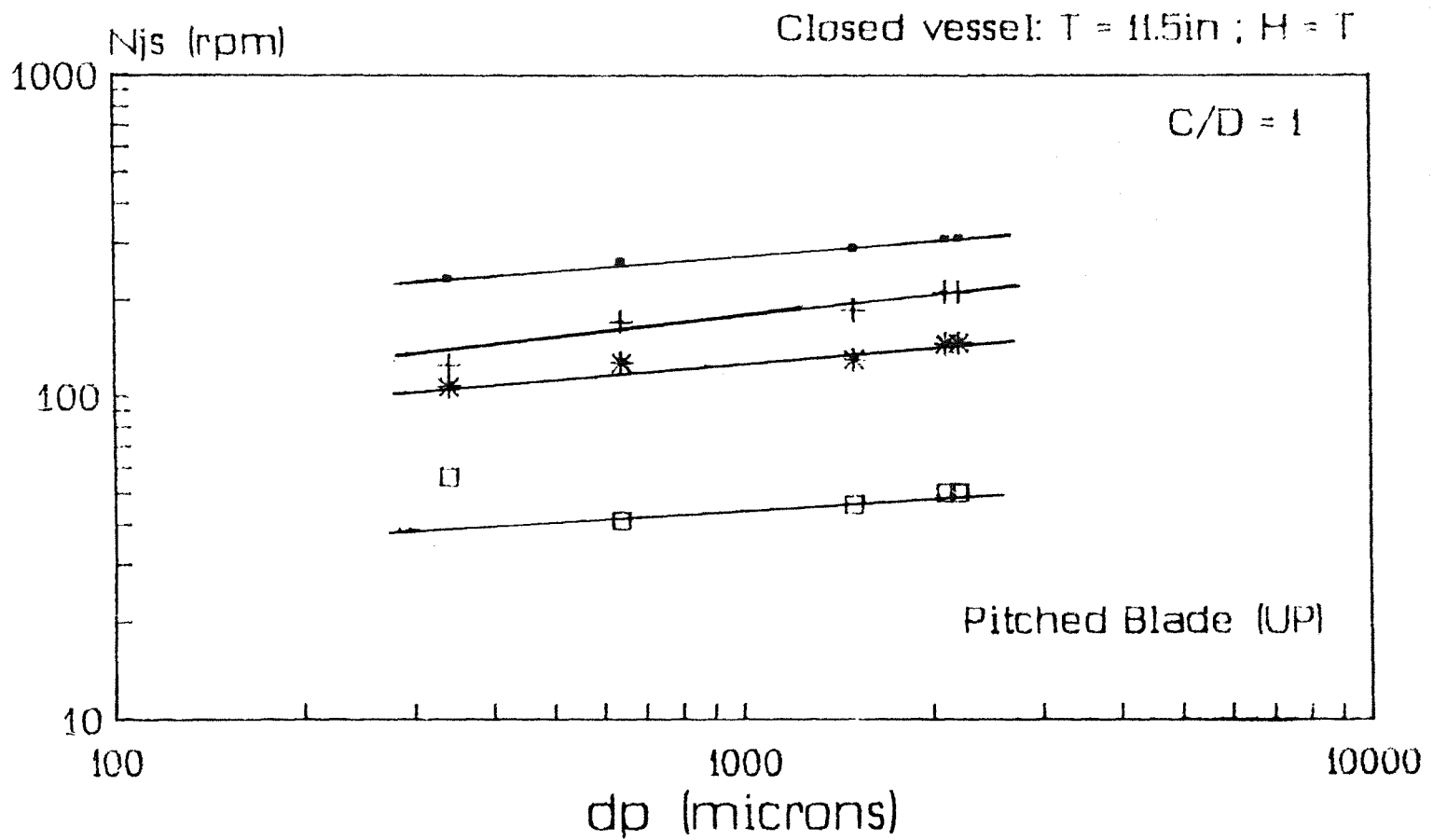
HD Polyethylene (897Kg/m³) / Water (996Kg/m³)



• D = 2.5in. + D = 3in. * D = 4in. □ D = 8in.

Figure 6.2.2 Effect of particle size on N_{js}

HD Polyethylene (897Kg/m³) / Water (996Kg/m³)



• D = 2.5in. + D = 3in. * D = 4in. □ D = 8in.

Figure 6.2.3 Effect of particle size on Njs

HD Polyethylene (897Kg/m³) / Water (996Kg/m³)

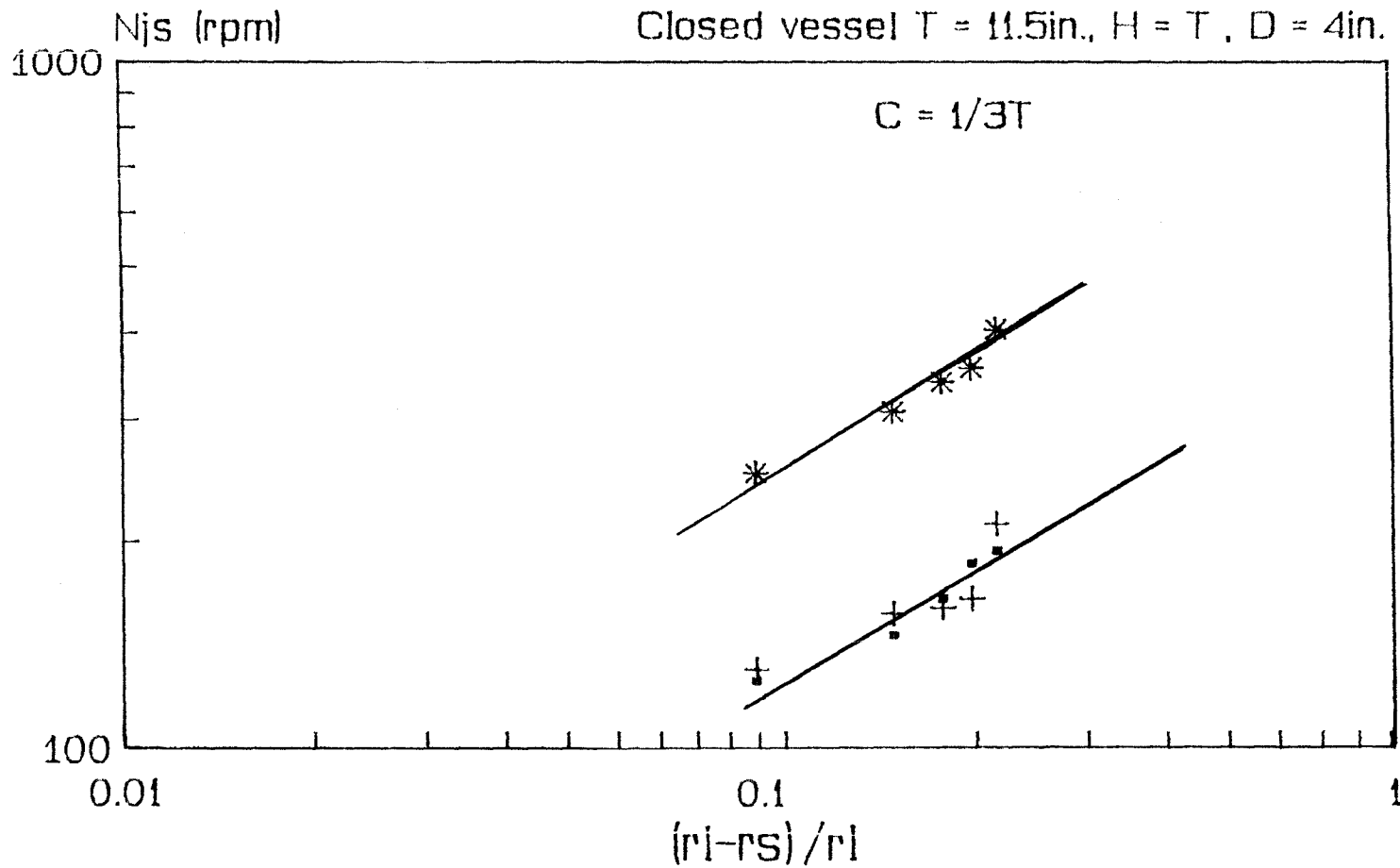
6.3 EFFECT OF DENSITY DIFFERENCE ON N_{js}

Figure 6.3.1 through 6.3.4 shows the graph of N_{js} vs. density difference factor ($\Delta r/r_1$) for the two most used impellers at two constant clearances. The indices for this factor (c_1) are shown in Table 6.4

Impeller Type	Index c_1 at	
	$C = 1/3T$	$C = 1/2T$
Disk turbine	0.506	0.555
Pitched Blade Turbine (UP)	0.444	0.860
Pitched Blade Turbine (DP)	0.506	0.742
Proposed equation	0.5	

Table 6.4 Index on $\Delta r/r_1$

The results above show that the model adequately predicts the functional dependence for the impellers at a clearance equal to $1/3T$. However, for different clearances and other impellers than the disk turbine the results are deficient. This shows that the model, as it stands it is still inadequate to incorporate clearance effects. The adjustment for clearance will be proposed in a section below.



▪ Disk Turbine + Pitched Blade (UP) * Pitched Blade (DP)

Figure 6.3.1 Density difference effect on N_{js}
 HD Polyethylene (2205microns)/Aqueous $ZnCl_2$ (0 to 14% w/w)

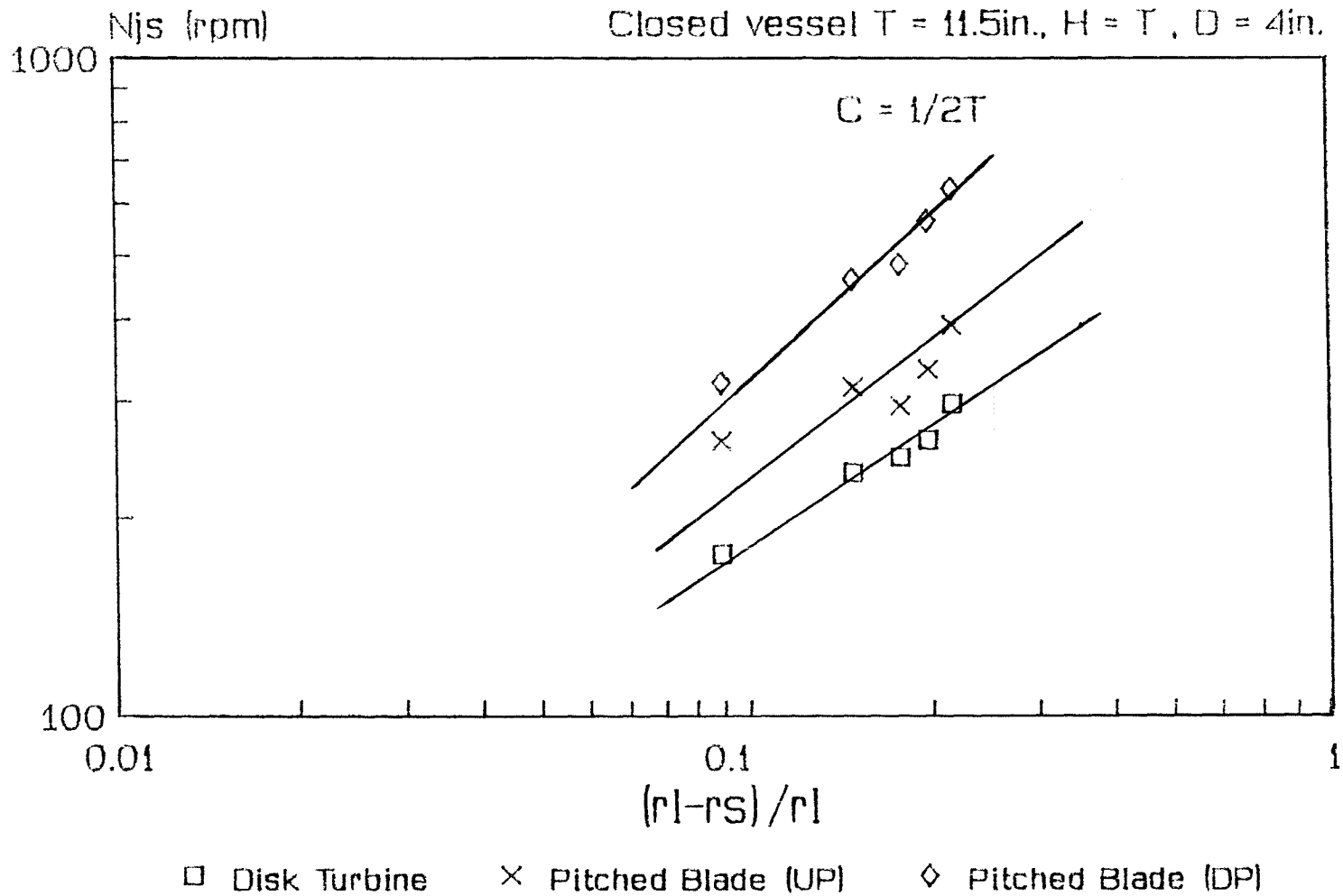


Figure 6.3.2 Density difference effect on N_{js}
 HD Polyethylene (2205microns)/Aqueous $ZnCl_2$ (0 to 14%)

6.4 EFFECT OF POWER NUMBER ON N_{js}

Figure 6.4 shows the graph of N_{js} vs. power number for different impellers. Table 6.5 shows the corresponding index obtained from linear regression results.

Impeller Type	Index c_4
Disk turbine	-0.312
Flat Blade Turbine	
Pitched Blade Turbine (DP)	
Pitched Blade Turbine (UP)	

Table 6.5 Index on N_p

The coefficient of correlation for the index for power number is poor if all the impellers and their pumping directions are included. However, if the data for pitched blade (pumping upwards) is excluded, the predicted index is closely approximated by the experimental results. This shows that actually the question of impeller type and pumping direction is more complicated and cannot be accounted by power number only. The flow pattern has to be taken into account also.

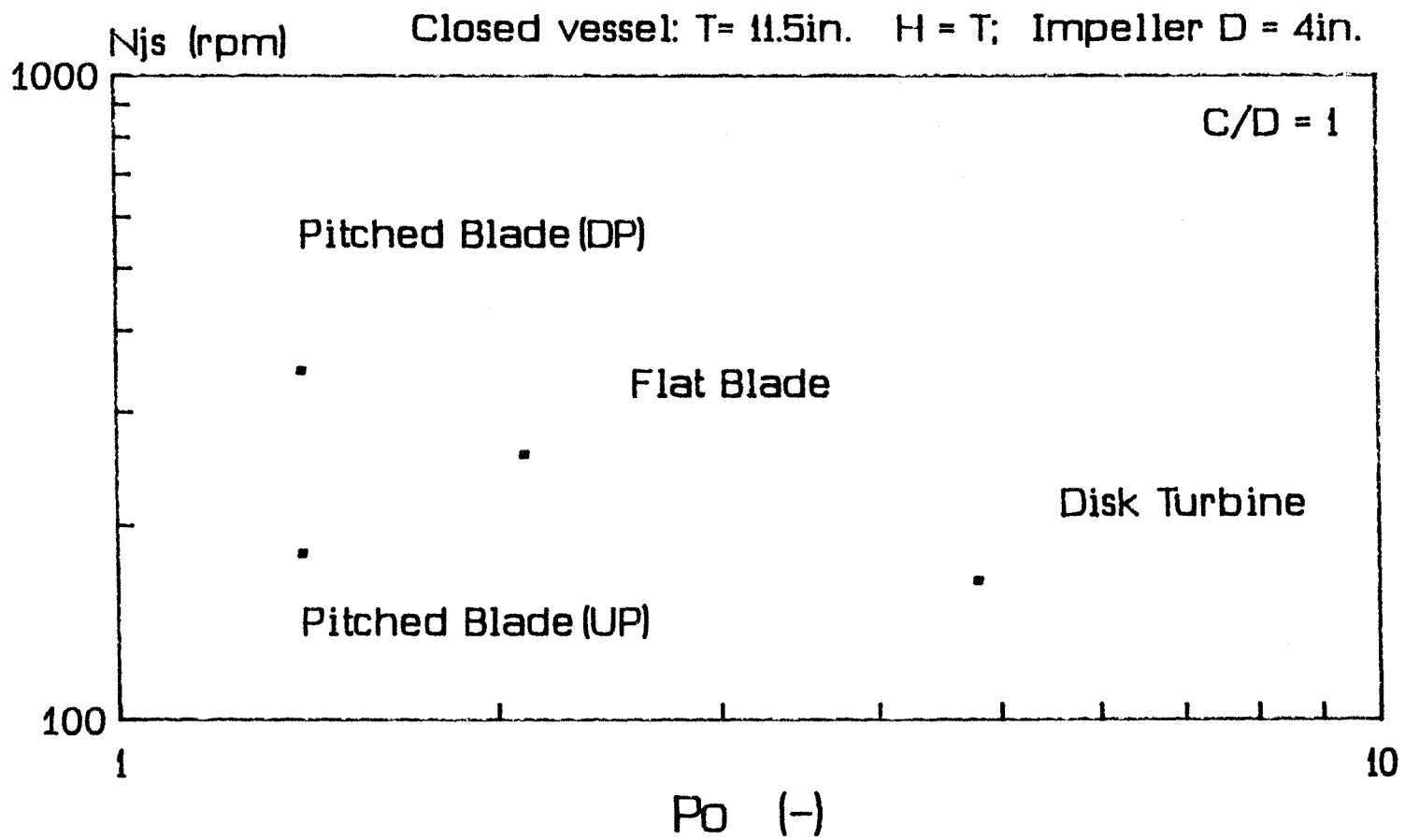


Figure 6.4 Effect of Po on N_{js}

Polypropylene (720Kg/m^3 , 2150microns) / Water (996Kg/m^3)

In Equation 3.20 the constant ϕ changes as the impeller type is changed and it is not appropriate to correlate the actions of the different kinds on impellers.

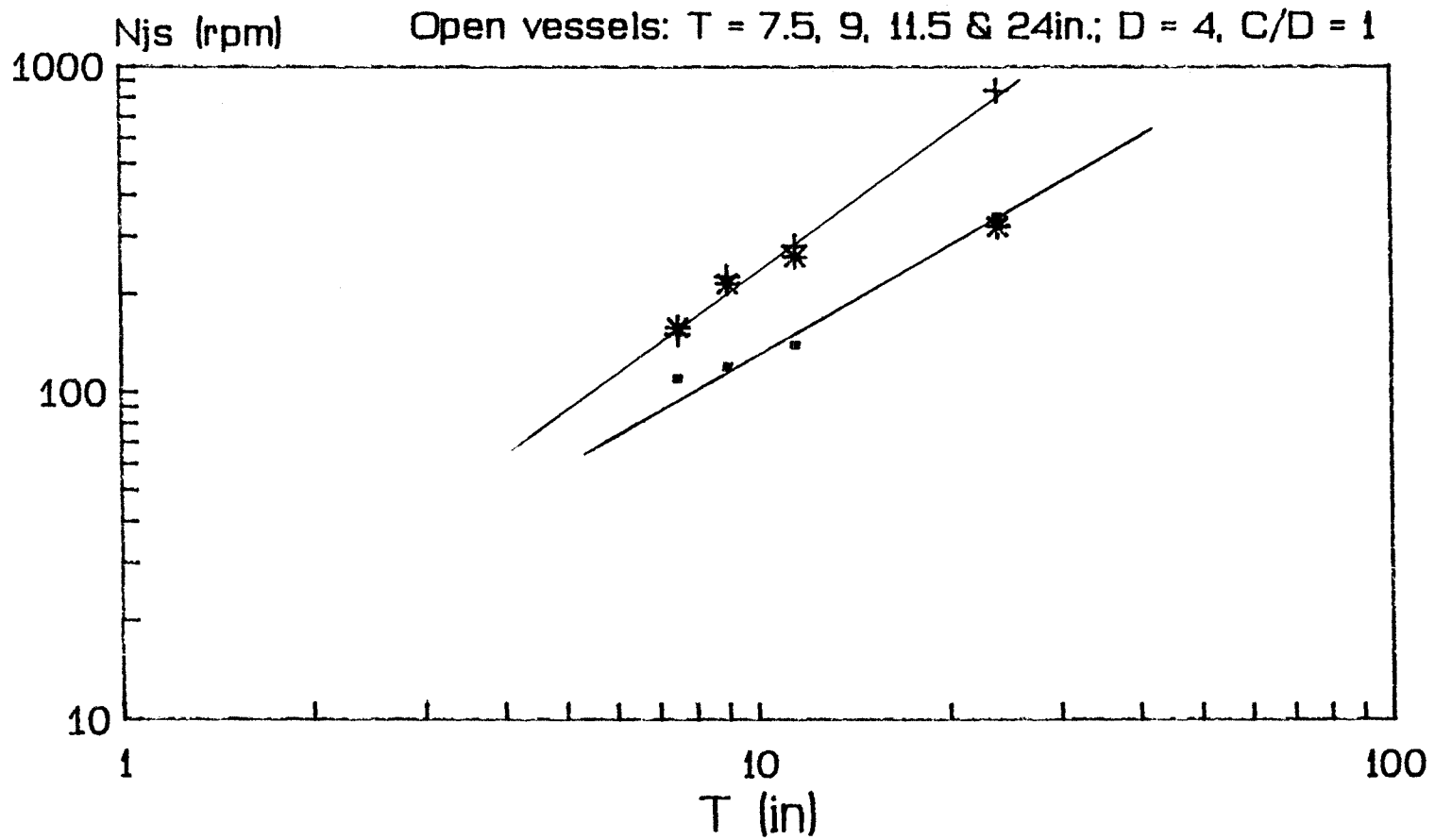
6.5 EFFECT OF TANK SIZE ON N_{js}

Figure 6.5.1 shows the effect of tank size on minimum suspension speed. The indices for correlation of the minimum speed with tank size for different impellers are shown in Table 6.6

Impeller type	Index c_3
Disk Turbine	1.04
Pitched Blade (DP)	1.45
Flat Blade	0.56
Pitched Blade (UP)	-0.60
Predicted Value	1.00

Table 6.6 Index on T for different Impellers (constant C and D)

It is interesting to note that it is only the disk blade turbine which so far agrees with the model prediction for all the parameters encountered so far.



• Disk Turbine + Pitched Blade (DP) * Flat Blade

Figure 6.5.1 Effect of tank size on N_{js}

LD Polyethylene (840Kg/m³, dp = 2200microns) / Water

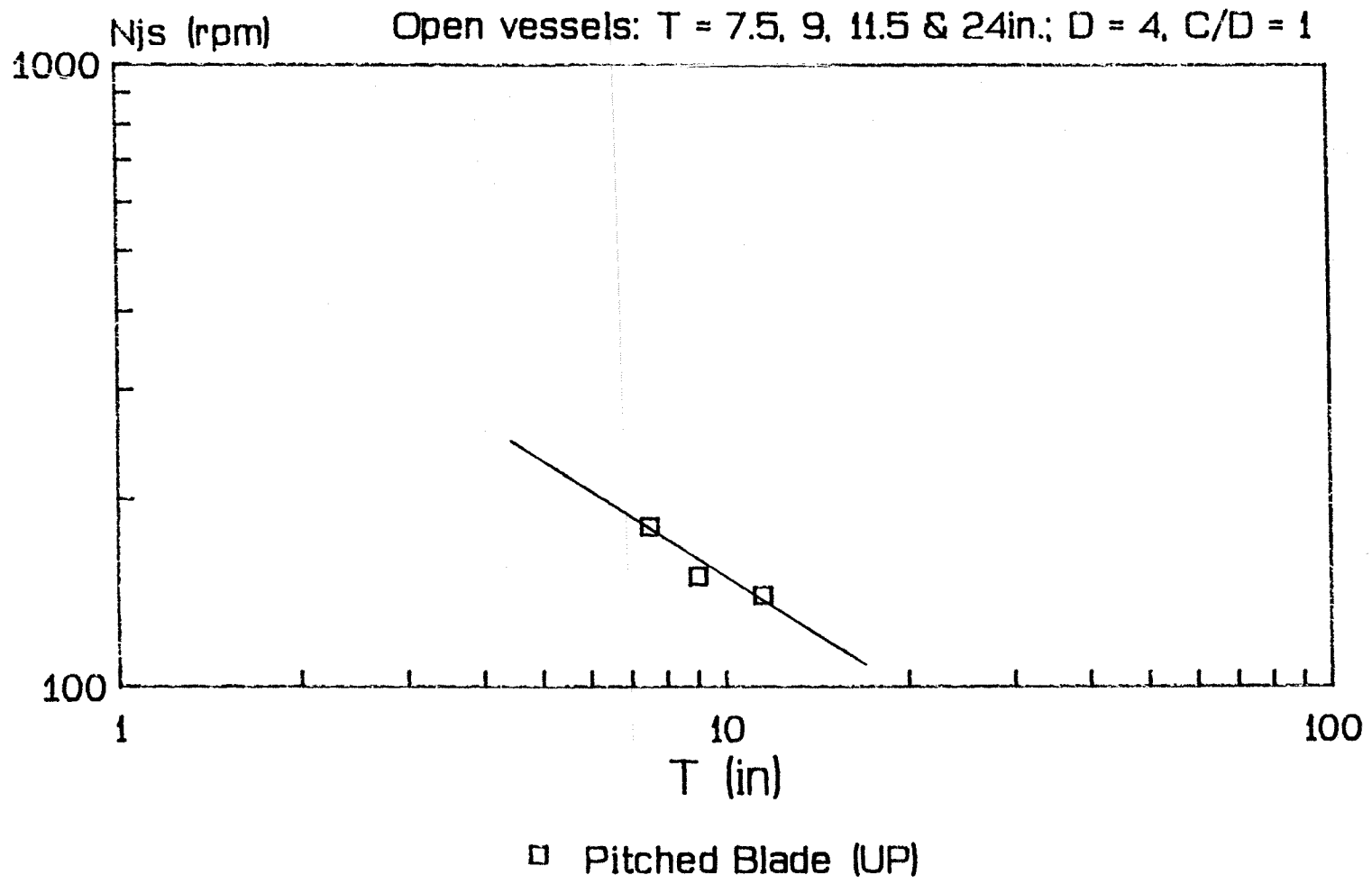


Figure 6.5.2 Effect of tank size on N_{js}
 LD Polyethylene (840Kg/m³, dp = 2200microns) / Water

The pitched blade turbine pumping upwards (Figure 6.5.2) shows opposite results with respect to the other impellers. As the tank size is increased the required minimum speed decreases.

Figure 6.5.3 shows the scale up effect. In this case, the same geometric ratios, C/D and T/D have been kept constant while changing the tank size.

Figure 6.5.4 shows yet another form of impeller scale up whereby for the same tank size the impeller size is changed while maintaining a constant C/D ratio. Results from this experiment are similar to results obtained by changing the tank size while keeping C and D the same.

Figure 6.5.5 shows the effect of C/T ratio on minimum drawdown speed. In this case, the clearance ratio is kept constant while impeller size is increased. The graph is similar to one obtained by changing tank size while maintaining constant C/D and T/D ratios.

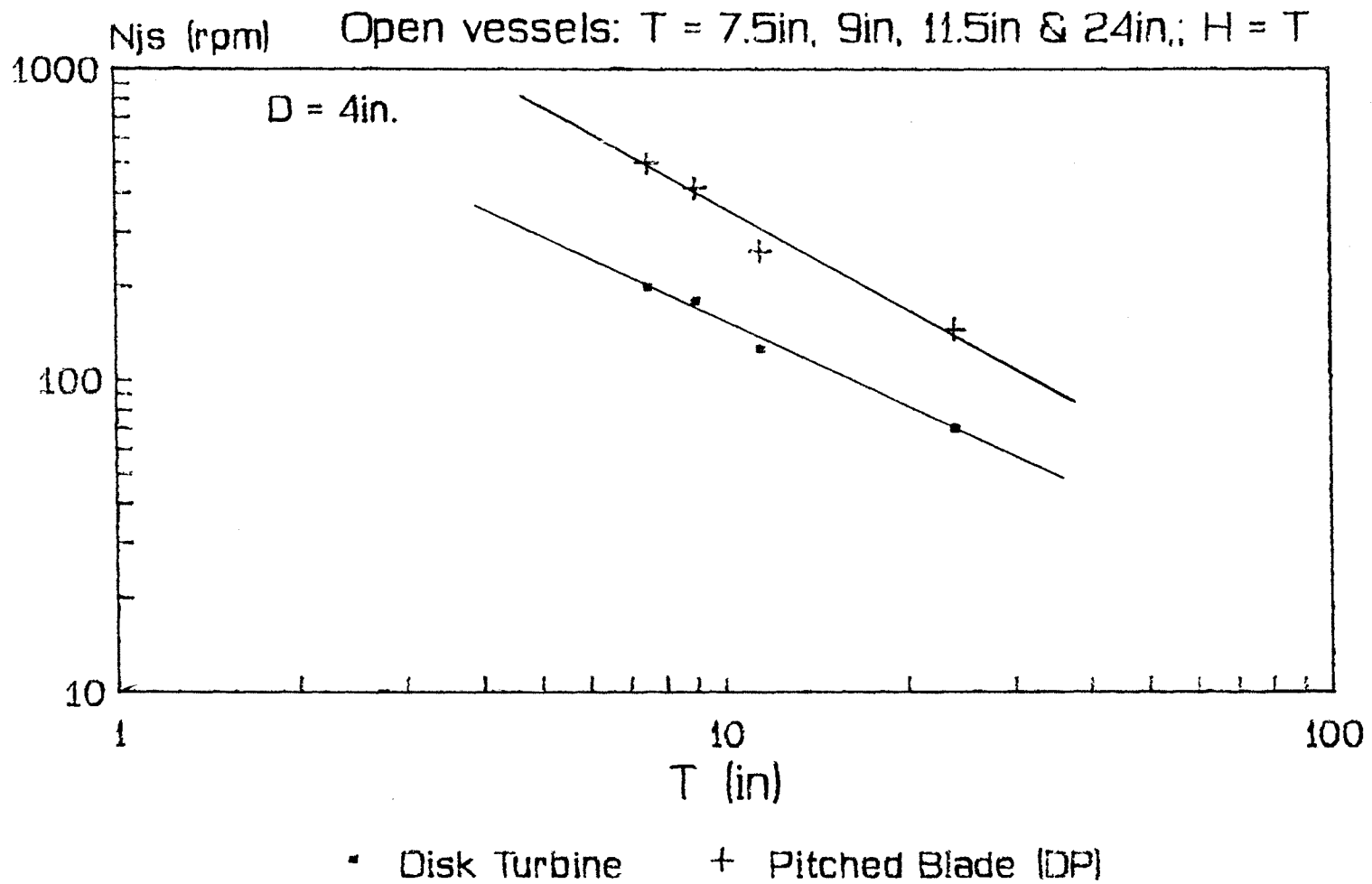
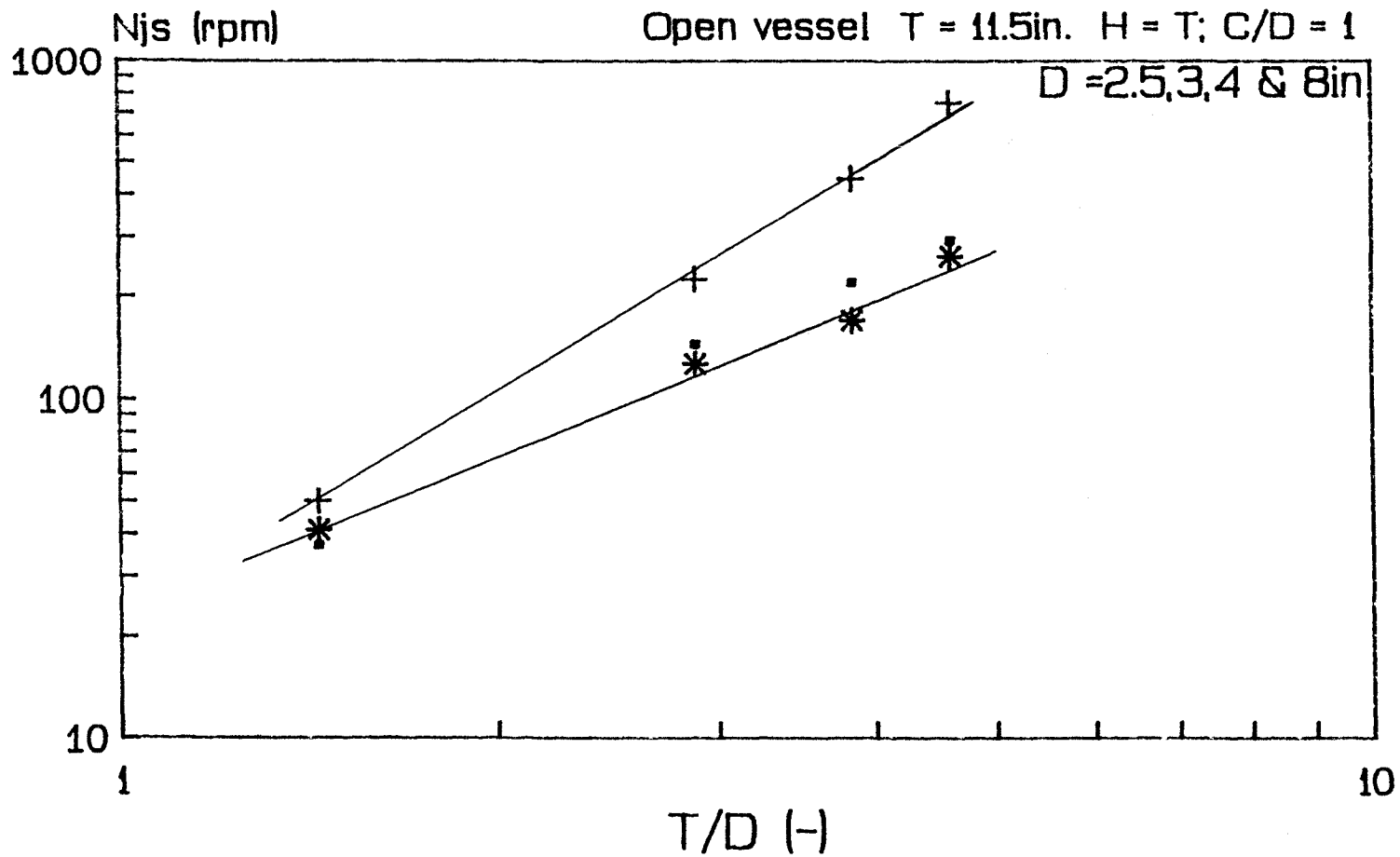


Figure 6.5.3 Effect of scale up on N_{js}

HD Polyethylene (897Kg/m³, 2205microns) / Water (996Kg/m³)



▪ Disk turbine + Pitched blade (UP) * Pitched blade (DP)

Figure 6.5.4 Effect of T/D ratio on N_{js}
 HD Polyethylene (897Kg/m^3 , $d_p=2205$ microns) / Water

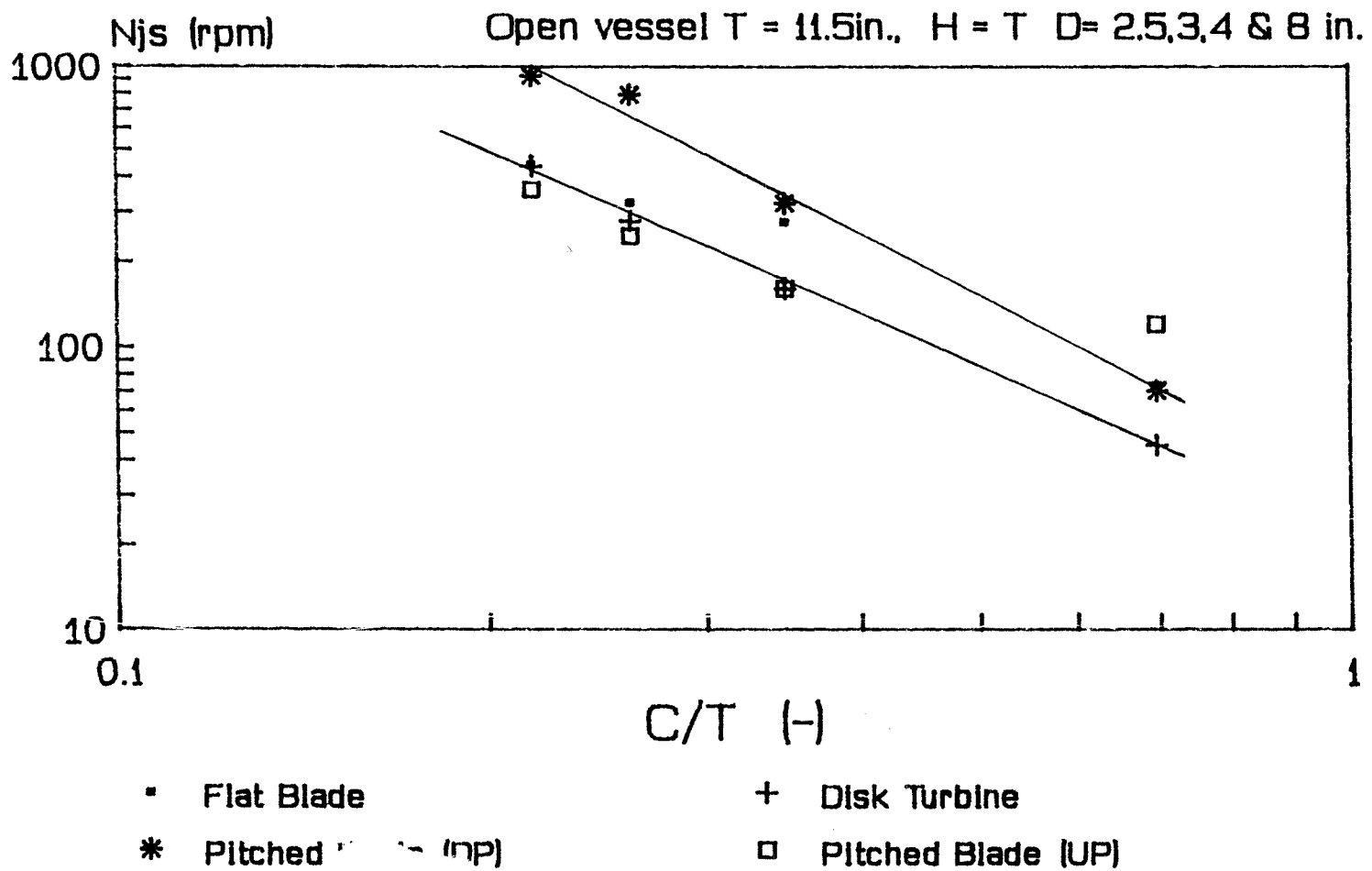


Figure 6.5.5 Effect of C/T ratio on N_{js} at $C/D = 1$
 System: HD Polyethylene (897Kg/m³) / Water (996Kg/m³)

6.6 EFFECT OF C/D RATIO ON N_{js}

The C/D ratio, although not appearing in the relationship directly, has a profound effect on the correlation between the predicted and experimental values for the indices in the model proposed. The C/D ratio equal to 1 has been found be the most convenient ratio to use in this model.

Figures 6.6.1 through 6.6.4 shows the variation for different systems. From all the graphs and data collected, one notes that the trend is to increase the required minimum speed for drawdown of solids as the C/D ratio increases. However, for the pitched blade impeller pumping downwards the required speed increases with C/D ratio for C/D values less than 2 and after this point, the minimum required speed decreases with increasing C/D ratio. This is attributed to the change in drawdown pattern. The C/D ratio corresponds to $C/T = 0.69$ which is very close to what was observed by Susanto [23] for settling solids suspension.

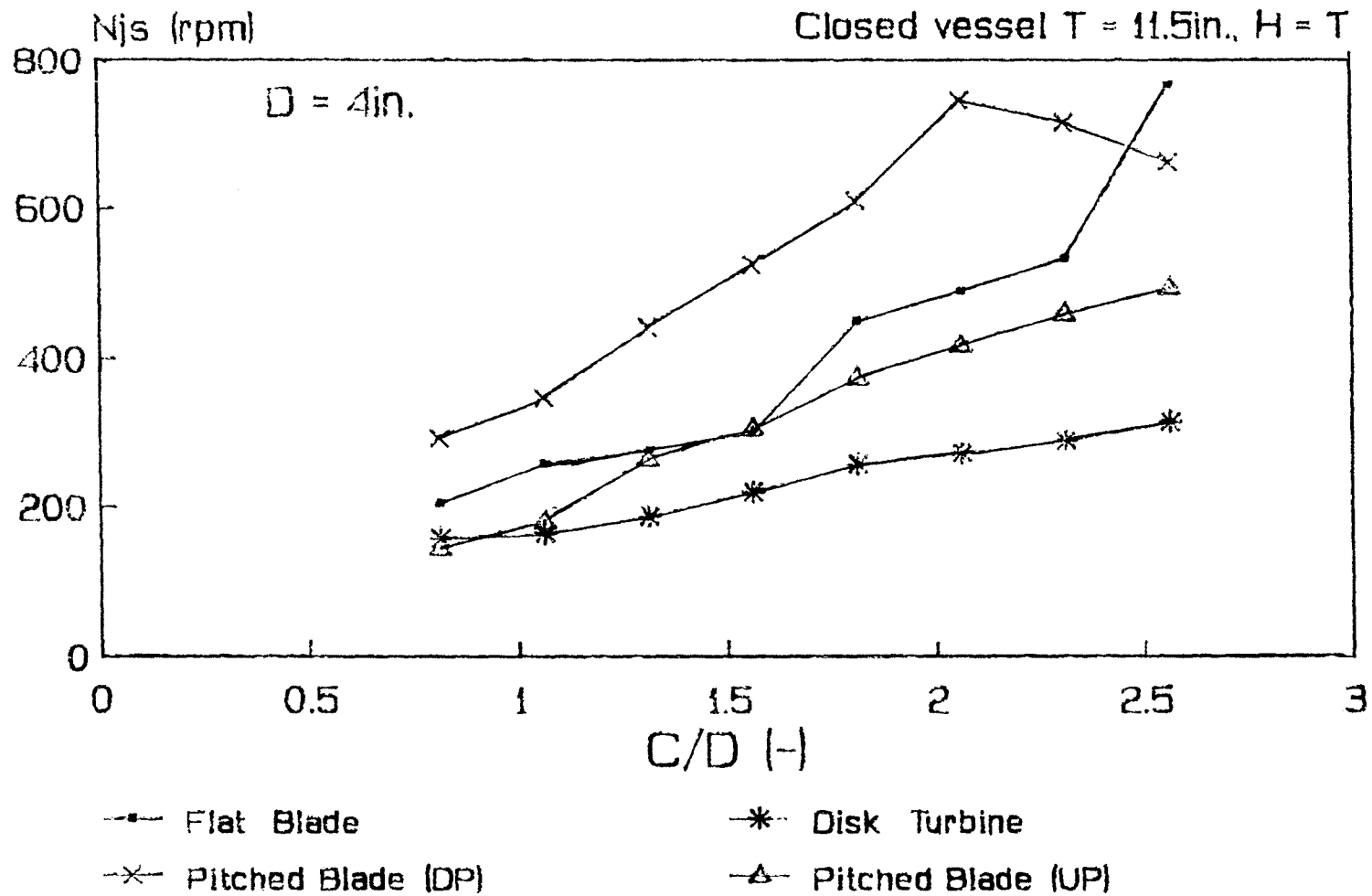


Figure 6.6.1 Effect of C/D ratio on Njs
 Polypropylene (2150microns, 720Kg/m³) + Water (996Kg/m³)

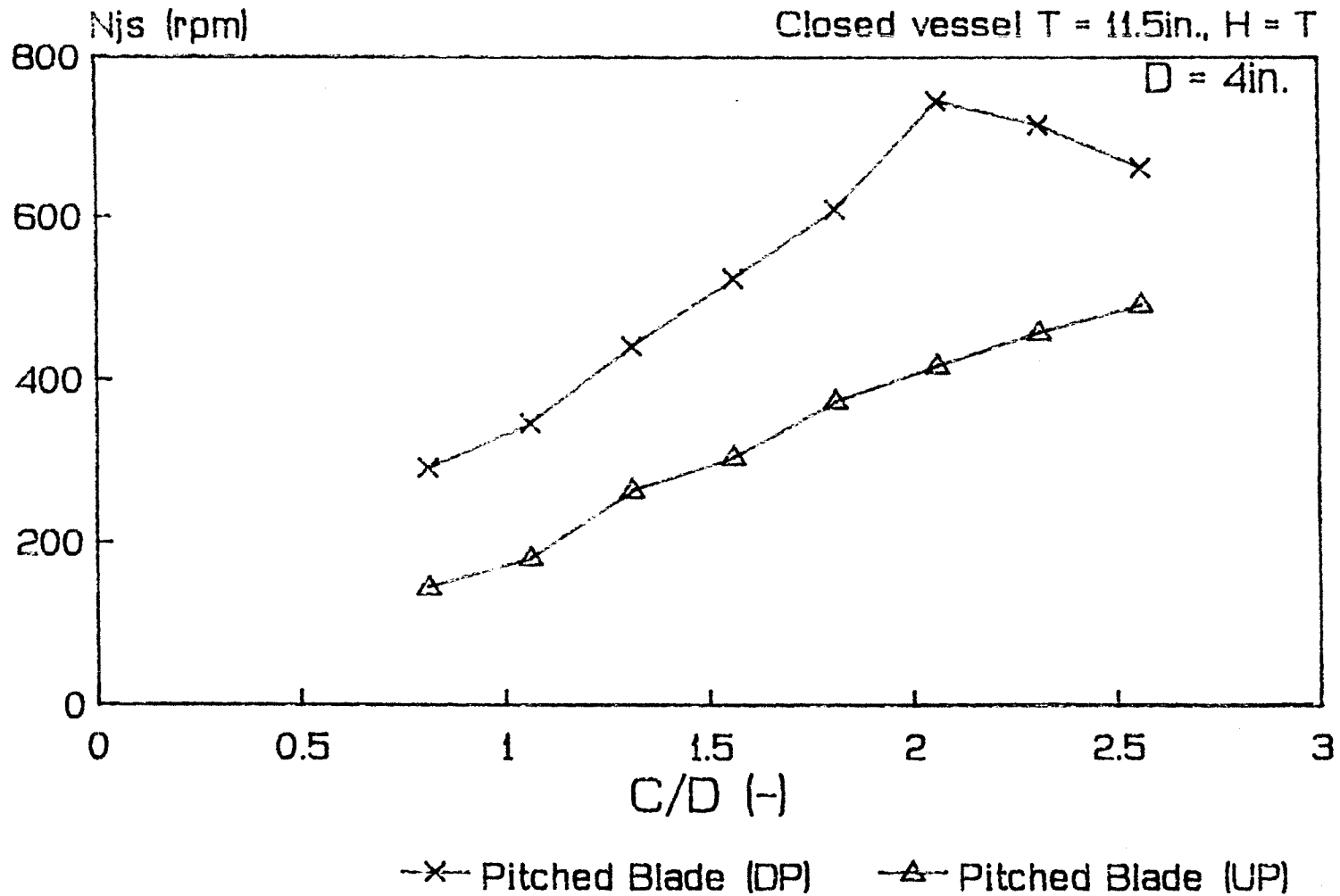


Figure 6.6.2 Effect of C/D ratio on N_{js}
 Polypropylene (2150microns, 720Kg/m³) + Water (996Kg/m³)

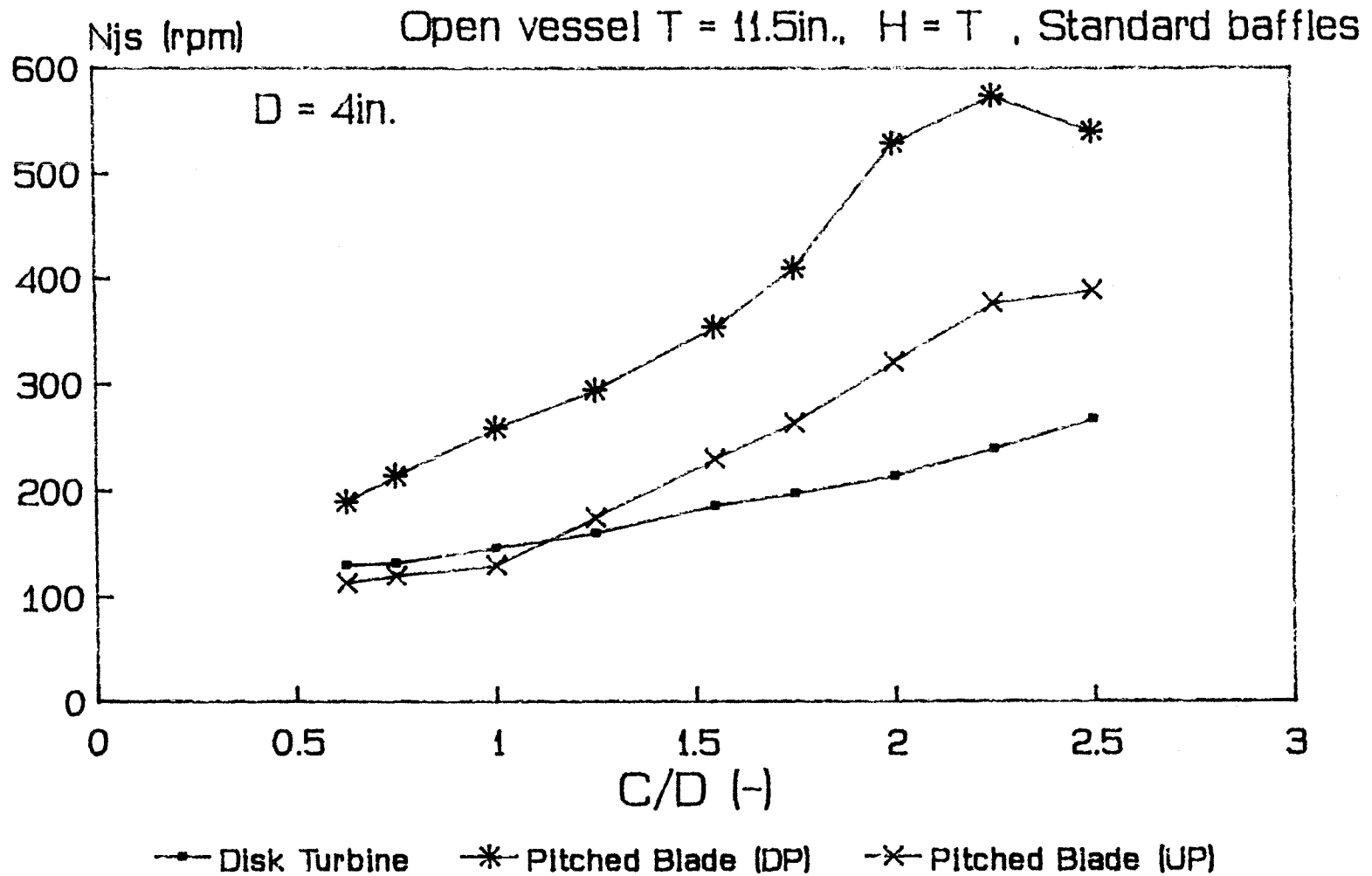


Figure 6.6.3 Variation of N_{js} with Clearance ratio
 HD Polyethylene ($d_p = 2205$ microns) + Water

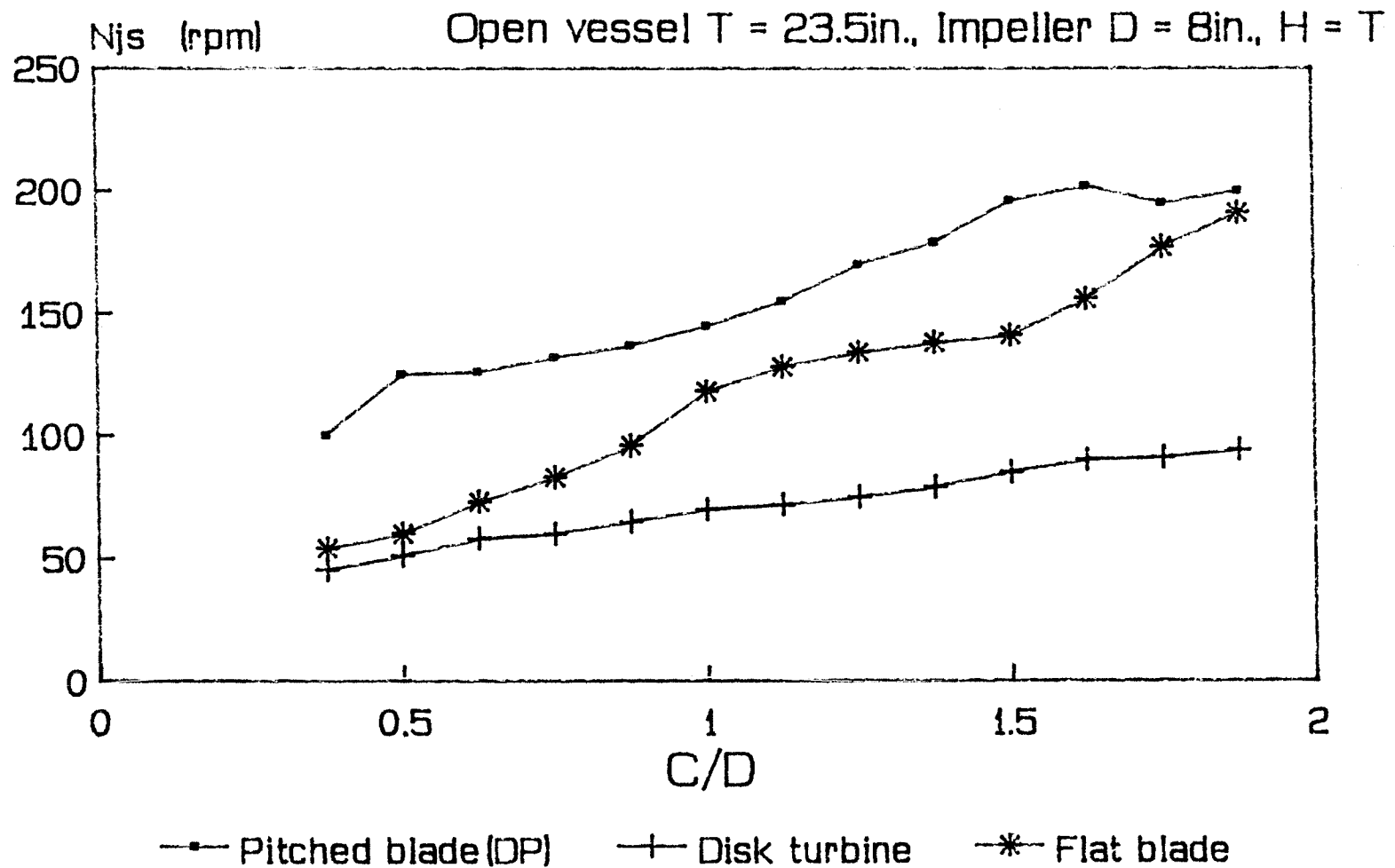


Figure 6.6.4 Effect of C/D ratio on N_{js}

Syssystem: HD Polyethylene (897Kg/m^3 , $d_p=2205$ microns) + Water

6.7 POWER CONSUMPTION

Figure 6.7.0 shows the plot of power number against Reynolds number for the various impellers used.

Figures 6.7.1 through 6.7.3 show the variation of power consumption for a disk turbine, flat blade turbine and pitched blade turbine, respectively.

6.7.1 Effect of Impeller size on Power Consumption

Figure 6.7.4 shows the variation of power consumption with impeller diameter for different impellers. This is an interesting graph because it shows just how differently these impellers behave. With the pitched blade turbine pumping upwards, the power consumption decreases as the impeller size is increased at constant C/D ratio, while for the disk blade turbine, the power consumption remains more or less the same as the impeller size is increased in the given range. For the pitched blade impeller pumping downwards, the power consumption actually increases within the given range.

It has been observed that large impellers consume much more power than small impellers for a fixed speed. Also the relative impeller clearance has been observed to have tremendous impact on the agitation requirements in terms of minimum speed and the power consumption accompanied. Therefore it is no doubt that the impeller clearance plays a significant role in determining the overall performance of

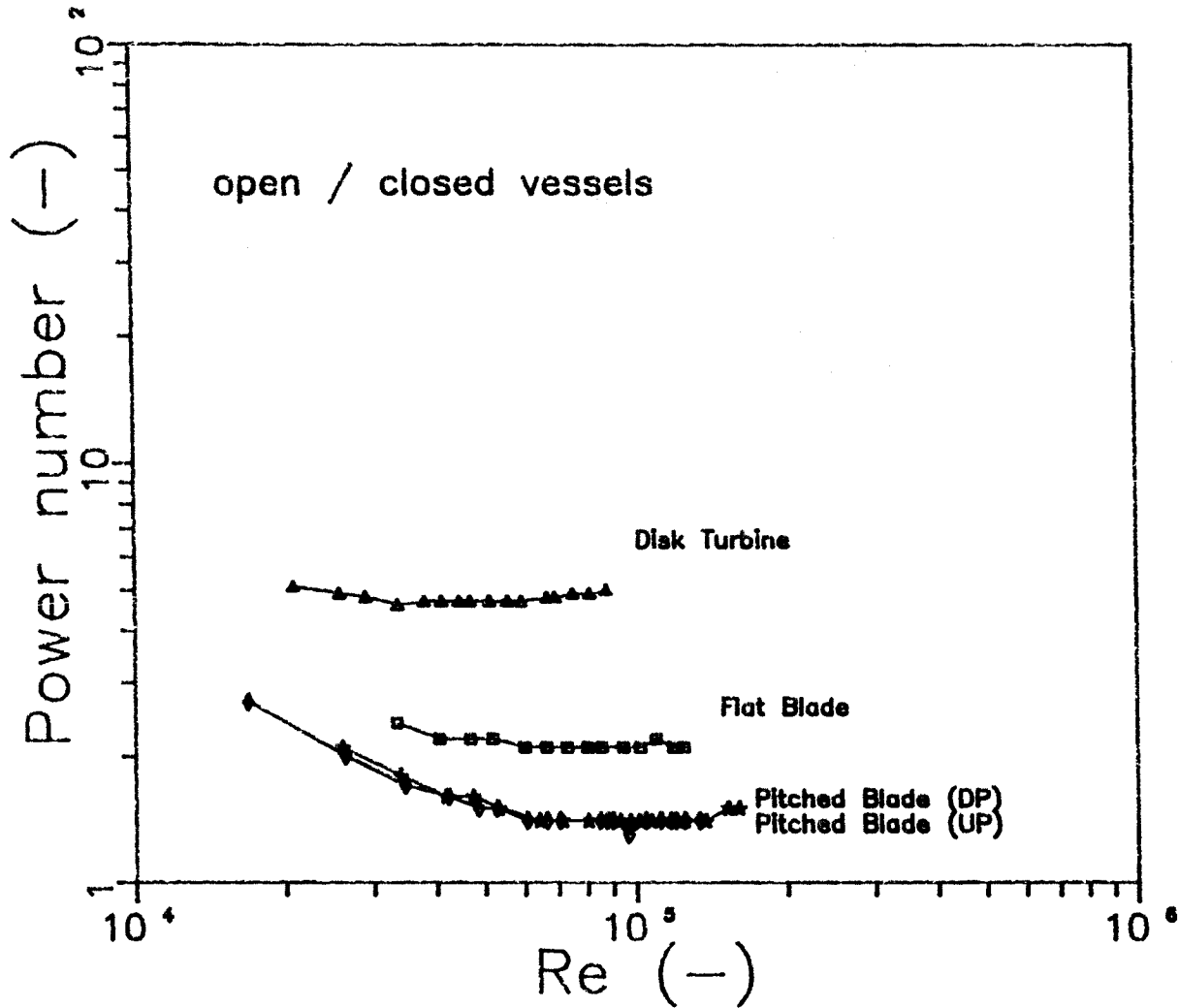


Figure 6.7.0 Power number curve
 $T = 11.5\text{in.}, H = T, D = 4\text{in.}, C = 4\text{in.}$

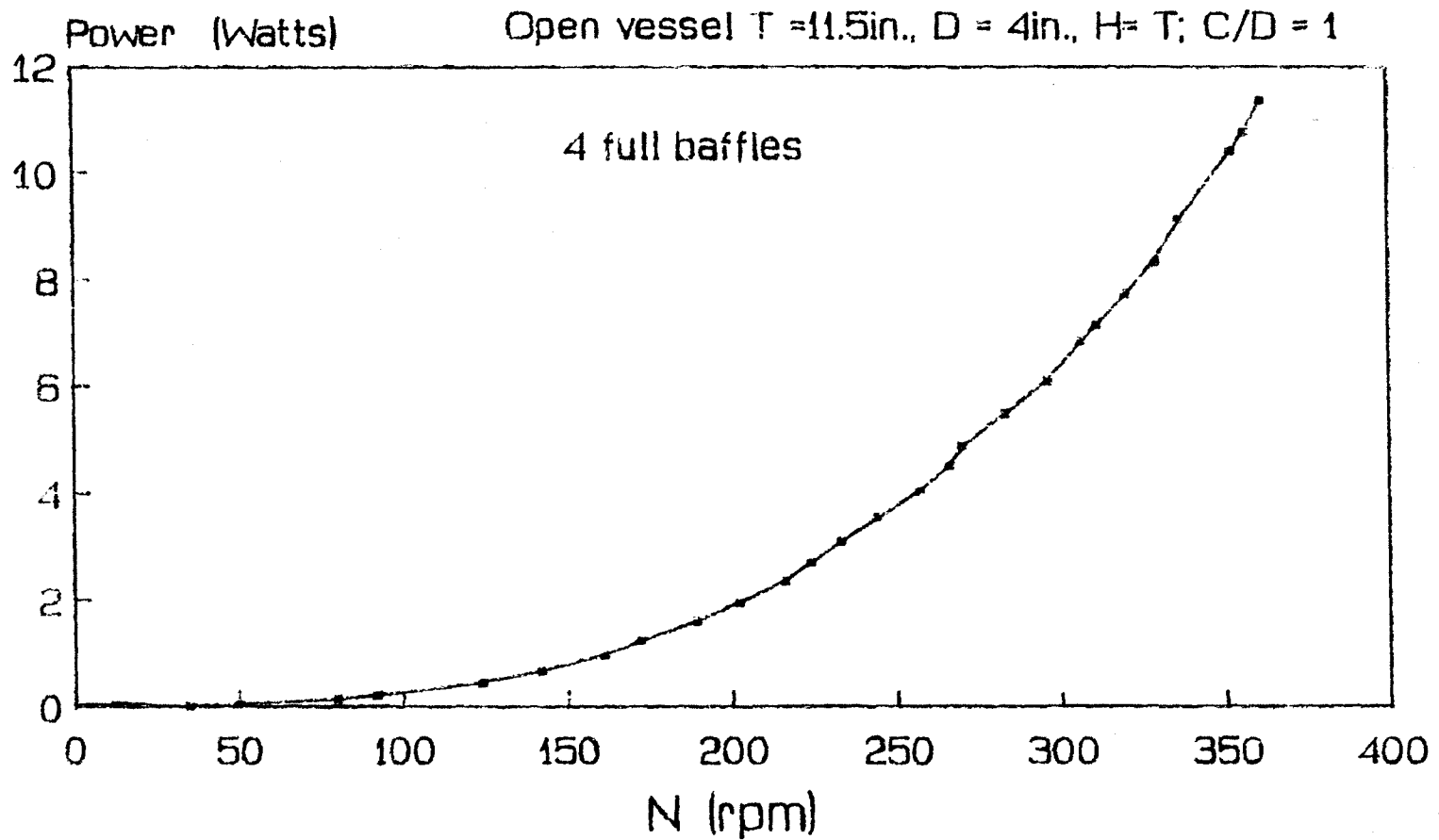


Figure 6.7.1 Power consumption curve for disk turbine
 System Water only (density = 996Kg/m^3)

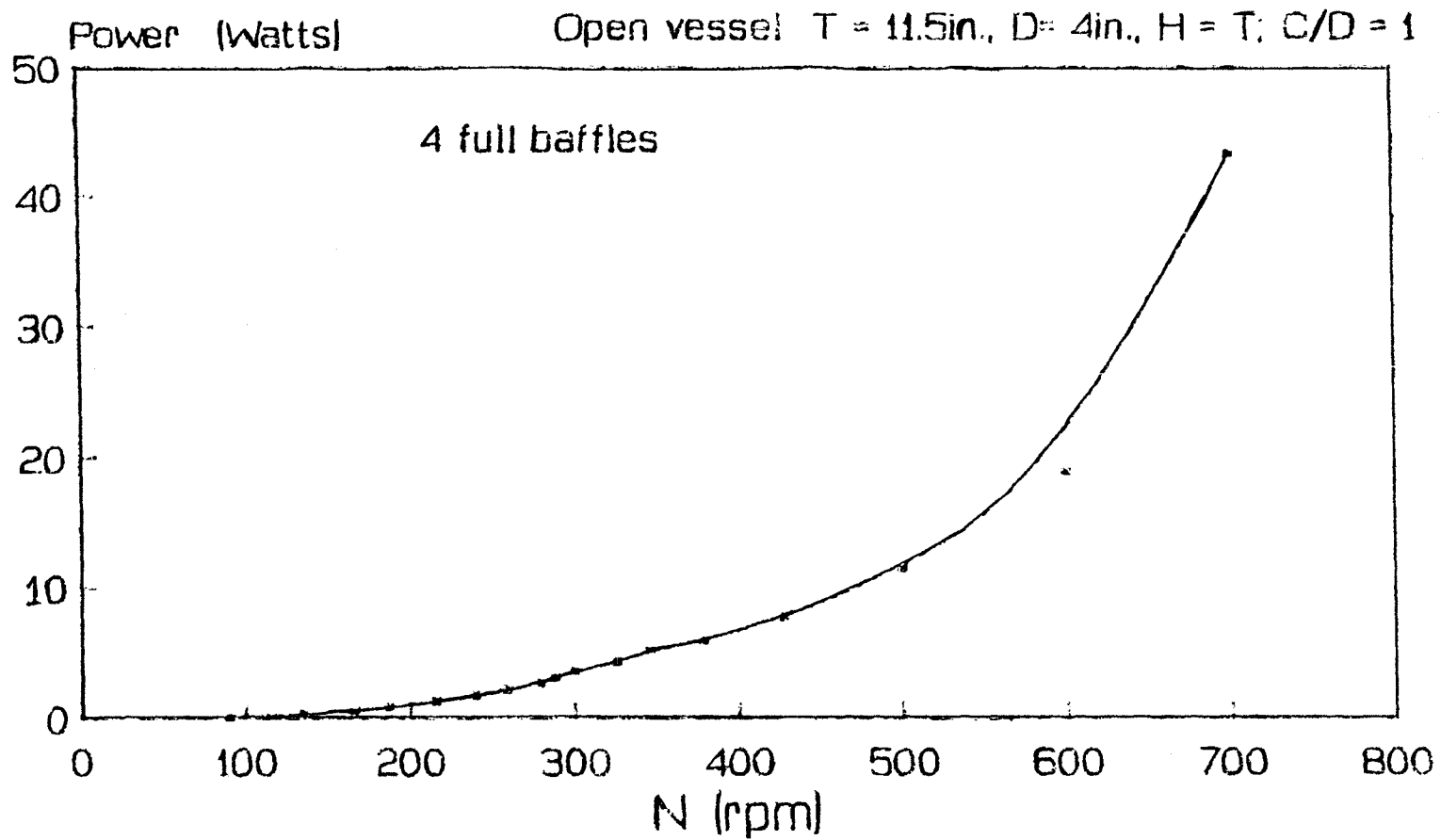


Figure 6.7.2 Power consumption with flat blade impeller

System: Water only (density = 996kg/m^3)

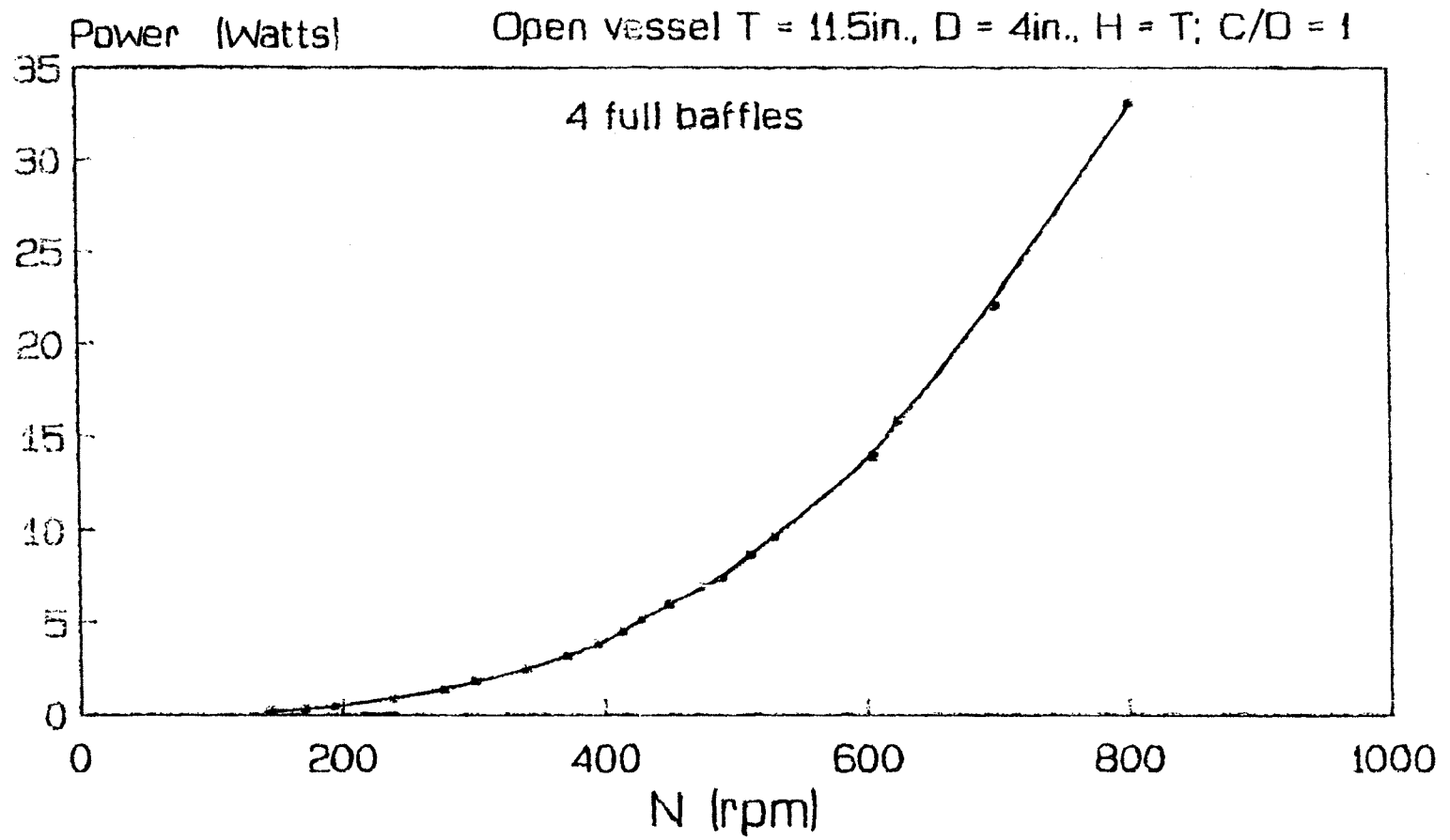


Figure 6.7.3 Power consumption for pitched blade turbine

System: Water only (density = 996Kg/m³)

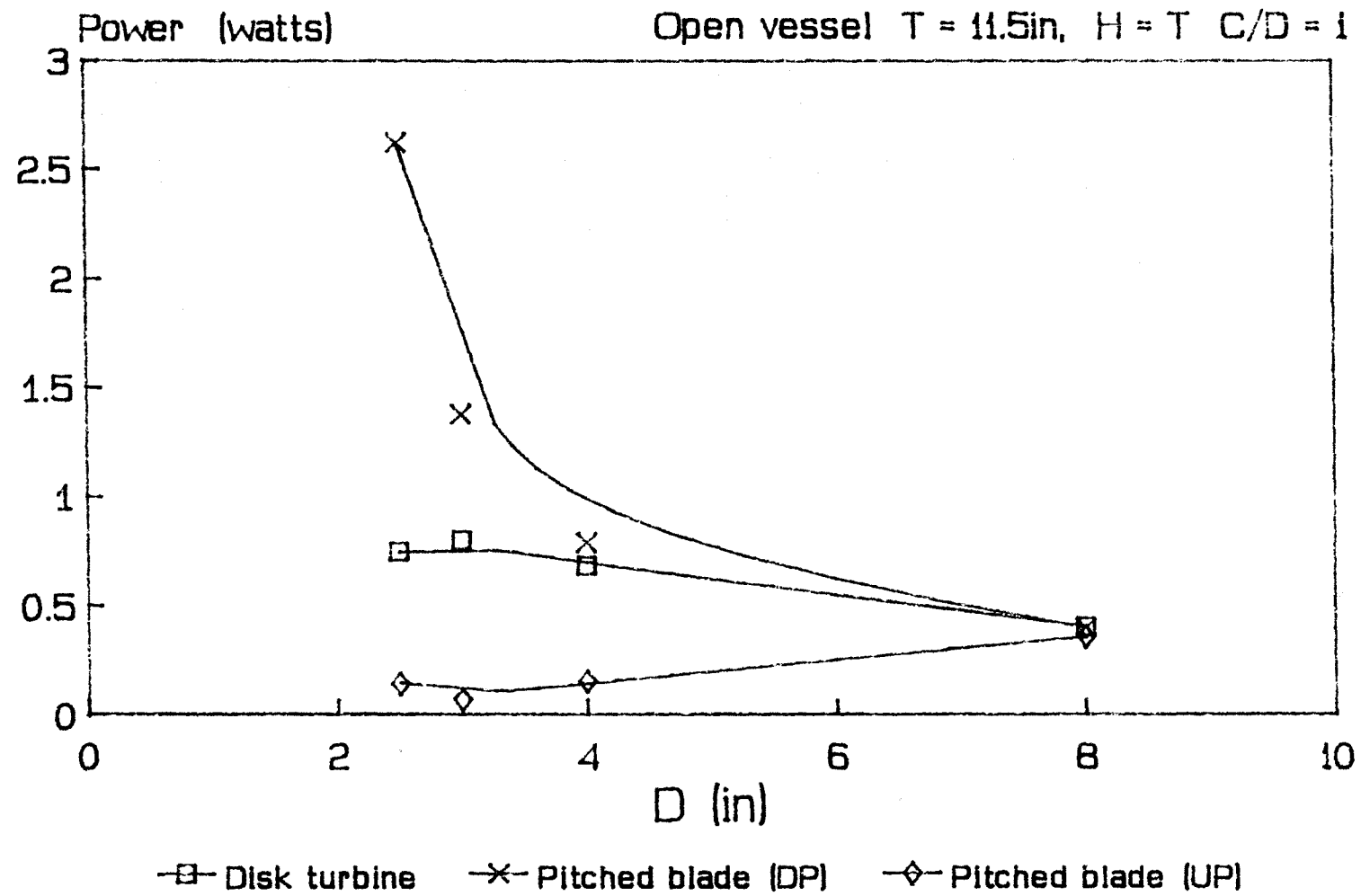


Figure 6.7.4 Effect of impeller size on power consumption at Njs
 System: HD Polyethylene (897Kg/m³, dp=2205microns) / Water

the mixing system. The clearance ratio C/D is best used to describe these two effects.

6.7.2 Effect of Impeller Clearance on Power Consumption

Figure 6.7.5 shows the power consumption of different impeller types at N_{js} as a function of the clearance ratio. We can infer from the results that the power required to achieve the minimum suspension speed increases as the impeller clearance increases.

We note from Figure 6.7.5 that the upward pumping pitched blade impeller performs more or less like the disk turbine in terms of power requirements. The flat blade impeller requires more power to achieve the same result as the disk turbine or pitched blade impeller pumping upwards. These observations help us narrow our search for an efficient impeller for floating solids draw-down.

For pitched blade turbine, the pumping direction is seen to be very decisive in determining the ease with which particles may be drawn down. Upward pumping impeller requires less speed and hence less power consumption than the conventional downward pumping impeller (Figure 6.7.6). This is a contrast to settling solids behavior [2,4,6]. The reason for this difference stems from the basic fact that in floating solids system, the particles are sitting at the top and hence for upward pumping impellers, the eddies have to travel a shorter distance before to reach the particles.

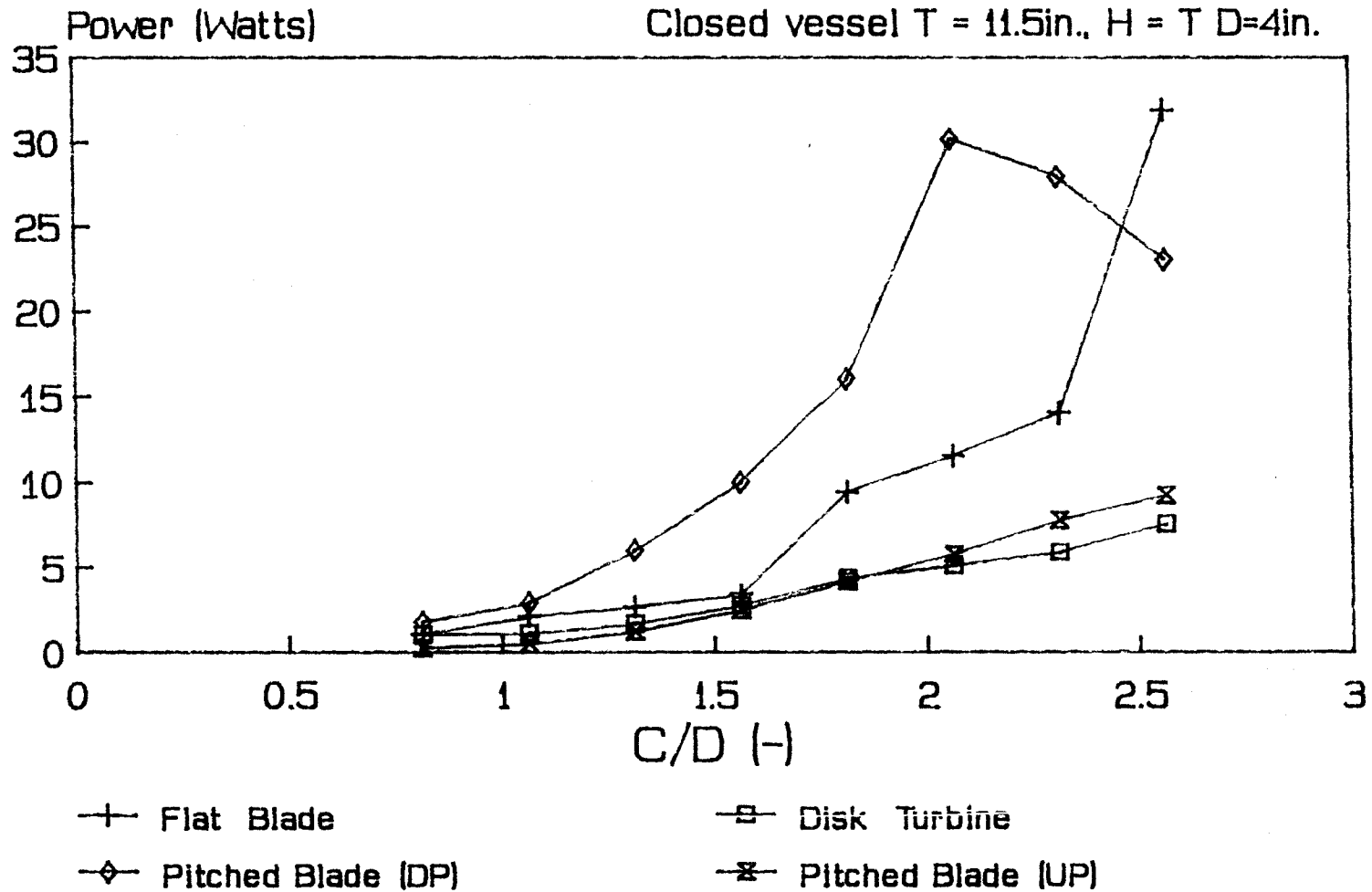


Figure 6.7.5 Effect of C/D ratio on power consumption at N_{js}
 Polypropylene (2105microns, 720Kg/m³) + Water (996Kg/m³)

However, from experimental observations it was noted that for clearances less than $1/3T$ the suspension criteria may easily be satisfied if the impeller is pumping upwards while at the same time distribution in the whole vessel is still very poor (see comments on Appendix A-1). This difference in behavior for the impellers does not depend on the type or size of impeller, or on tank or properties of the fluid/solid phases employed. The same trend was observed in the different vessels used and also for different particle density and sizes. It is because of this observation that the overall process requirement and definition has to be given further consideration in terms of what has been achieved beyond the attainment of the 'just suspended state' remedied. The use of multiple impellers is proposed to alleviate the problem of uneven distribution.

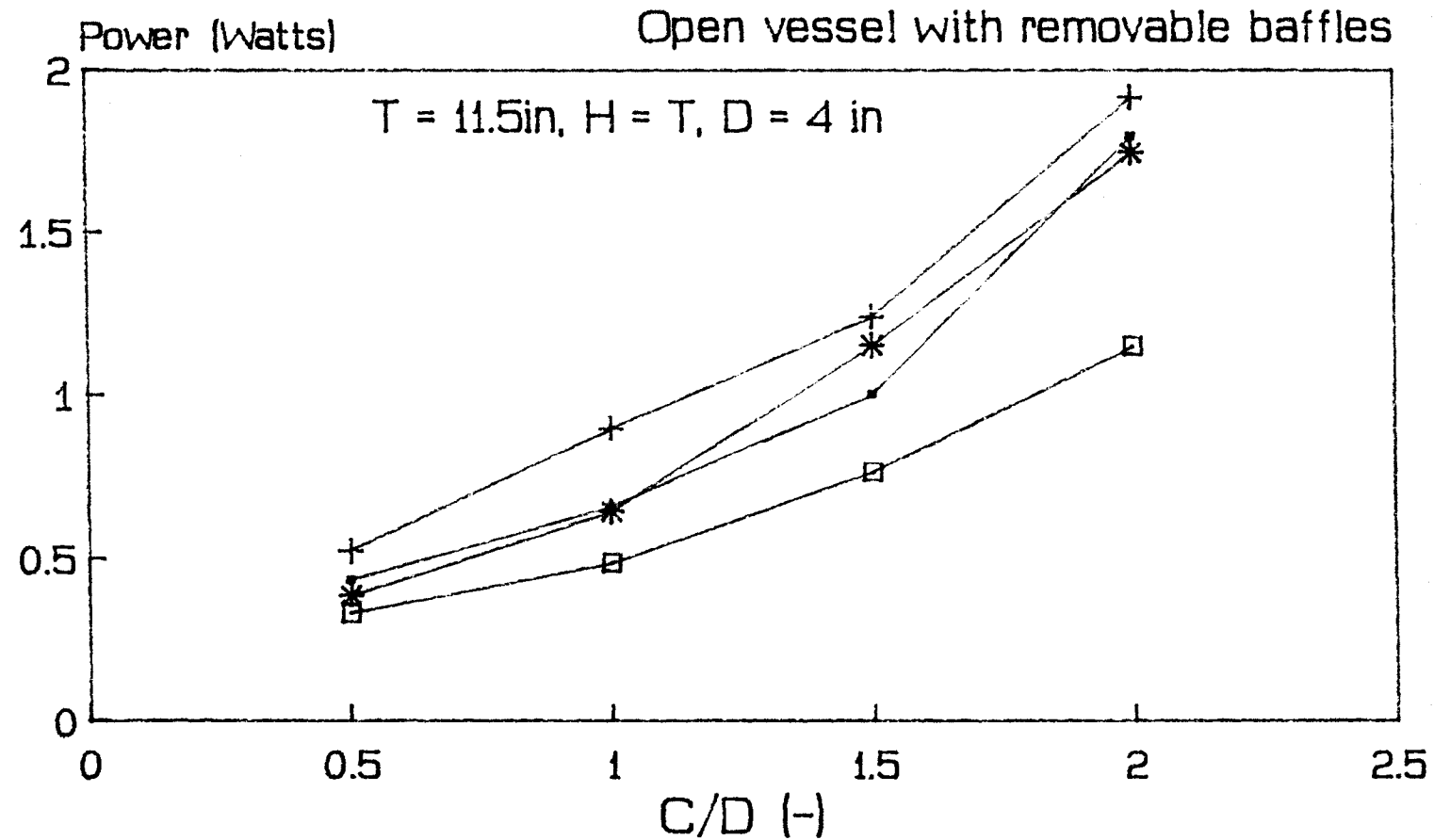
6.8 THE USE OF DIFFERENT BAFFLING SYSTEMS

A number of different baffling systems has been tried to see which one will work best for floating solids drawdown. Table 6.7 shows the systems and the associated notation.

System Baffle notation	Description
4 2/3H	4 baffles extending to 2/3 of the liquid height from the bottom.
3 2/3H & 1F	3 baffles extending to 2/3 of the liquid height from the bottom and 1 full baffle extending over liquid height
2 2/3H & 2F	2 baffles extending to 2/3 of liquid height and 2 full baffles extending over the liquid height.
2 2/3H & 2 1/2H alternating	2 baffles extending to 2/3 of liquid height and 2 baffles covering half the liquid height from the top surface

Table 6.7 Baffling notation

Figure 6.8.1 and 6.8.2 shows the power consumption at N_{js} for different impeller positions and varying number of baffles. It is observed that the system with 4 full baffles has the highest power consumption for all clearance ratios while the configuration with 2 2/3H baffles and 2 1/2 alternating baffles has the least power consumption over the



→ 4 full baffles + 3 full baffles * 2 full baffles □ 1 full baffle
 Figure 6.8.1 Effect of number of baffles on power at N_{js}
 LD Polyethylene (840Kg/m³, $d_p=2200\text{microns}$) / Water (996Kg/m³)

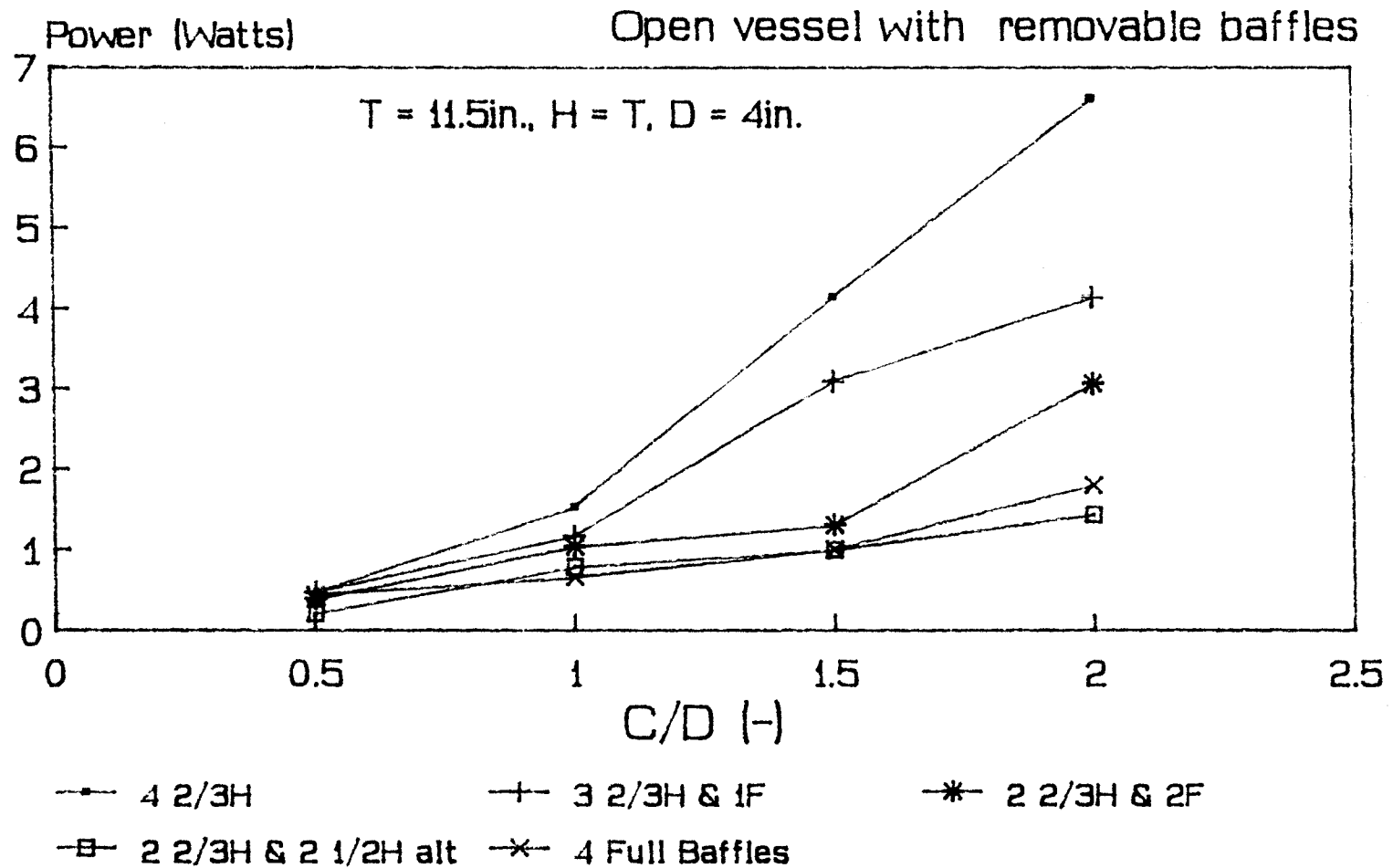


Figure 6.8.2 Power consumption for different baffling systems at Njs LD Polyethylene (840Kg/m³, dp= 2200microns) / Water (996Kg/m)

C/D range studied. Also, the power consumption does not vary as rapidly as it does for the other configurations.

Figures 6.8.3 and 6.8.4 show the corresponding minimum speed required for the selected baffle configurations. Again the 2/3H & 2 1/2H alt. configuration has the lowest minimum speed requirement. It is interesting to note that the curve for 2/3H & 2 1/2H alt. and curve for 4 full baffles do not differ much in terms of power consumption at Njs. From the power curve and speed curve, the former arrangement appears to be preferred.

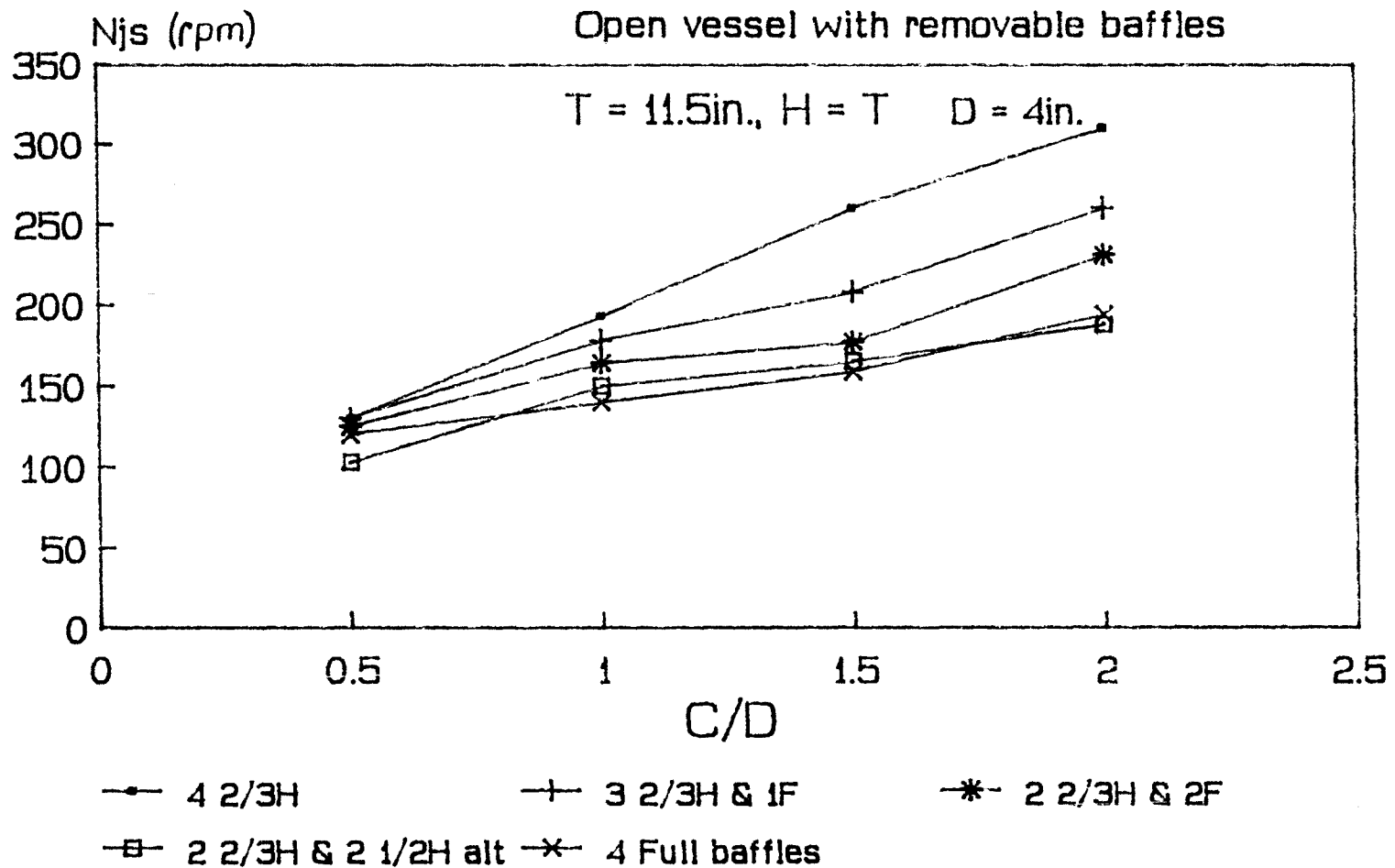


Figure 6.8.3 Njs for different baffling systems

LD Polyethylene (840Kg/m³, dp = 2200microns) / Water

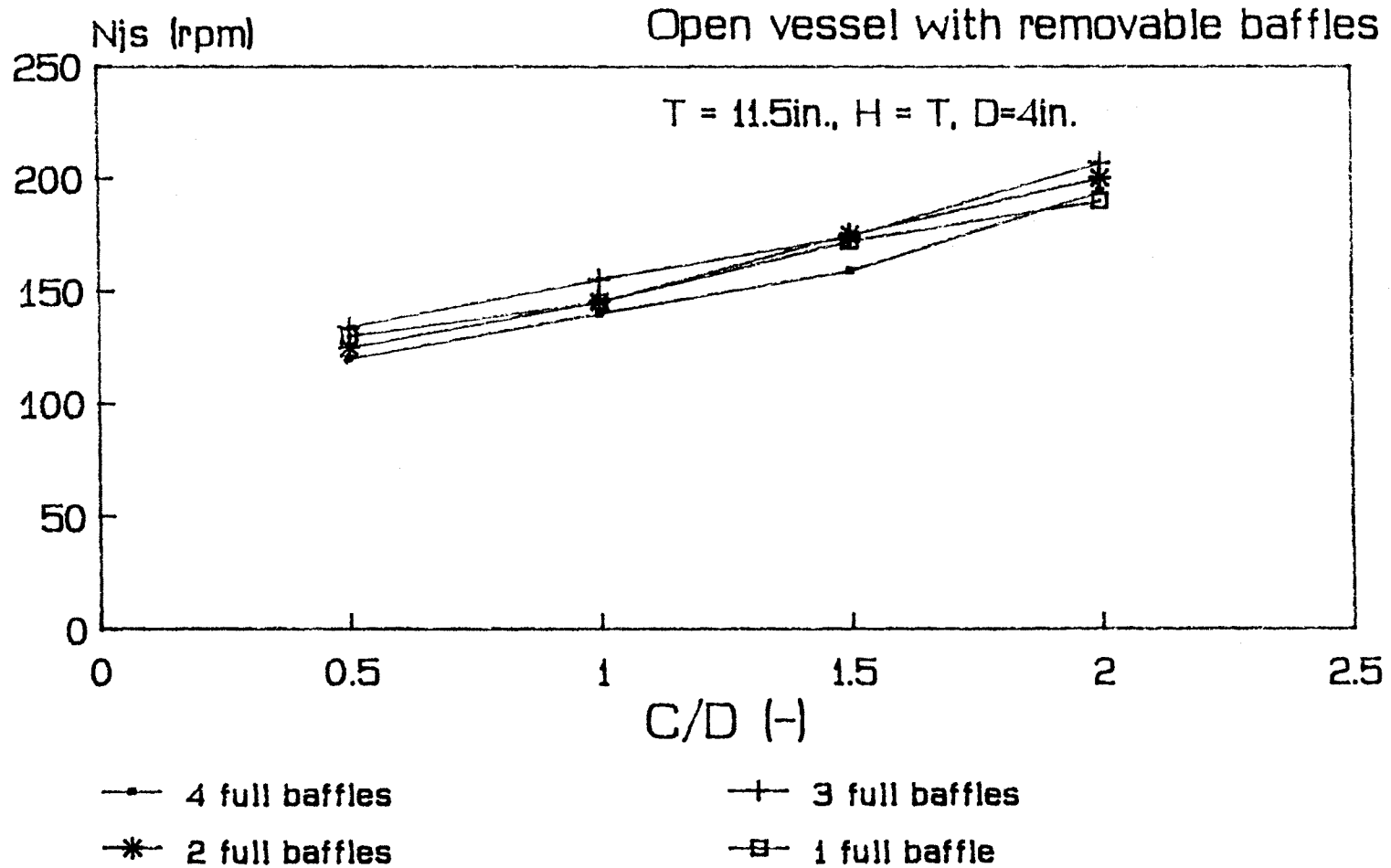


Figure 6.8.4 Effect of number of baffles on N_{js}

LD Polyethylene ($840\text{Kg/m}^3, dp=2200\text{microns}$) / Water (996Kg/m^3)

6.9 THE PROPORTIONALITY PARAMETER Φ

6.9.1 First Approach

As first approach to model the parameter Φ , a simple exponential decay was assumed.

The proposed equation then takes the form

$$N_{js} = \Phi \cdot ((\Delta r/r_1) \cdot g)^{1/2} \cdot \left(\frac{1}{Po} \right)^{1/3} (T^2 \cdot H)^{1/3} \cdot (dp)^{1/6} D^{-5/3} \quad (6.1)$$

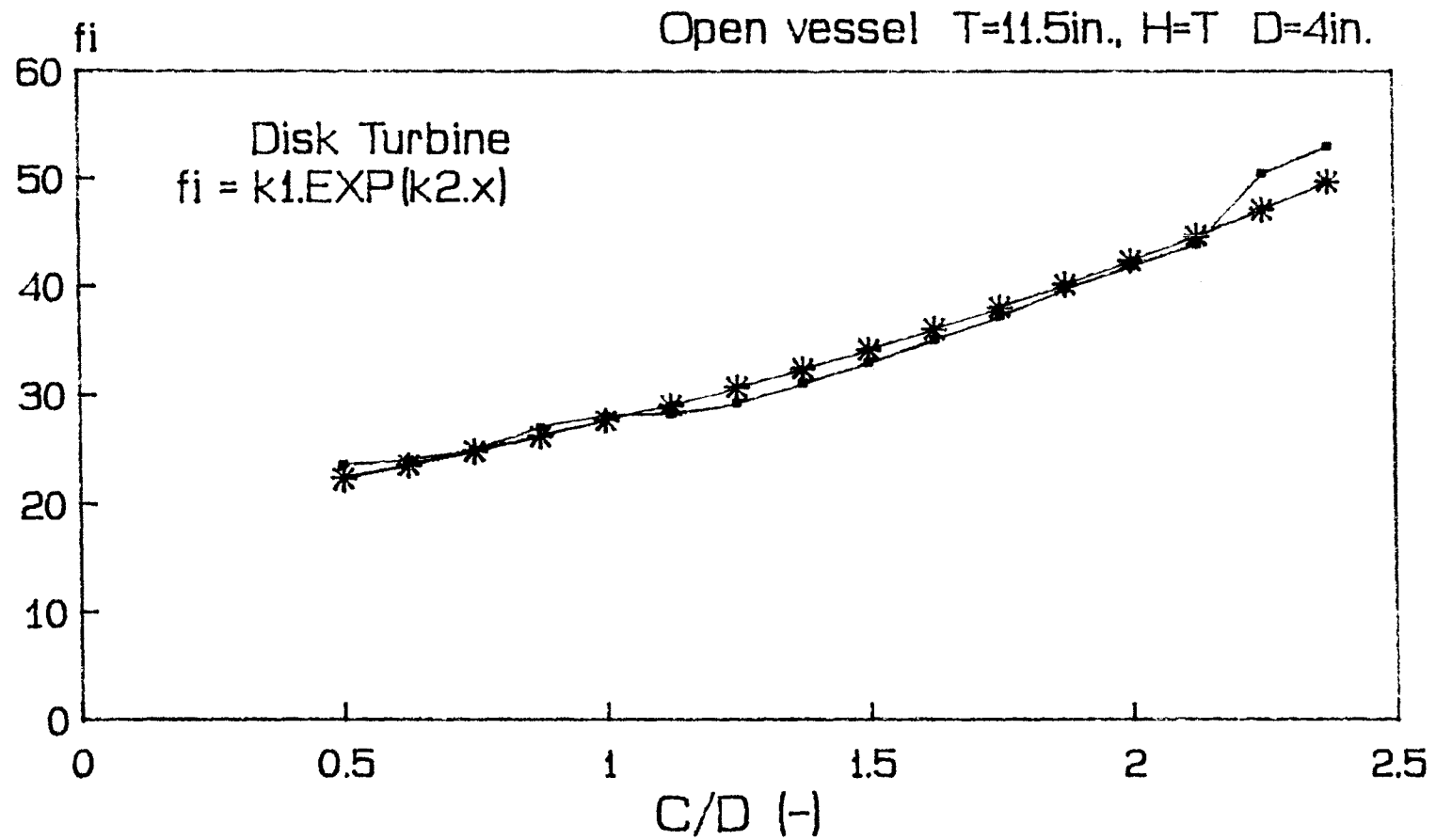
$$\text{with } \Phi = k_1 \cdot \text{EXP}(k_2 \cdot x)$$

Table 6.8 shows the constants k_1 and k_2 for the two optimal impellers for floating solids drawdown used in this work.

Impeller type	x	k1	k2
Disk Turbine	C/D+T/D-1	8.35	0.463
Pitched blade turbine UP	C/D + T/2D	4.56	0.671
Pitched blade turbine DP	3T/D - C/D	2100	-0.517

Table 6.8 Parameters for Φ

Figures 6.9.1 through 6.9.5 show a comparison of the values for the constant Φ as predicted by the equation and the values obtained experimentally. It is evident that the equation predictions are reasonable within the limits of the experimental range covered. However, no general trend can be drawn from the constants, and the constants



—•— experimental
—+— calculated
 Figure 6.9.1 Predicted and experimental values for f_i
 LD Polyethylene (840Kg/m³, dp=2200microns) / Water (996Kg/m³)

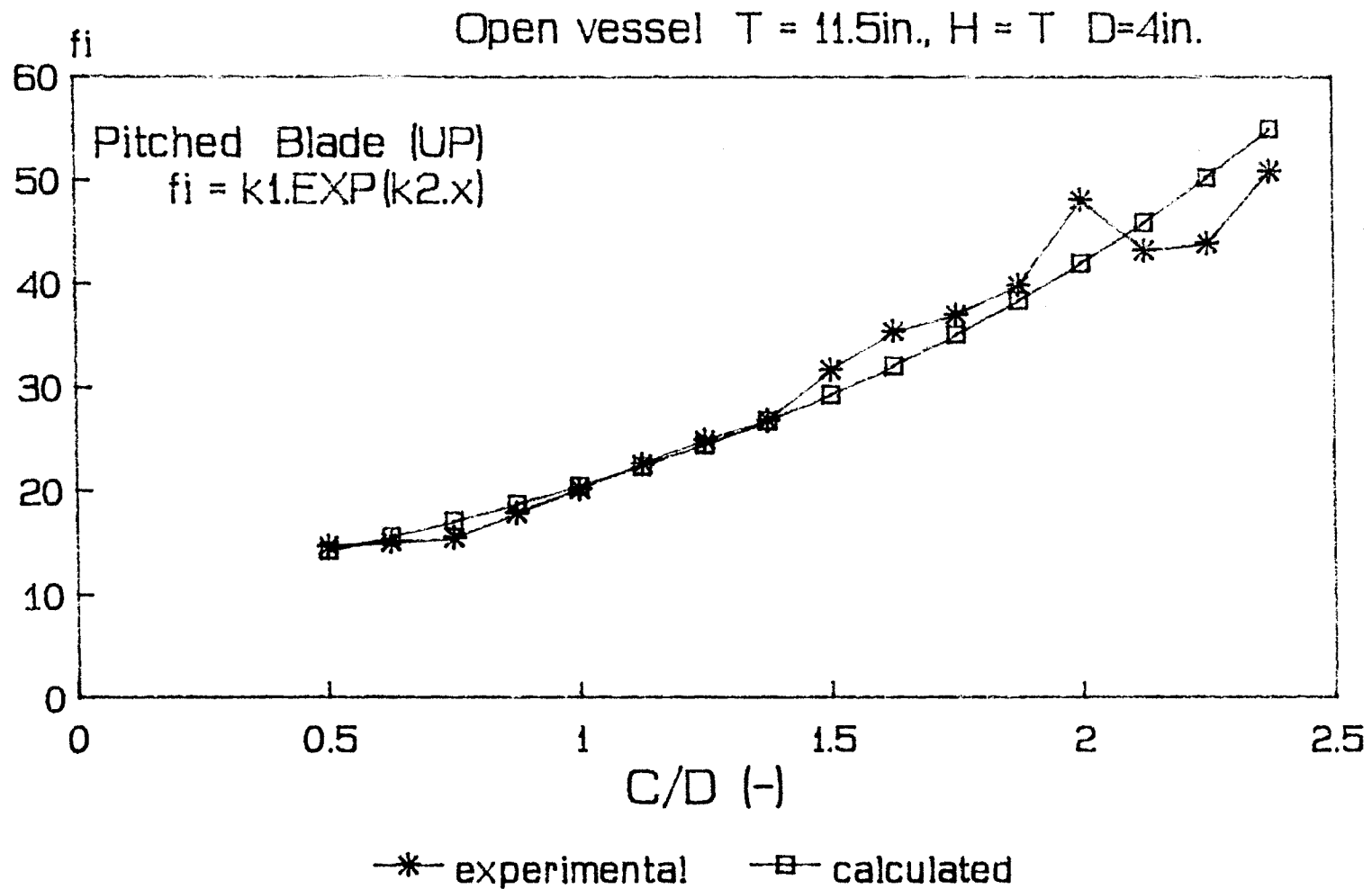
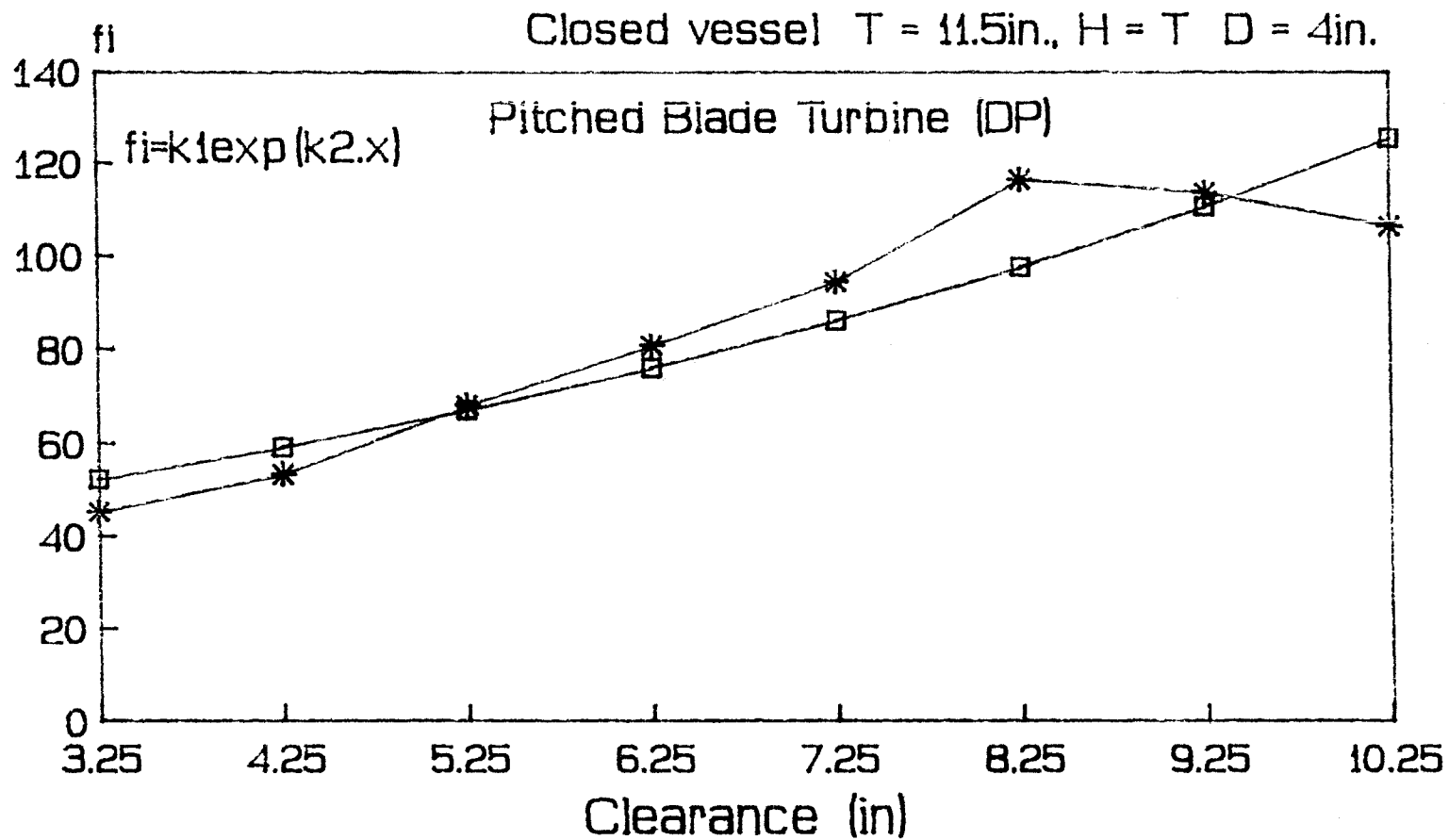


Figure 6.9.2 Predicted and experimental values for f_i
 LD Polyethylene (840Kg/m³, dp=2200microns) / Water (996Kg/m³)



* Experimental □ Calculated

Figure 6.9.4 Predicted and experimental values for
HD polyethylene (897Kg/m³, dp =2205microns) / Water

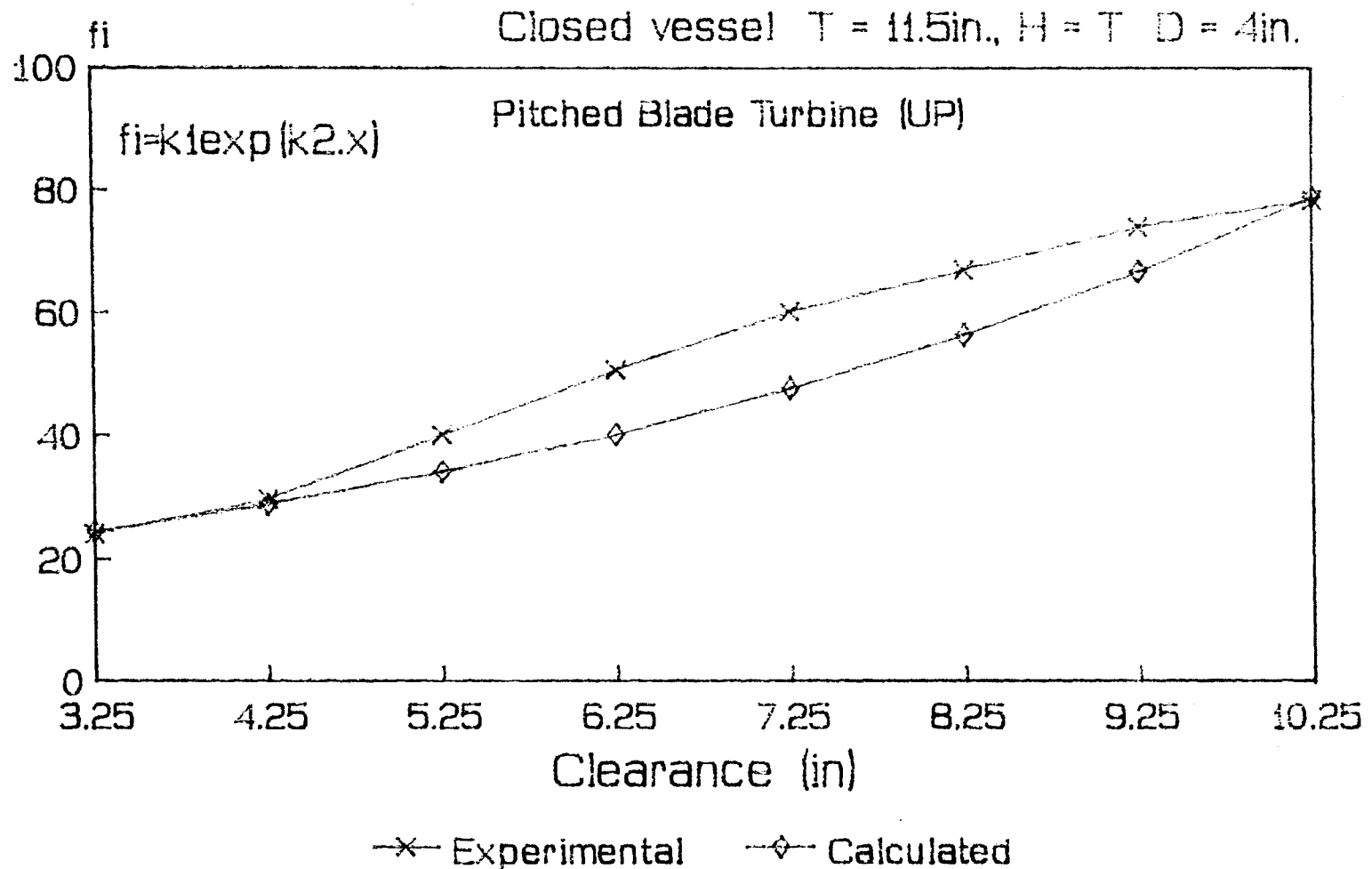


Figure 6.9.5 Predicted and experimental values for
 HD polyethylene (897Kg/m³, dp =2205microns) / Water

for pitched blade turbine pumping downwards seems to be way off the others.

6.9.2 Second Approach

Figure 6.9.6 shows the plot of ϕ vs. simple flow path function (x). It is interesting to note that data for the disk turbine, pitched blade turbine (UP) and flat blade fall within a region of slope 1.4 to 2.1. On the other hand, data for the pitched blade turbine pumping downwards lies on a line of negative slope (-4).

The average values of constants k_1 and k_2 are shown in table 6.9.

Impeller type	k_1	k_2
Disk turbine	7.3	1.35
Pitched blade (UP)	4.1	1.99
Pitched blade (DP)	86909	3.56

Table 6.9 Constants for ϕ using power function

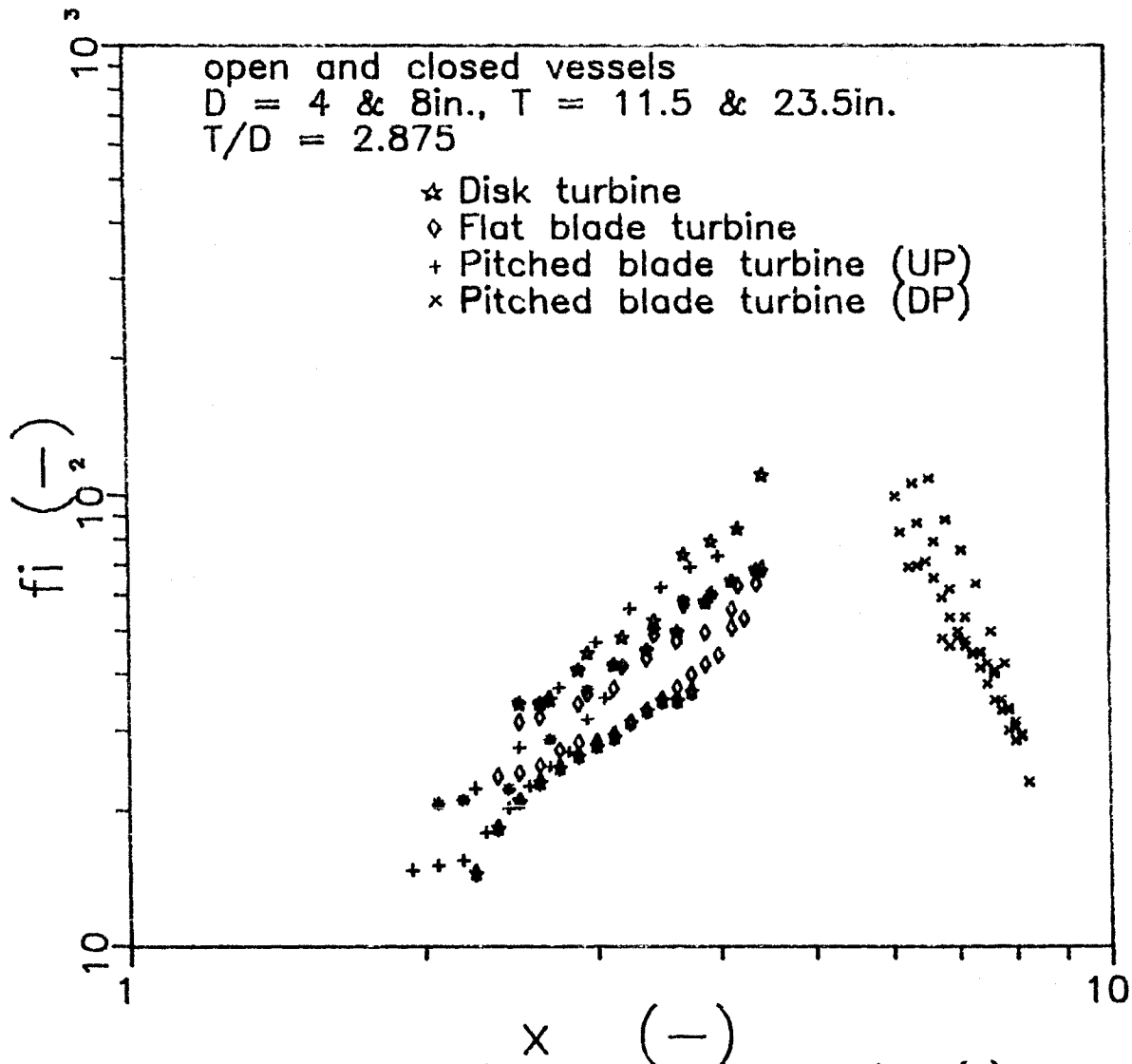


Figure 6.9.6 Plot of f_i vs flow path function (x)
 (using simple flow path function)

Figure 6.9.7 shows the plot of ϕ vs \bar{x} as defined in Table 6.10 and also in Section 3.2.3. This seems to be a better plot than the first approach because the data for pitched blade turbine pumping downwards now shows the same trend as the other impellers, although the value for constants in ϕ are still in their own range.

From experimental observations, the change in the macroscopic flow pattern does not always occur in correspondence of $C/T = 0.71$ (or $C/T = 0.21$ for the upward pumping case) for the pitched blade turbine, as predicted by theory. Therefore, the macroscopic flow path function can be redefined as $\bar{\bar{x}}$, according to the definition in Table 6.10 and Section 3.2.3 where $(C/T)_{crit}$ is the experimentally determined point where the transition in flow pattern occurs.

Figure 6.9.8 shows the same plot using macroscopic flow path ($\bar{\bar{x}}$). This figure shows that almost all the points for the pitched blade turbine (DP) are now grouped together.

Impeller type	Macroscopic flow path function
Disk turbine	$x = C/D + T/D - 1$
Flat blade turbine	$x = C/D + T/D - 1$
Pitched blade turbine (upward pumping)	$x = C/(2D) + T/2$
Pitched blade turbine (downward pumping)	$x = 3T/D - C$
Disk turbine	$\bar{x} = x$
Flat blade turbine	$\bar{x} = x$
Pitched blade turbine (upward pumping)	$\bar{x} = \sqrt{2} \left(\frac{T}{2D} - 1/4 \right) + \left(\frac{C}{D} - \frac{T}{2D} - 1/4 \right) + \frac{T}{2D} \quad \text{for } C/T > 0.29$ $\bar{x} = \sqrt{2} \cdot C/D + \left(\frac{T}{2D} - C/D - 1/4 \right) \quad \text{for } C/T < 0.29$
Pitched blade turbine (downward pumping)	$\bar{x} = \sqrt{2} \left(\frac{T}{D} - C/D \right) + \left(\frac{2T}{D} - 1/4 - C/D \right) \quad \text{for } C/T > 0.71$ $\bar{x} = \sqrt{2} \left(\frac{T}{2D} - 1/4 \right) + \left(\frac{T}{D} + C/D \right) - 1/4 \quad \text{for } C/T < 0.71$
Disk turbine	$\bar{\bar{x}} = x$
Flat blade turbine	$\bar{\bar{x}} = x$
Pitched blade turbine (upward pumping)	$\bar{\bar{x}} = \sqrt{2} \left(\frac{T}{2D} - 1/4 \right) + \left(\frac{C}{D} - \frac{T}{2D} - 1/4 \right) + \frac{T}{2D} \quad \text{for } C/T > (C/T)_{\text{crit. UP}}$ $\bar{\bar{x}} = \sqrt{2} \cdot C/D + \left(\frac{T}{2D} - C/D - 1/4 \right) \quad \text{for } C/T < (C/T)_{\text{crit. UP}}$
Pitched blade turbine (downward pumping)	$\bar{\bar{x}} = \sqrt{2} \left(\frac{T}{D} - C/D \right) + \left(\frac{2T}{D} - 1/4 - C/D \right) \quad \text{for } C/T > (C/T)_{\text{crit. DP}}$ $\bar{\bar{x}} = \sqrt{2} \left(\frac{T}{2D} - 1/4 \right) + \left(\frac{T}{D} + C/D \right) - 1/4 \quad \text{for } C/T < (C/T)_{\text{crit. DP}}$

Table 6.10 Macroscopic flow path functions

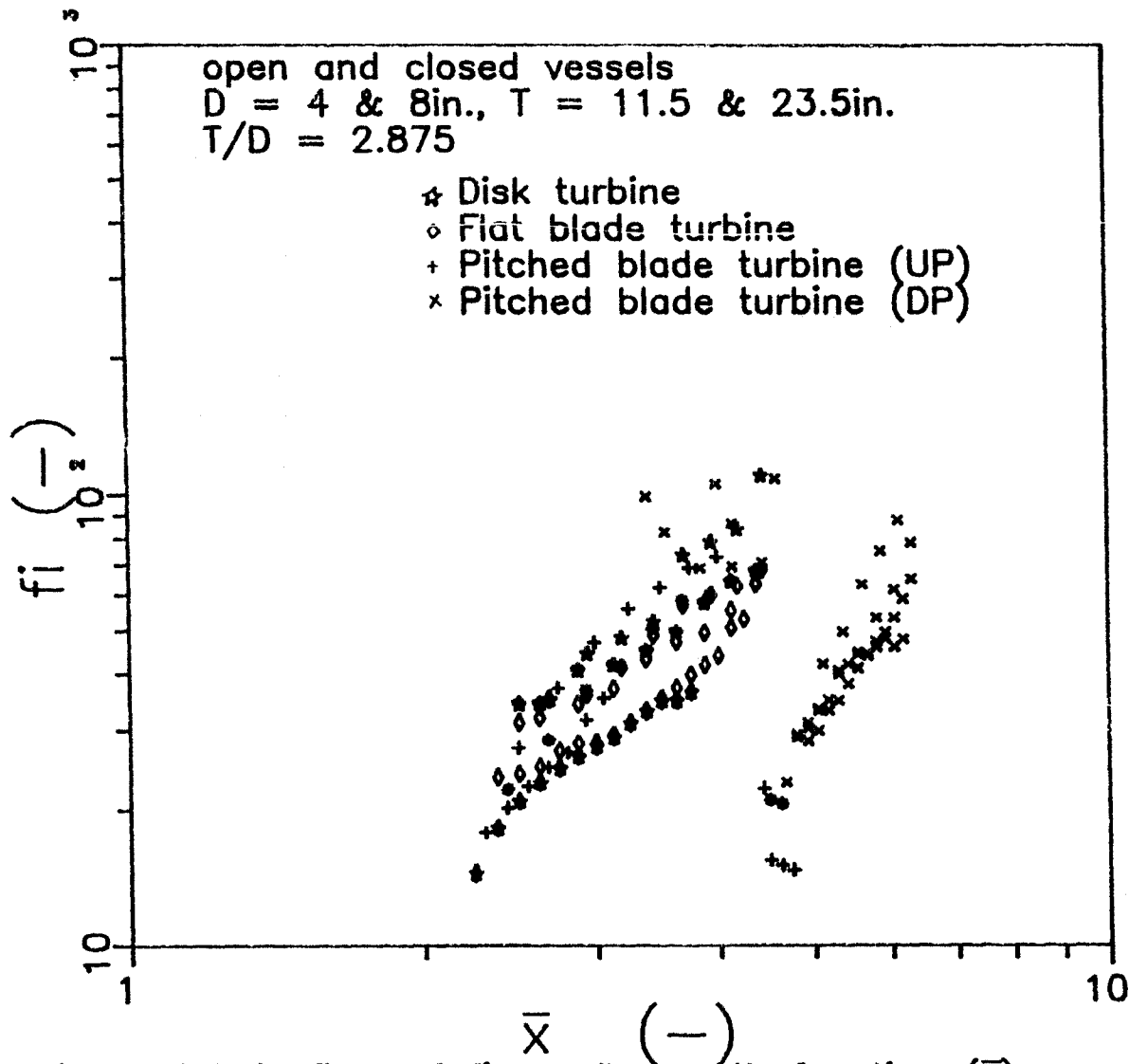


Figure 6.9.7 Plot of f_i vs. flow path function (\bar{x})
 (flow path modified according to theory)

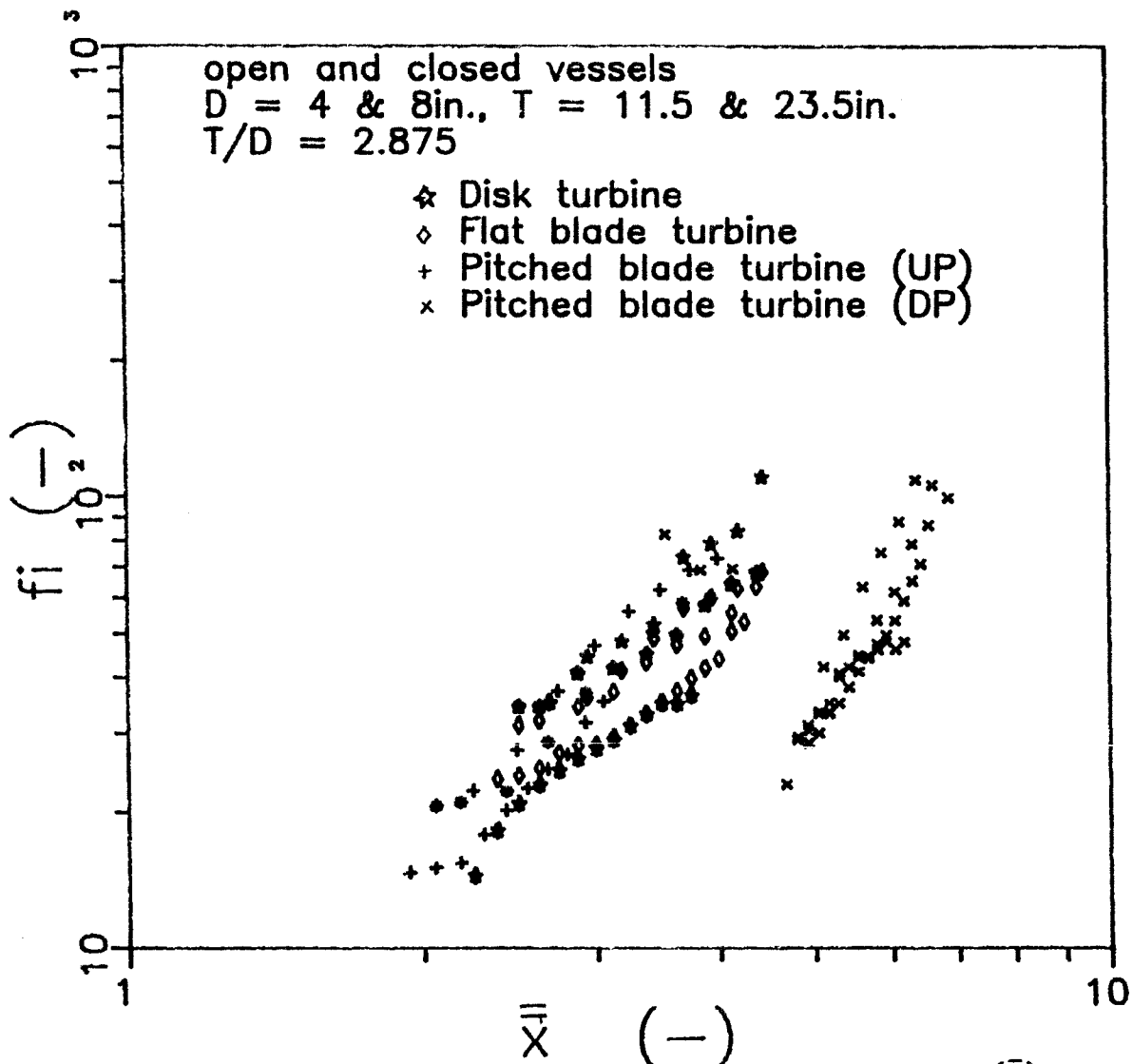


Figure 6.9.8 Plot of f_i vs. flow path function (\bar{X})
 (flow path modified at actual transition points)

6.10 VESSEL DRAW-OFF EFFECTS

Figure 6.10.1 shows a plot of the minimum speed for just suspended state against the liquid height in a vessel. Here the impeller clearance varied as more liquid was removed and the liquid level in the tank decreased. It is clear from the graph that, as liquid height in a vessel changes, the speed required to satisfy the process requirements also changes.

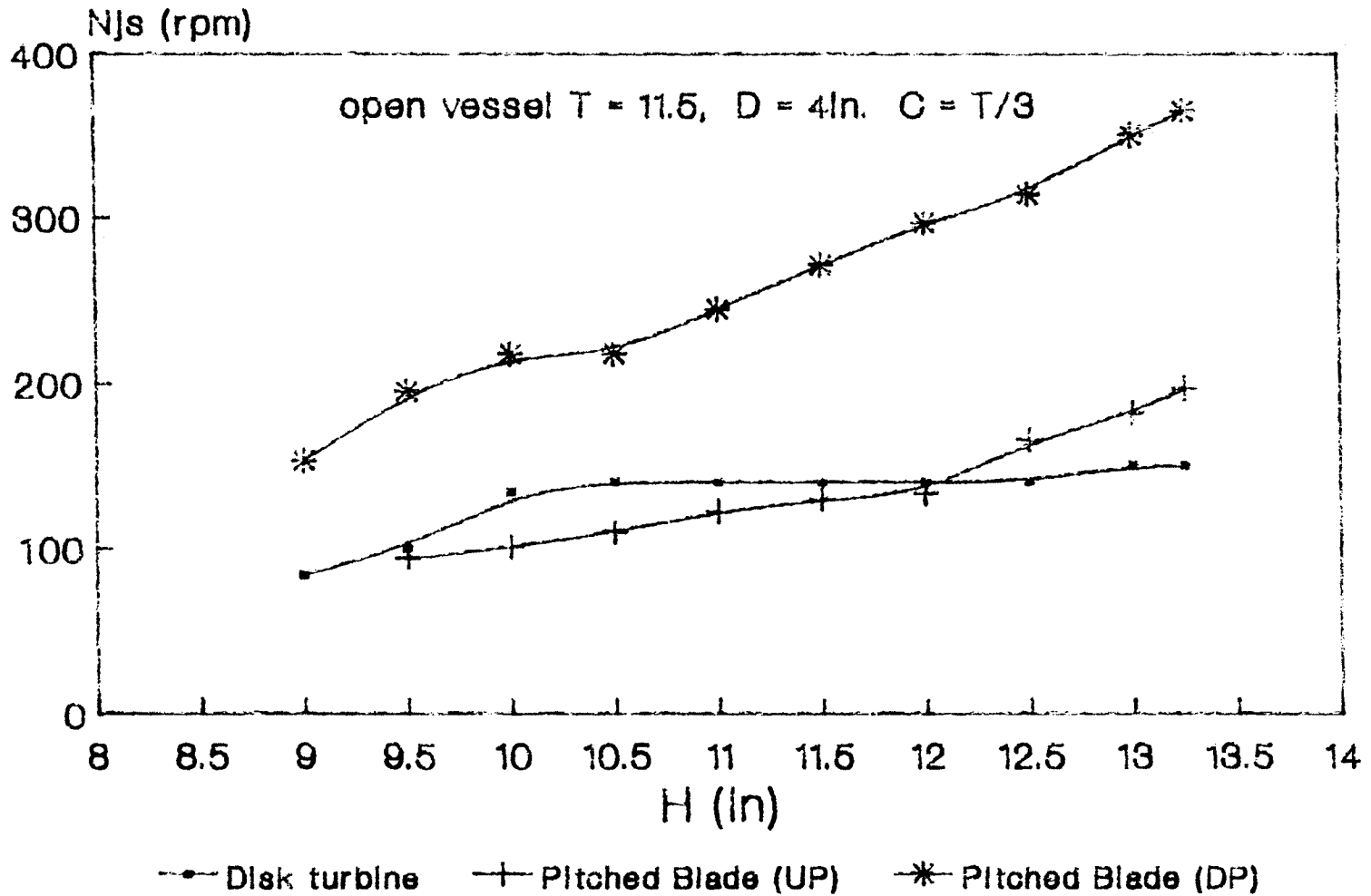


Figure 6.10.1 Effect of vessel draw-off on Njs

LD Polyethylene (840Kg/m³, dp = 2200microns) / Water(996Kg)

6.11 COMPARISON OF OPEN AND CLOSED VESSELS

Figures 6.11.1 through 6.11.5 shows the comparison minimum drawdown speed in closed vessel and open vessel for different impellers used. It is observed that for density differences ratios less than 0.3 the difference in minimum drawdown speed for the two situations is not significant, considering a margin of error in the observed minimum drawdown speed (2 to 5%). However, for larger differences in density and/or for large particle sizes, (Figures 6.11.6 through 6.11.8) the difference is significant. Experimental observations reveal that, in order to drawdown particles in this range, more agitation is required to overcome the surface effects which come into play.

For the case where high agitation levels are required, the floating solid-liquid system becomes a three phase situation, where the entrapped air is the third phase, playing a significant role in determining the ease or difficulty in particle drawdown. For the case of small particle sizes, surface tension effects may also come into play if the particles are partially immersed. The use of a closed vessel enabled the exclusion of such effects, if any.

These observations are in agreement with the experimental evidence obtained by Bruining and Frijlink [5] in the drawdown of particles in this regime. The probable reason that made these investigators not able to come up

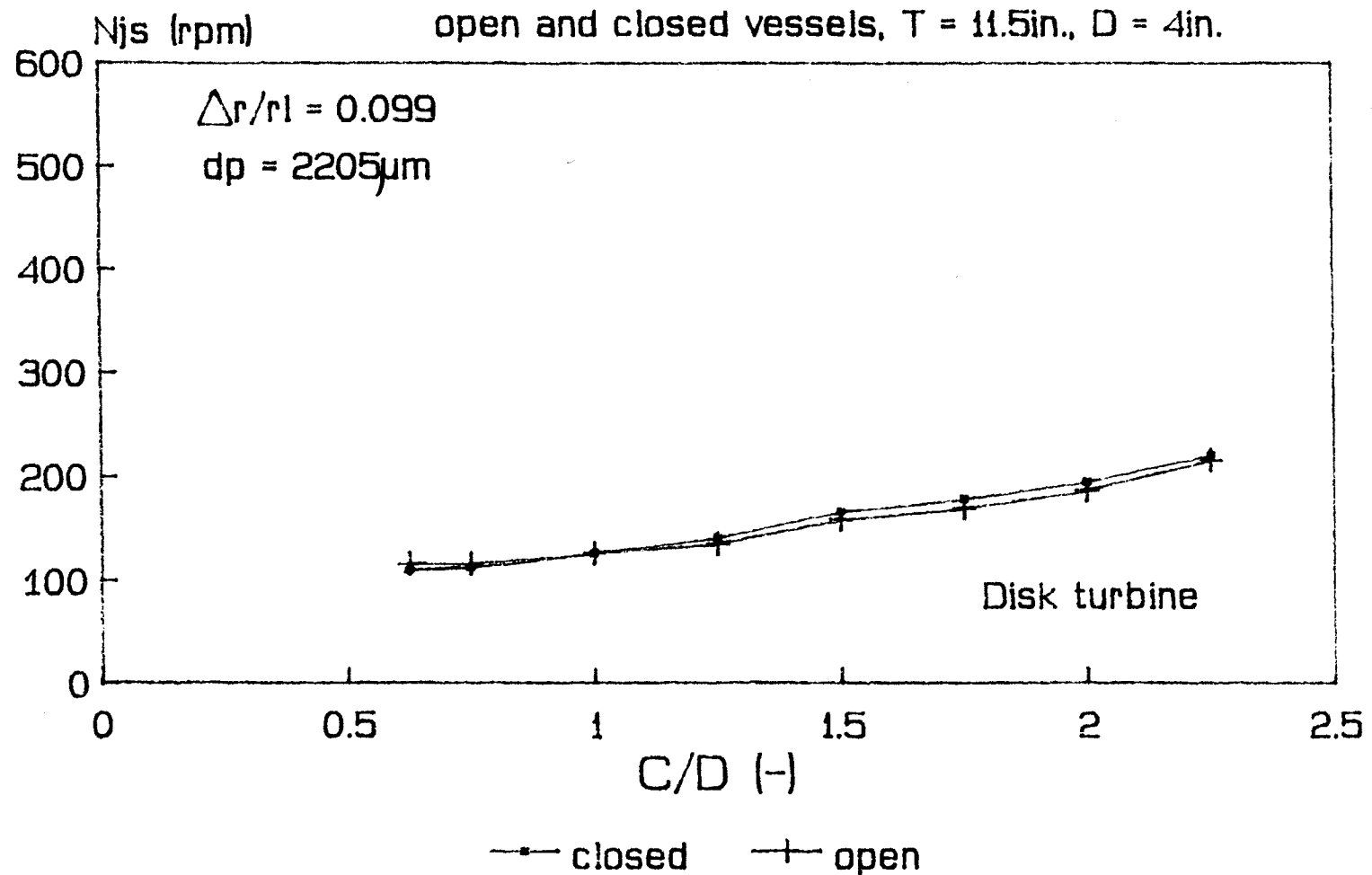


Figure 6.11.1 Comparison of N_{js} for open and closed vessels
 System: HD Polyethylene (897kg/m³, $dp=2205$ microns) / Water

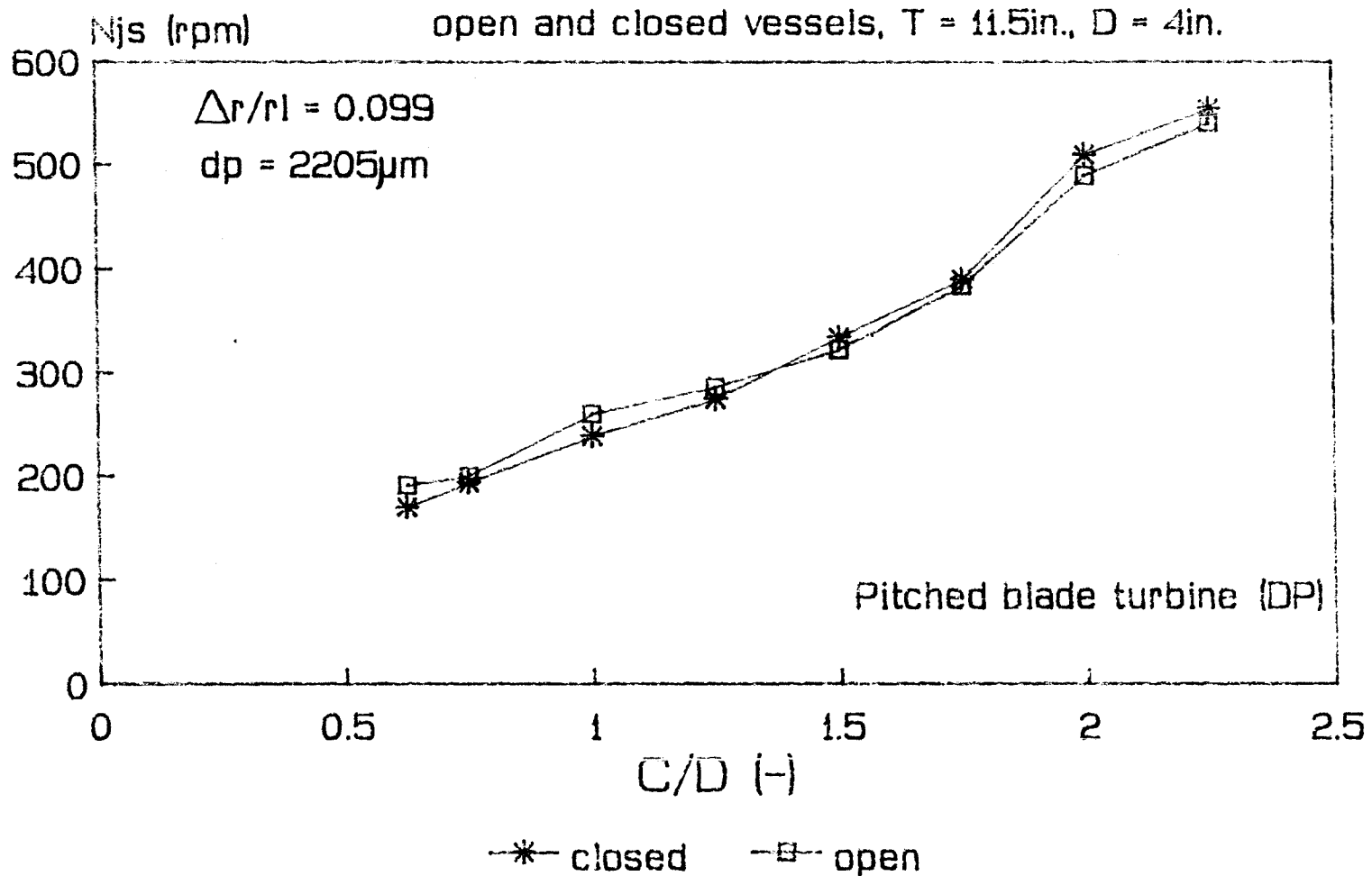


Figure 6.11.2 Comparison of N_{js} for open and closed vessels
 System: HD Polyethylene (897kg/m³, dp=2205 microns)/ Water

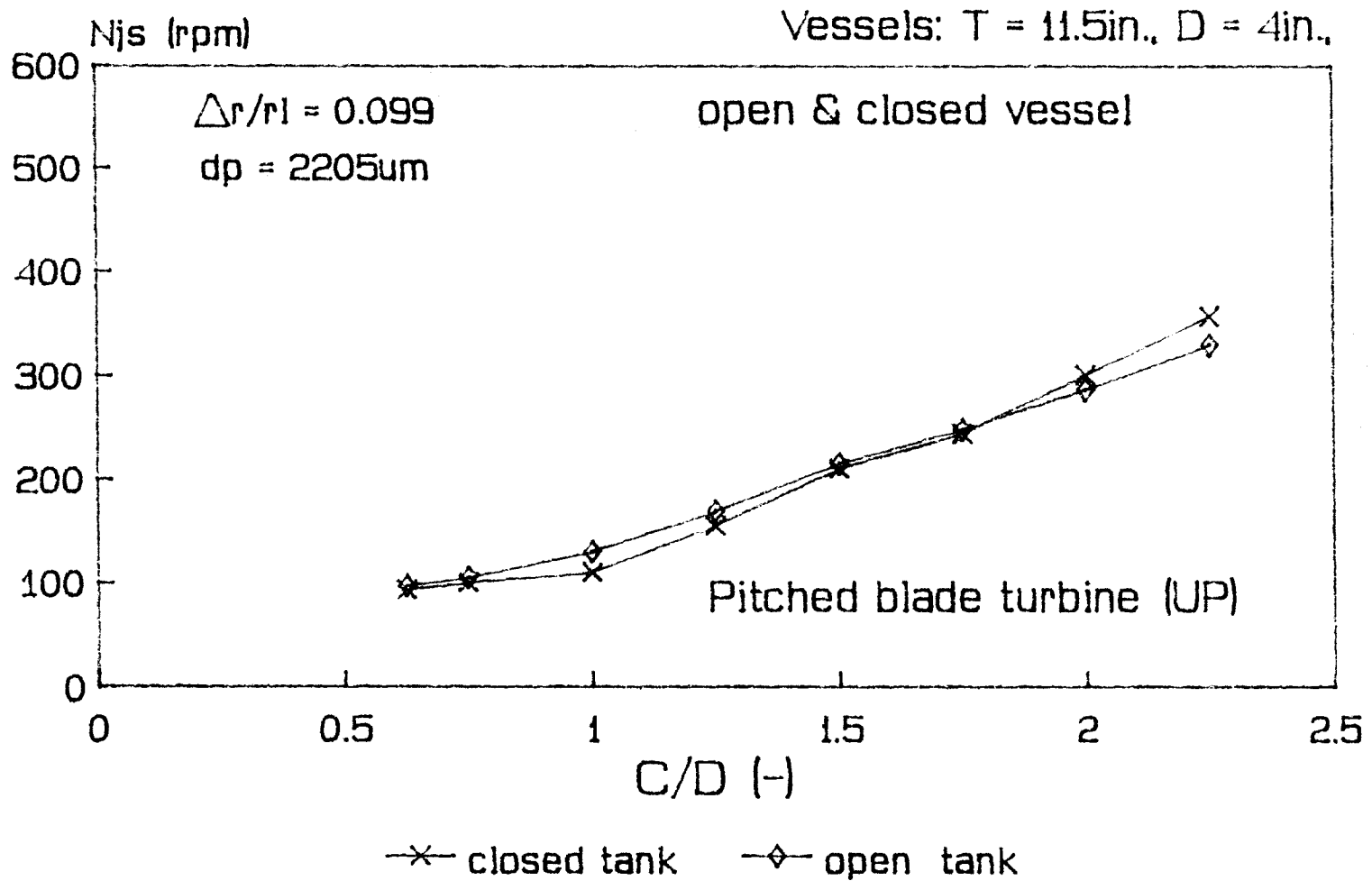


Figure 6.11.3 Comparison of N_{js} for open and closed vessel

System: Hd Polyethylene (897kg/m³, $dp = 2205$ microns) / Water

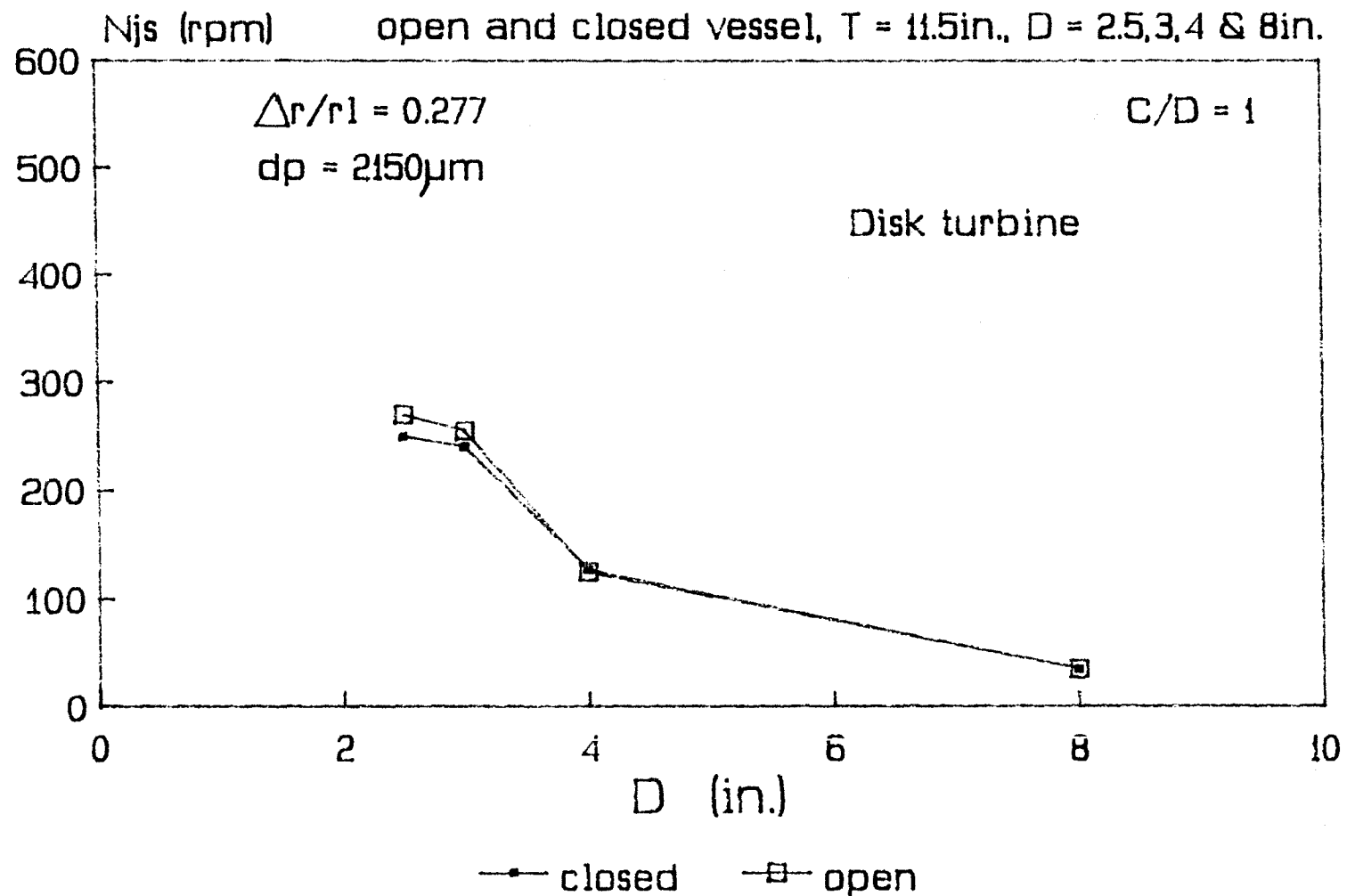


Figure 6.11.4 Plot of D vs. Njs for open and closed vessels
 System: Polypropylene (720kg/m³, dp=2150microns) / water

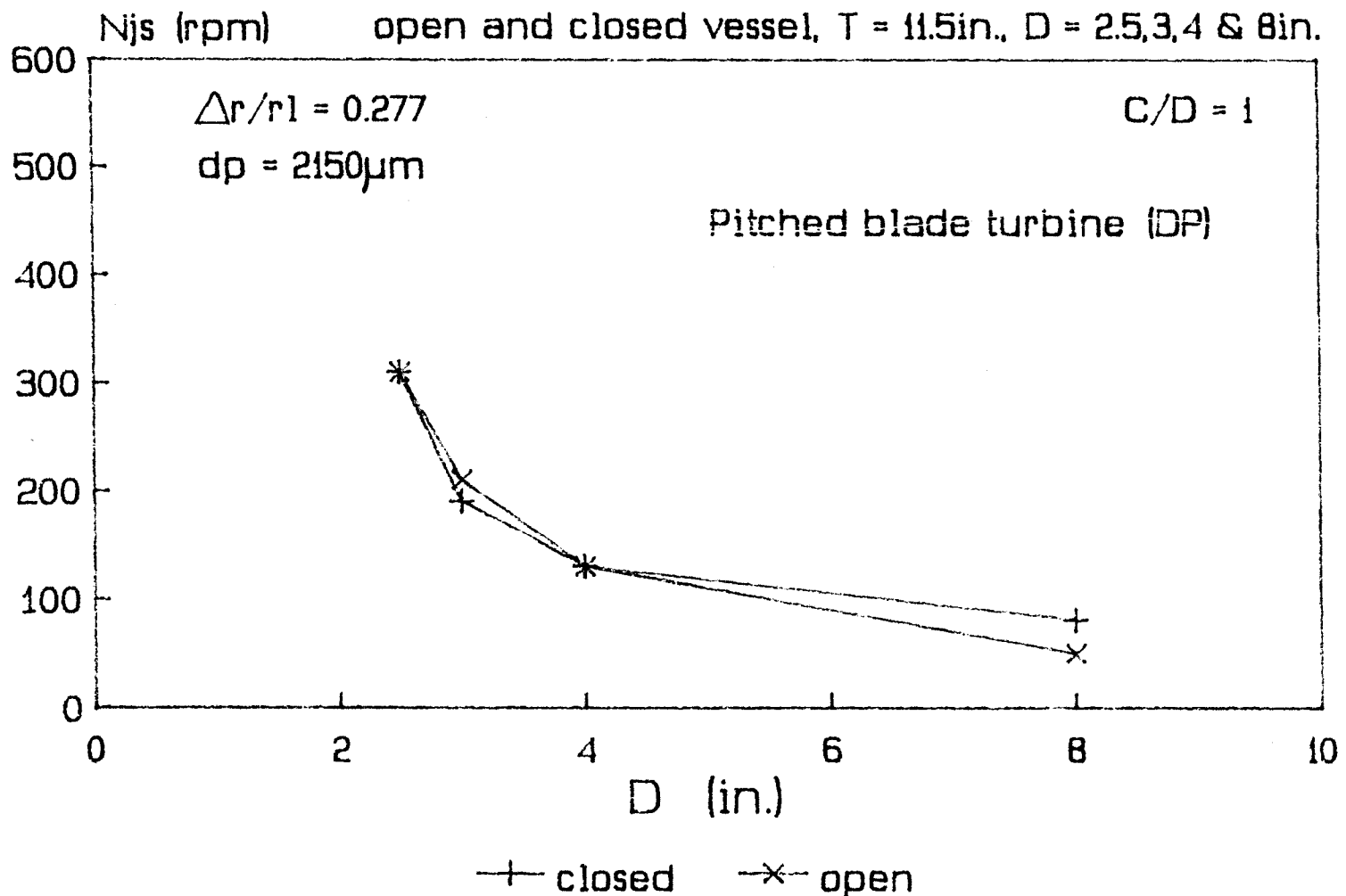


Figure 6.11.5 Plot of D vs. Njs for open and closed vessels
 System: Polypropylene (720kg/m³, dp=2150microns) / water

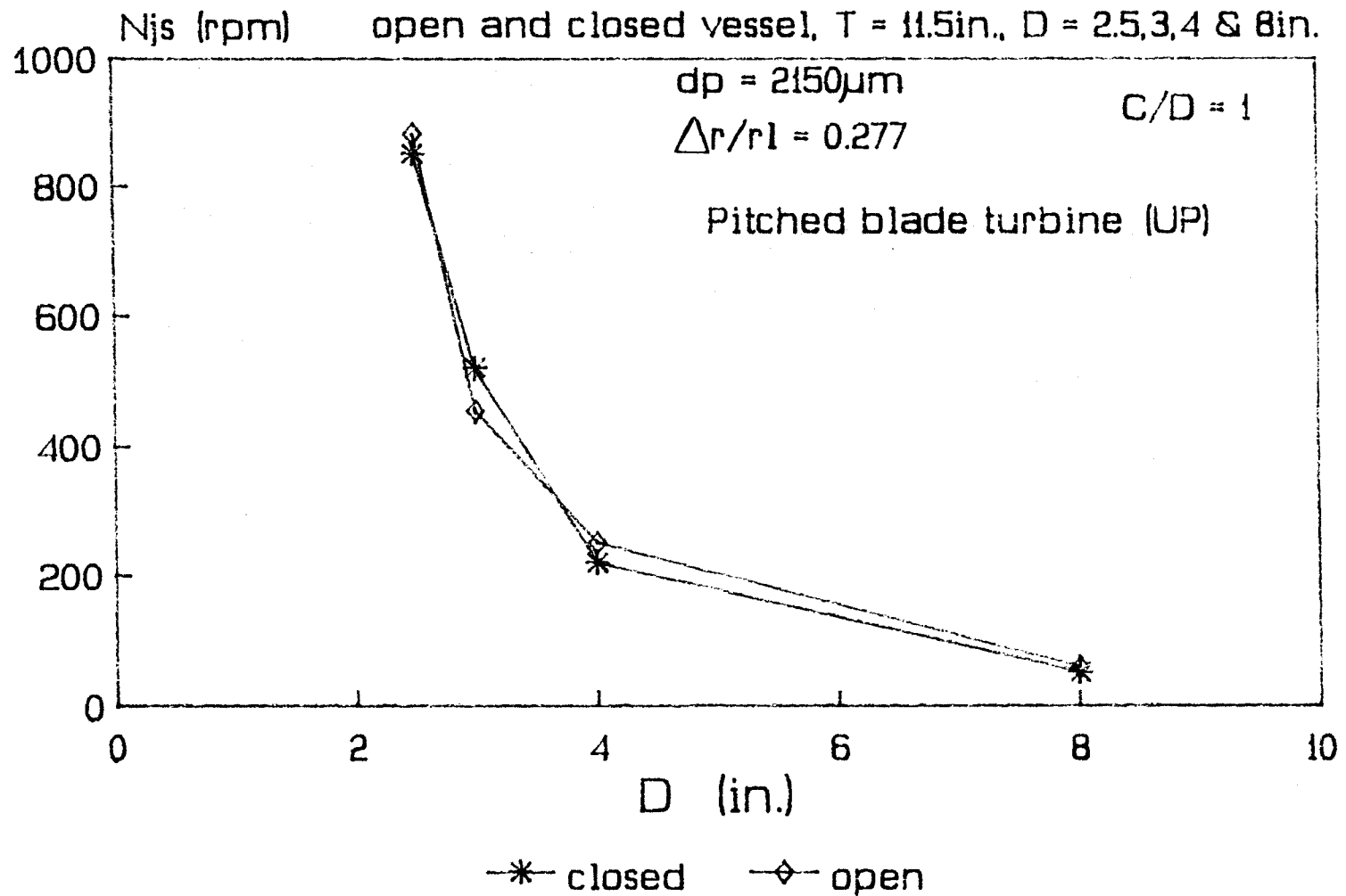


Figure 6.11.6 Plot of D vs. Njs for open and closed vessels
 System: Polypropylene (720kg/m³, dp=2150microns) / water

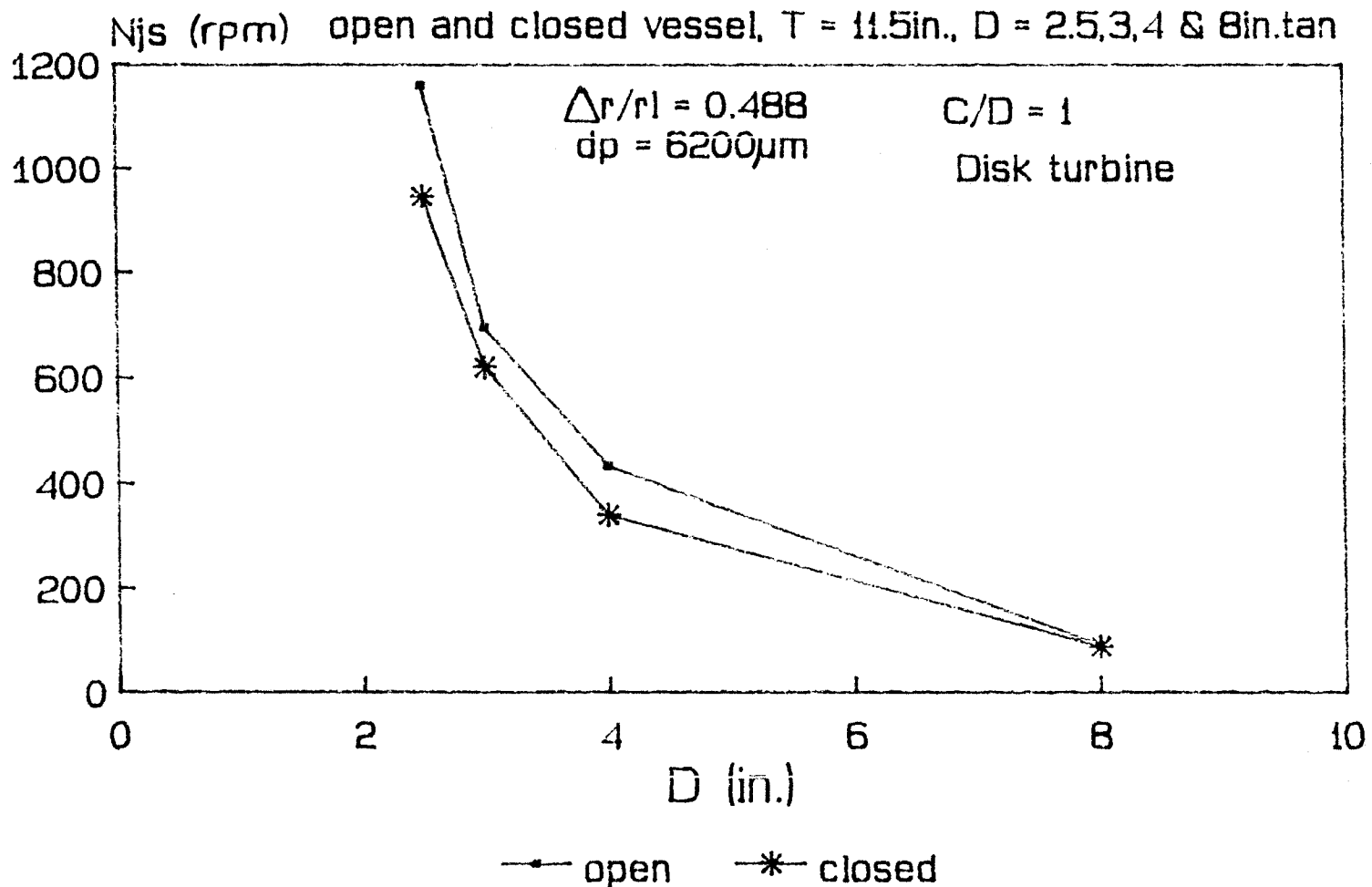


Figure 6.11.7 Plot of D vs. Njs for open and closed vessels
 System : Cork (density=510Kg/m³), dp =6200microns) / Water

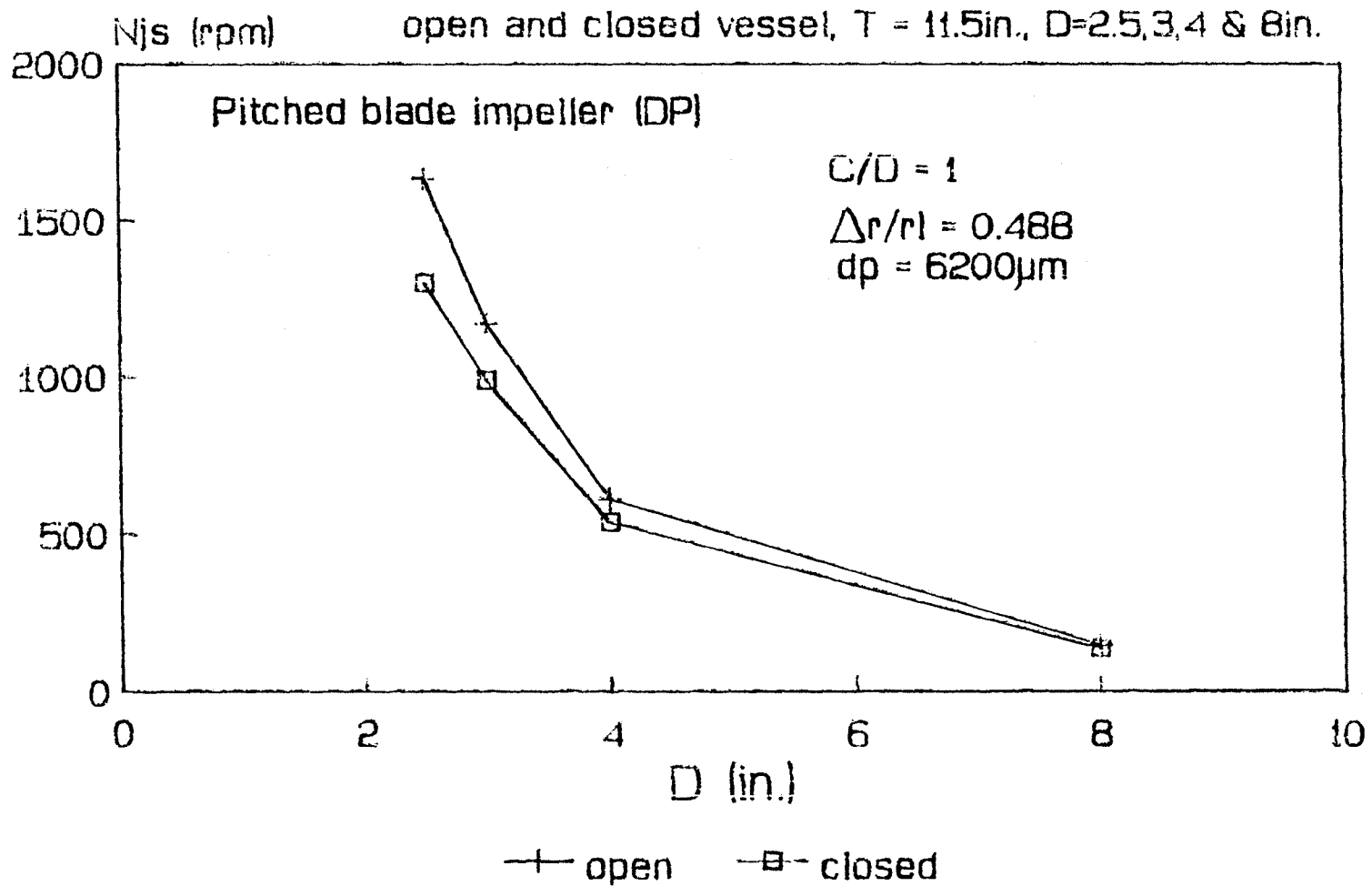


Figure 6.11.8 Plot of D vs. Njs for open and closed vessels

System : Cork (density=510Kg/m³), dp =6200microns) / Water

with a correlation is that they did not distinguish these two regimes, and their experiments were done in both.

The distinction of these regimes is the first step towards the achievement of a better model for floating solids drawdown.

CHAPTER 7

CONCLUSIONS AND RECOMMENDATIONS

7.1 CONCLUSIONS

- 1 A model has been derived and experimentally shown to be able to predict the minimum speed for drawdown of floating solids within the range of experimental values.
- 2 There is a noticeable similarity between floating solids drawdown and settling solids suspension for small density difference ranges ($0 - 300\text{kg/m}^3$) and medium particle sizes ($300-2500\mu\text{m}$).
- 3 The derived model can be compared to Baldi's equation [8] for settling solids suspension in the range specified above.
- 4 Drawdown of floating solids with particles size less than $300\mu\text{m}$ and/or density differences greater than $500\mu\text{m}$ produces a three phase dispersion with the inclusion of air sucked-in from the liquid free surface due to high impeller speeds. In this case, vortex formation dominates the particle drawdown mechanism. Since the proposed equation does not account for such mechanisms, the proposed equation loses its validity in this regime.
- 5 The 45° pitched blade turbine (6-blade) pumping upwards is more efficient in drawing floating particles when situated at clearance of $1/2 T$ of the air/liquid interface.

- 6 The disk turbine (6-blade) is most favored when placed at a clearance of $1/3T$ from the air/liquid interface.
- 7 Cylindrical tanks with flat bottom and partial baffles have the best performance in floating solid drawdown.
- 8 The position of the impeller plays a major role in particle drawdown. An impeller placed close to the floating solids requires less power consumption than an impeller placed close to the tank bottom.
- 9 The pumping direction for axial impellers has an influence on the minimum required speed and the power consumption even though there is no change in the power number.
- 10 The equations previously proposed (e.g. by Joosten et al. (1977)) seem to be valid for a fixed impeller clearance and do not account for some important aspects of the floating solids drawdown mechanism.
- 11 The drawdown of floating solids is affected by the solid concentration in the liquid at high particle concentrations.
- 12 The type of impeller used has a major effect on both the minimum drawdown speed and the power consumption as observed by previous investigators both in floating solids drawdown and settling solids suspension.
- 13 From experiments done with open and closed tanks, surface tension effects do not affect the requirements for drawdown when density difference is small and the particle size range is medium.

- 14 However, when particle size and/or density difference is large, there is a significant difference between results from open and closed vessels.
- 15 Change in the level of the liquid in a vessel affects the minimum required speed.
- 16 Baffle configuration does have an effect on the minimum drawdown speed and the associated power consumption.

7.2 RECOMMENDATIONS FOR FUTURE WORK

It is recommended to continue this work with extensive examination of the turbulent flow field in order to get a clear insight of particle drawdown when three phase system is involved. More insight is required to be able to understand the particle-liquid interaction. Computational analysis and numerical techniques can be explored to model fluid particleinteraction.

The use of a Laser Doppler technique to monitor the fluctuating velocities can be attempted.

CHAPTER 8

NOMENCLATURE

Symbol	Description	Units
A	Area	m^2
A'	Submerged area	m^2
C	Clearance	m
c'	Constant in Equation 2.1	-
ci	Constants in Equation 4.1	-
D	Impeller diameter	m
d	Distance	m
dp	Particle diameter	m
F_B	Buoyancy force	N
H	Liquid height	m
Fr	Froude's number	-
g	Acceleration due to gravity	$m.s^{-2}$
k1,k2	Constants in Equation 3.21	-
L	Length	m
m	Mass	Kg
M	Torque	N.m
N	Impeller speed	s^{-1}
Njs	Impeller speed at just drawdown state	s^{-1}
p	Constant in Equation 2.1	-
P	Power consumption	Watts
Po	Power number	-

q	Constant in equation 2.1	-
R	Radius	m
Re	Reynolds number	-
r	Density	Kg.m^{-3}
r_l	Liquid density	Kg.m^{-3}
r_s	Solid density	Kg.m^{-3}
T	Tank diameter	m
\hat{u}'	Root mean square fluctuating velocity	m.s^{-1}
v'	Fluctuating velocity	m.s^{-1}
V	Volume	m^3
V_s	particle volume	m^3
V'_1	Volume of displaced fluid	m^3
x	Macroscopic flow path function	m
\bar{x}	Macroscopic flow path function (modified for transition points)	m
$\bar{\bar{x}}$	Macroscopic flow path function (modified at critical points only)	m
Greek letters		
β	Universal function (eqn. 6.3)	-
Φ, f_i	Constant in equation (3.19a)	-
τ	Shear stress	N.m^{-2}
η	Kolmogoroff's length scale	m
ν	Kinematic viscosity	m^2s^{-1}
μ	Viscosity	Ns.m^{-2}
ϵ	Energy dissipation rate unit per unit mass	N.m.kg^{-1}

Subscripts

min.	minimum
max.	maximum
js	just suspended

APPENDIX A-1

STATES OF SUSPENSION

VARYING SPEED AT CONSTANT CLEARANCE

SYSTEM: Polypropylene (720kg/m³, dp=2150μm) / WaterClosed vessel T = 11.5in. (29.12cm) (996kg/m³)

D = 4in. (6.54cm)

FLAT BLADE TURBINE

C = 1/3T

SPEED (rpm)	OBSERVATION / COMMENTS
0	All particles sitting at the top
20	"
100	Very slight disturbance at the bottom of the floating mass of solids
115	1 or 2 particles move down 1 - 2 cm and come back once in a while
120	1 particle drawn down to the impeller once in a while.
140	Disturbance increases
150	3 to 5 particles drawn down to the impeller and thrown down to the bottom zone. All particles go back to the top. Downward journey along impeller axis while upward journey along side wall.
160	The few particles drawn down lingers a

little longer in the upper zone

170 Still bulk of the particles stationary at the top.

200 More disturbance. More particles drawn down at any point in time there are particles in suspension. Still more particle concentration at the top. Particles at the surface are still stationary.

220 More particles drawn down. Top layer stationary.

300 Larger percentage of particles in motion. Still non uniform. Accumulation spots the the surface near baffles (Figure A-1.1)

400 More suspension. Still some stationary spots on the surface.

500 Agitation more vigorous in the middle and bottom zone.

550 Drawdown more or less complete.

600 Further increase in speed does not really affect the distribution now, although there are still some stationary spots created by the baffles.

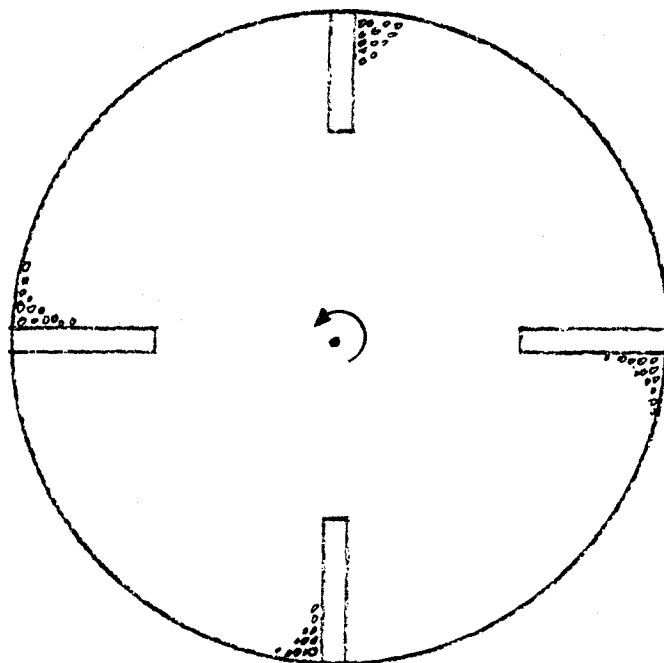


Figure A-1.1 Vessel top view showing accumulation spots

PITCHED BLADE TURBINE(DP)

$$C = 1/3T$$

SPEED (rpm)	OBSERVATION / COMMENTS
0	Nothing
100	"
175	"
200	One particle shooting out and back (very occasional) practically nothing happens.
250	2 - 3 particles shooting out. Mostly do not reach the impeller but are pushed back to the top. One particle may succeed to go past the impeller zone but gets back in no time.
300	Occasional 'shocks' at the bottom of the pile. some particles manage to travel down as a result of the shock. When such a particle gets near the impeller pumping zone it is thrown to the region below the impeller and can make some swirls up and down between the impeller and the bottom before being swept to the top again.
350	Particles swept down seems to come from specific locations at the top. Some particles remain in suspension.

400 More disturbance. Still a lot of particles are stagnant at the top, but particles drawn into the turbulent zone are somewhat well distributed.

500 Greater part of the material has been drawn down into 'system'.

600 Some particles are still stationary at the top

730 Complete drawdown criteria satisfied

DISK TURBINE

$$C' = 1/3T$$

SPEED (rpm)	OBSERVATION / COMMENTS
0	Everything still
100	2 to 3 particles drawn down and back. clusters of 2 to 4 particles forming.
130	Random draw down. No particular path for going down or up
140	More particles drawn into the upper zone. 1 or 2 particles going down into the lower zone and back (fast).
200	More disturbance. A lot of particles in the middle zone. Particles at the plane of the e impeller and below it are moving at a higher velocity. The surface is still stationary.
300	90% homogeneity. Some spots at the top are still stationary (around the shaft and on one side of the baffles (Fig. A-1.2)
400	Complete drawdown criteria satisfied

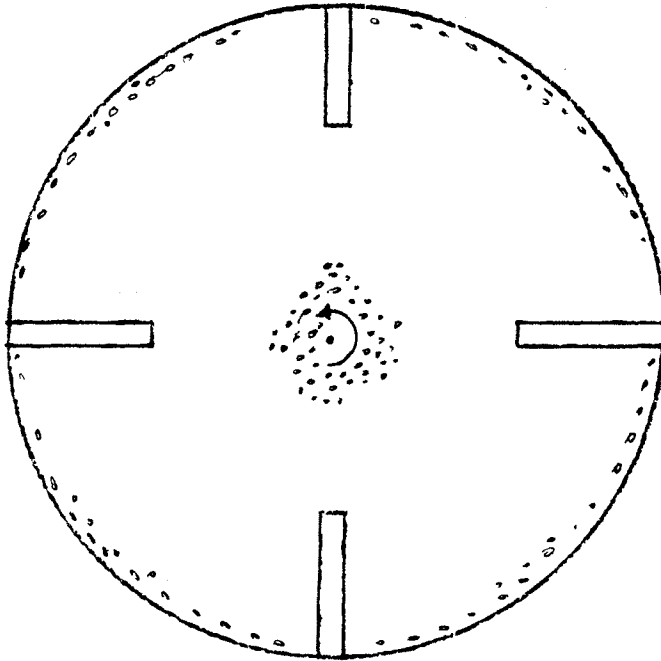


Figure A-1.2 Accumulation spots

DISK TURBINE

$$C = 1/3T$$

SPEED (rpm)	OBSERVATION / COMMENTS
0	Nothing
80	Slight disturbance
100	More particles drawn down
150	More dissipation beyond the impeller. Particles travel up to 2/3 of the area bellow impeller. Top surface still stationary.
200	More disturbance. Still non-uniform. stationary layer at the very top
300	Uniform suspension except for a layer around the impeller at the top. (maybe a vortex could help this down)
400	At this speed all particles are in suspension, not because of vortex but heavy recirculation currents formed.

PITCHED BLADE TURBINE (UP)

$$C' = 1/3T$$

SPEED (rpm)	OBSERVATION / COMMENTS
0	Nothing
160	A single particle shooting out and back
200	2 - 3 particles shooting out regularly. Particles at the top pile rearranges. agglomeration towards the center. (Figure A-1.3)
250	Number of particles drawn down increases.
300	More particles going into the 'bulk'
500	More and more particles in suspension
600	Some spots of stationary material still at the top but the distribution is quite uniform. Further increase in speed causes instability in the vessel leading to spillage.

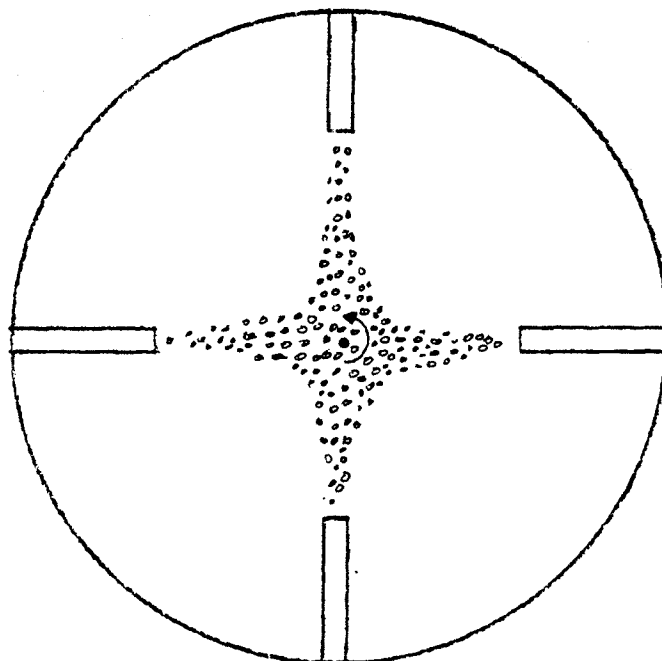


Figure A-1.3 Particles swept towards the center

FLAT BLADE TURBINE

$$C = 1/3T$$

SPEED	OBSERVATION / COMMENTS
0	Nothing
100	Very slight disturbance
160	Disturbance. Some particles are drawn down while the rest tend to agglomerate towards the axis.
200	More disturbance
300	High disturbance. Not many particles reach the bottom. Some particles still cling to the axis.
400	More or less homogeneous distribution (say 90%) More speed causes instability.

PITCHED BLADE TURBINE (DP)

$$C = 1/3T$$

SPEED (rpm)	OBSERVATION / COMMENTS
0	Nothing
65	Slight disturbance
100	Disturbance. particles drawn down up to the middle of the vessel. Particles remaining at the top are pushed to the walls (opposite effect to flat blade).
150	More or less half ground play. Baffles seems to be the cause of stagnant zones.
200	Good distribution for about 2/3 of vessel from top
250	Same distribution as at 200 rpm but more vigorous.
300	Good distribution for 80% of vessel. Bottom no good.
above	Increase in speed causes instability and spillage

PITCHED BLADE TURBINE (UP)

$$C = 1/3T$$

SPEED (rpm)	OBSERVATION / COMMENTS
0	Nothing
100	Still nothing happens
120	Slight disturbance
150	Agglomeration pattern different. Heavy concentration on the sides of the baffles and at the shaft axis
200	Half the particles still sitting at the top
300	Near complete distribution, but some agglomeration near baffles.
400	Good distribution 80%
500	Excellent distribution

APPENDIX-A2

DATA BANK #1

LEGEND:

- 1: DISK TURBINE
- 2: FLAT BLADE
- 3: PITCHED BLADE (DOWNWARD PUMPING)
- 4: PITCHED BLADE (UPWARD PUMPING)

SYSTEM : HIGH DENSITY POLYETHYLENE / WATER

OPEN TANK

RUN	dp	rs	rl	T	D	C/T	TYPE	N	Emf
#	μm	kg/m^3	kg/m^3	cm	cm	-	-	rpm	mV
1	2205	897	996	29.21	6.54	1/3T	1	400.0	34
2	2205	897	996	29.21	7.62	1/3T	1	251.0	34
3	2205	897	996	29.21	10.1	1/3T	1	139.0	37.5
4	2205	897	996	29.21	20.3	1/3T	1	37.5	56
5	2205	897	996	29.21	6.54	1/2T	1	495.0	41.5
6	2205	897	996	29.21	7.62	1/2T	1	325.0	43
7	2205	897	996	29.21	10.1	1/2T	1	195.5	54.5
8	2205	897	996	29.21	20.3	1/2T	1	41.8	60
9	2205	897	996	29.21	6.54	1/3T	2	549.0	34.5
10	2205	897	996	29.21	7.62	1/3T	2	331.0	33
11	2205	897	996	29.21	10.1	1/3T	2	185.0	35
12	2205	897	996	29.21	20.3	1/3T	2	57.0	75
13	2205	897	996	29.21	6.54	1/2T	2	848.0	52
14	2205	897	996	29.21	7.62	1/2T	2	441.0	40

Run #	dp	rs	rl	T	D	C/T	TYPE	N	Emf
15	2205	897	996	29.21	10.1	1/2T	2	315.0	70
16	2205	897	996	29.21	20.3	1/2T	2	54.5	70
17	2205	897	996	29.21	6.54	1/3T	3	907.0	40
18	2205	897	996	29.21	7.62	1/3T	3	639.0	45
19	2205	897	996	29.21	10.1	1/3T	3	259.0	42
20	2205	897	996	29.21	20.3	1/3T	3	36.0	35
21	2205	897	996	29.21	6.54	1/2T	3	1412.0	62
22	2205	897	996	29.21	7.62	1/2T	3	930.0	70
23	2205	897	996	29.21	10.1	1/2T	3	400.0	60
24	2205	897	996	29.21	20.3	1/2T	3	55.0	56
25	2205	897	996	29.21	6.54	1/3T	4	330.0	26
26	2205	897	996	29.21	7.62	1/3T	4	228.0	26
27	2205	897	996	29.21	10.1	1/3T	4	147.0	27.5
28	2205	897	996	29.21	20.3	1/3T	4	56.0	53.5
29	2205	897	996	29.21	6.54	1/2T	4	605.0	31
30	2205	897	996	29.21	7.62	1/2T	4	450.0	33
31	2205	897	996	29.21	10.1	1/2T	4	261.0	39
32	2205	897	996	29.21	20.3	1/2T	4	83.0	94
33	2100	897	996	29.21	6.54	1/3T	1	397.0	34
34	2100	897	996	29.21	7.62	1/3T	1	249.0	33
35	2100	897	996	29.21	10.1	1/3T	1	138.0	37
36	2100	897	996	29.21	20.3	1/3T	1	37.0	56
37	2100	897	996	29.21	6.54	1/2T	1	491.0	41
38	2100	897	996	29.21	7.62	1/2T	1	322.0	43
39	2100	897	996	29.21	10.1	1/2T	1	194.0	54

Run #	dp	rs	rl	T	D	C/T	TYPE	N	Emf
40	2100	897	996	29.21	20.3	1/2T	1	41.0	41.5
41	2100	897	996	29.21	6.54	1/3T	2	545.0	34
42	2100	897	996	29.21	7.62	1/3T	2	328.0	33
43	2100	897	996	29.21	10.1	1/3T	2	184.0	35
44	2100	897	996	29.21	20.3	1/3T	2	57.0	57
45	2100	897	996	29.21	6.54	1/2T	2	841.0	51.5
46	2100	897	996	29.21	7.62	1/2T	2	437.0	40
47	2100	897	996	29.21	10.1	1/2T	2	312.0	70
48	2100	897	996	29.21	20.3	1/2T	2	54.0	70
49	2100	897	996	29.21	6.54	1/3T	3	900.0	40
50	2100	897	996	29.21	7.62	1/3T	3	634.0	44.5
51	2100	897	996	29.21	10.1	1/3T	3	257.0	42
52	2100	897	996	29.21	20.3	1/3T	3	36.0	35
53	2100	897	996	29.21	6.54	1/2T	3	1401.0	62
54	2100	897	996	29.21	7.62	1/2T	3	922.0	69.5
55	2100	897	996	29.21	10.1	1/2T	3	397.0	60
56	2100	897	996	29.21	20.3	1/2T	3	55.0	56
57	2100	897	996	29.21	6.54	1/3T	4	327.0	27
58	2100	897	996	29.21	7.62	1/3T	4	226.0	27
59	2100	897	996	29.21	10.1	1/3T	4	146.0	27
60	2100	897	996	29.21	20.3	1/3T	4	56.0	53
61	2100	897	996	29.21	6.54	1/2T	4	600.0	31
62	2100	897	996	29.21	7.62	1/2T	4	446.0	33
63	2100	897	996	29.21	10.1	1/2T	4	259.0	40
64	2100	897	996	29.21	20.3	1/2T	4	82.0	90

Run #	dp	rs	rl	T	D	C/T	TYPE	N	Emf
65	1500	897	996	29.21	6.54	1/3T	1	381.0	34
66	1500	897	996	29.21	7.62	1/3T	1	270.0	39
67	1500	897	996	29.21	10.1	1/3T	1	135.0	38
68	1500	897	996	29.21	20.3	1/3T	1	35	53
69	1500	897	996	29.21	6.54	1/2T	1	450.0	40
70	1500	897	996	29.21	7.62	1/2T	1	360.0	48
71	1500	897	996	29.21	10.1	1/2T	1	185.0	50.5
72	1500	897	996	29.21	20.3	1/2T	1	39.0	56
73	1500	897	996	29.21	6.54	1/3T	3	840.0	37
74	1500	897	996	29.21	7.62	1/3T	3	495.0	35
75	1500	897	996	29.21	10.1	1/3T	3	235.0	34
76	1500	897	996	29.21	20.3	1/3T	3	34.0	33
77	1500	897	996	29.21	6.54	1/2T	3	1310.0	58
78	1500	897	996	29.21	7.62	1/2T	3	867.0	61
79	1500	897	996	29.21	10.1	1/2T	3	334.0	50
80	1500	897	996	29.21	20.3	1/2T	3	52.0	53
81	1500	897	996	29.21	6.54	1/3T	4	310.0	24
82	1500	897	996	29.21	7.62	1/3T	4	212.0	23.5
83	1500	897	996	29.21	10.1	1/3T	4	137.0	25
84	1500	897	996	29.21	20.3	1/3T	4	53.0	50
85	1500	897	996	29.21	6.54	1/2T	4	564.0	30
86	1500	897	996	29.21	7.62	1/2T	4	381.0	29
87	1500	897	996	29.21	10.1	1/2T	4	235.0	34
88	1500	897	996	29.21	20.3	1/2T	4	77.0	90
89	640	897	996	29.21	6.54	1/3T	1	323.0	32

Run #	dp	rs	rl	T	D	C/T	TYPE	N	Emf
90	640	897	996	29.21	7.62	1/3T	1	268.0	38.5
91	640	897	996	29.21	10.1	1/3T	1	145.0	38
92	640	897	996	29.21	20.3	1/3T	1	31.0	49
93	640	897	996	29.21	6.54	1/2T	1	444.0	40
94	640	897	996	29.21	7.62	1/2T	1	329.0	47
95	640	897	996	29.21	10.1	1/2T	1	200.0	69
96	640	897	996	29.21	20.3	1/2T	1	37.0	61
97	640	897	996	29.21	6.54	1/3T	3	950.0	40
98	640	897	996	29.21	7.62	1/3T	3	556.0	39
99	640	897	996	29.21	10.1	1/3T	3	213.0	32
100	640	897	996	29.21	20.3	1/3T	3	29.0	29
101	640	897	996	29.21	6.54	1/2T	3	1306.0	55
102	640	897	996	29.21	7.62	1/2T	3	744.0	50
103	640	897	996	29.21	10.1	1/2T	3	360.0	52
104	640	897	996	29.21	20.3	1/2T	3	45.0	45
105	640	897	996	29.21	6.54	1/3T	4	308.0	23
106	640	897	996	29.21	7.62	1/3T	4	190.0	23
107	640	897	996	29.21	10.1	1/3T	4	122.0	24
108	640	897	996	29.21	20.3	1/3T	4	46.0	43
109	640	897	996	29.21	6.54	1/2T	4	510.0	27
110	640	897	996	29.21	7.62	1/2T	4	383.0	29
111	640	897	996	29.21	10.1	1/2T	4	196.0	32
112	640	897	996	29.21	20.3	1/2T	4	67.5	75
113	340	897	996	29.21	6.54	1/3T	1	288	29
114	340	897	996	29.21	7.62	1/3T	1	209	29

Run #	dp	rs	rl	T	D	C/T	TYPE	N	Emf
115	340	897	996	29.21	10.1	1/3T	1	96	29
116	340	897	996	29.21	20.3	1/3T	1	28	41
117	340	897	996	29.21	6.54	1/2T	1	343	30
118	340	897	996	29.21	7.62	1/2T	1	240	32
119	340	897	996	29.21	10.1	1/2T	1	144	37
120	340	897	996	29.21	20.3	1/2T	1	32	41
121	340	897	996	29.21	6.54	1/3T	3	660	31
122	340	897	996	29.21	7.62	1/3T	3	468	35
123	340	897	996	29.21	10.1	1/3T	3	190	30
124	340	897	996	29.21	20.3	1/3T	3	28	35
125	340	897	996	29.21	6.54	1/2T	3	1040	43
126	340	897	996	29.21	7.62	1/2T	3	678	49
127	340	897	996	29.21	10.1	1/2T	3	295	41
128	340	897	996	29.21	20.3	1/2T	3	37	35
129	340	897	996	29.21	6.54	1/3T	4	248	23
130	340	897	996	29.21	7.62	1/3T	4	170	24
131	340	897	996	29.21	10.1	1/3T	4	110	24
132	340	897	996	29.21	20.3	1/3T	4	44	40
133	340	897	996	29.21	6.54	1/2T	4	450	26
134	340	897	996	29.21	7.62	1/2T	4	335	28
135	340	897	996	29.21	10.1	1/2T	4	187	30
136	340	897	996	29.21	20.3	1/2T	4	54	61
137	2205	897	996	29.21	6.54	1	3	881.0	39
138	2205	897	996	29.21	7.62	1	3	455.0	35
139	2205	897	996	29.21	10.1	1	3	260.0	39

Run #	dp	rs	rl	T	D	C/T	TYPE	N	Emf
140	2205	897	996	29.21	20.3	1	3	60.0	60
141	2205	897	996	29.21	6.54	1	1	350.0	31
142	2205	897	996	29.21	7.62	1	1	275.0	36.5
143	2205	897	996	29.21	10.1	1	1	146.0	40
144	2205	897	996	29.21	20.3	1	1	48.0	32
145	2205	897	996	29.21	6.54	1	2	394.0	30
146	2205	897	996	29.21	7.62	1	2	265.0	28.5
147	2205	897	996	29.21	10.1	1	2	214.5	43
148	2205	897	996	29.21	20.3	1	2	57.0	75
149	2205	897	996	29.21	6.54	1	4	310.0	25
150	2205	897	996	29.21	7.62	1	4	210	25
151	2205	897	996	29.21	10.1	1	4	146	27
152	2205	897	996	29.21	20.3	1	4	50	65
153	1500	897	996	29.21	6.54	1	1	355	32.5
154	1500	897	996	29.21	7.62	1	1	260	36
155	1500	897	996	29.21	10.1	1	1	155	40
156	1500	897	996	29.21	20.3	1	1	45	30
157	1500	897	996	29.21	6.54	1	3	822	36.2
158	1500	897	996	29.21	7.62	1	3	440	32
159	1500	897	996	29.21	10.1	1	3	240	35
160	1500	897	996	29.21	20.3	1	3	56	55
161	1500	897	996	29.21	6.54	1	4	289	23.5
162	1500	897	996	29.21	7.62	1	4	185	23.5
163	1500	897	996	29.21	10.1	1	4	130	24.5
164	1500	897	996	29.21	20.3	1	4	46	61

Run #	dp	rs	rl	T	D	C/T	TYPE	N	Emf
165	2100	897	996	29.21	6.54	1	1	391	30
166	2100	897	996	29.21	7.62	1	1	263	28
167	2100	897	996	29.21	10.1	1	1	213	44
168	2100	897	996	29.21	20.3	1	1	58	76
169	2100	897	996	29.21	6.54	1	3	874	40
170	2100	897	996	29.21	7.62	1	3	451	35
171	2100	897	996	29.21	10.1	1	3	258	38
172	2100	897	996	29.21	20.3	1	3	60	60
173	2100	897	996	29.21	6.54	1	4	308	25
174	2100	897	996	29.21	7.62	1	4	210	25
175	2100	897	996	29.21	10.1	1	4	145	30
176	2100	897	996	29.21	20.3	1	4	50	64
177	640	897	996	29.21	6.54	1	1	292	30
178	640	897	996	29.21	7.62	1	1	220	34
179	640	897	996	29.21	10.1	1	1	145	38
180	640	897	996	29.21	20.3	1	1	37	61
181	640	897	996	29.21	6.54	1	3	750	33.5
182	640	897	996	29.21	7.62	1	3	445	32
183	640	897	996	29.21	10.1	1	3	225	33.5
184	640	897	996	29.21	20.3	1	3	40	50
185	640	897	996	29.21	6.54	1	4	262	22.5
186	640	897	996	29.21	7.62	1	4	170	22
187	640	897	996	29.21	10.1	1	4	127	25
188	640	897	996	29.21	20.3	1	4	43	50
189	340	897	996	29.21	6.54	1	1	264	28.5

Run #	dp	rs	rl	T	D	C/T	TYPE	N	Emf
190	340	897	996	29.21	7.62	1	1	189	27.5
191	340	897	996	29.21	10.1	1	1	103	30
192	340	897	996	29.21	20.3	1	1	36	55
193	340	897	996	29.21	6.54	1	3	639	31
194	340	897	996	29.21	7.62	1	3	335	29
195	340	897	996	29.21	10.1	1	3	190	30
196	340	897	996	29.21	20.3	1	3	45	41
197	340	897	996	29.21	6.54	1	4	232	22
198	340	897	996	29.21	7.62	1	4	225	25
199	340	897	996	29.21	10.1	1	4	107	23.5
200	340	897	996	29.21	20.3	1	4	56	64
201	340	897	996	29.21	6.54	2/3T	1	588	51.5
202	340	897	996	29.21	7.62	2/3T	1	320	42
203	340	897	996	29.21	10.1	2/3T	1	186	49
204	340	897	996	29.21	20.3	2/3T	1	46	76
205	340	897	996	29.21	6.54	2/3T	3	1156	51
206	340	897	996	29.21	7.62	2/3T	3	743	56
207	340	897	996	29.21	10.1	2/3T	3	430	65
208	340	897	996	29.21	20.3	2/3T	3	56	53
209	340	897	996	29.21	6.54	2/3T	4	632	30
210	340	897	996	29.21	7.62	2/3T	4	434	32
211	340	897	996	29.21	10.1	2/3T	4	260	37
212	340	897	996	29.21	20.3	2/3T	4	76	76

APPENDIX A-3

DATA BANK #2AGITATION REQUIREMENTS FOR COMPLETE DRAWDOWN OF
FLOATING SOLIDS IN DIFFERENT SYSTEMSSYSTEM: Polypropylene (dp=2150 μ m, density = 720kg/m³)Water (density 996kg/m³)

D = 4in. (6.54cm)

T = 11.5in. (29.12cm)

Closed vessel

Impeller D = 4"

Flat Blade Turbine

C in.	C/D -	C/T -	Njs rpm	Emf (mV)	Torque (Nm)	Power (watts)	Np -	fi -
3.25	0.8125	0.2826	204	39.125	0.0480	1.0269	2.4	35.063
4.25	1.0625	0.3696	258	50.6	0.0771	2.0844	2.4	44.395
5.25	1.3125	0.4565	277	56.2	0.0915	2.6540	2.5	48.118
6.25	1.5625	0.5435	300	62.93	0.1087	3.4161	2.5	52.342
7.25	1.8125	0.6304	450	98.6	0.2000	9.4307	2.1	73.427
8.25	2.0625	0.7174	490	108.3	0.2249	11.5442	2.0	78.547
9.25	2.3125	0.8043	533	118.8	0.2518	14.0587	1.9	83.880
10.2	2.5625	0.8913	766	175.6	0.3972	31.8777	1.4	110.19

Table A-3.1

SYSTEM: Polypropylene ($dp=2150\mu\text{m}$, density = 720kg/m^3)

Water (density 996kg/m^3)

D = 4in. (6.54cm)

T = 11.5in. (29.12cm)

Closed vessel

IMPELLER : Disk Turbine

C in.	C/D -	C/T -	Njs Njs	Emf (mV)	Torque (Nm)	Power (watts)	Np -	fi -
3.25	0.8125	0.2826	158	44.78	0.0622	1.0297	5.2	35.096
4.25	1.0625	0.3696	164	45.66	0.0645	1.1076	5.0	35.958
5.25	1.3125	0.4565	187	53.94	0.0857	1.6783	5.1	41.302
6.25	1.5625	0.5435	220	66.87	0.1188	2.7377	5.2	48.619
7.25	1.8125	0.6304	257	83.8	0.1621	4.3655	5.2	56.800
8.25	2.0625	0.7174	272	90.3	0.1788	5.0946	5.1	59.802
9.25	2.3125	0.8043	289	96.07	0.1936	5.8604	4.9	62.659
10.2	2.5625	0.8913	314	110	0.2292	7.5409	4.9	68.153

Table A-3.2

SYSTEM: Polypropylene ($dp=2150\mu m$, density = $720\text{kg}/\text{m}^3$)

Water (density $996\text{kg}/\text{m}^3$)

D = 4in. (6.54cm)

T = 11.5in. (29.12cm)

Closed vessel

IMPELLER: PITCHED BLADE (DP)

C in.	C/D -	C/T -	Njs Njs	Emf (mV)	Torque (Nm)	Power (watts)	Np -	fi -
3.25	0.8125	0.2826	292	43.02	0.0577	1.7652	1.4	42.002
4.25	1.0625	0.3696	347	51.58	0.0796	2.8946	1.4	49.530
5.25	1.3125	0.4565	442	71.15	0.1297	6.0078	1.4	63.180
6.25	1.5625	0.5435	525	91.7	0.1824	10.0306	1.4	74.952
7.25	1.8125	0.6304	610	118.71	0.2515	16.0750	1.4	87.712
8.25	2.0625	0.7174	745	171.4	0.3865	30.1643	1.5	108.18
9.25	2.3125	0.8043	715	166.2	0.3732	27.9521	1.5	105.47
10.2	2.5625	0.8913	662	150.1	0.3319	23.0206	1.6	98.866

Table A-3.3

SYSTEM: Polypropylene ($dp=2150\mu\text{m}$, density = 720kg/m^3)

Water (density 996kg/m^3)

D = 4in. (6.54cm)

T = 11.5in. (29.12cm)

Closed vessel

IMPELLER : PITCHED BLADE (UP)

C in.	C/D -	C/T -	Njs Njs	Emf (mV)	Torque (Nm)	Power (watts)	Np -	fi -
3.25	0.8125	0.2826	145	27.27	0.0174	0.2638	1.7	22.29
4.25	1.0625	0.3696	181	30.65	0.0260	0.4935	1.7	27.46
5.25	1.3125	0.4565	265	37.82	0.0444	1.2323	1.3	37.26
6.25	1.5625	0.5435	306	50.61	0.0771	2.4730	1.7	46.99
7.25	1.8125	0.6304	375	61.83	0.1059	4.1594	1.6	55.89
8.25	2.0625	0.7174	419	71.63	0.1310	5.7492	1.6	62.26
9.25	2.3125	0.8043	460	83.42	0.1612	7.7668	1.6	68.82
10.2	2.5625	0.8913	494	90.02	0.1781	9.2156	1.5	72.86

Table A-3.3

SYSTEM: Polyethylene (dp = 2205 μ m, density = 897Kg/m³)

Water (density 996kg/m³)

D = 4in. (6.54cm)

T = 11.5 in. (29.12cm)

Open vessel

Disk Turbine

C in.	C/D -	C/T -	Njs rpm	Emf (mV)	Torque (Nm)	Power (watts)	Np -	fi -
2	0.5	0.1733	110	29	0.0218	0.2512	3.8	23.602
2.5	0.625	0.2166	116	29	0.0218	0.2649	3.4	24.023
3	0.75	0.2600	116	30	0.0244	0.2960	3.8	24.930
3.5	0.875	0.3033	122	32	0.0295	0.3768	4.2	27.017
4	1	0.3466	126	33	0.0320	0.4230	4.2	28.078
4.5	1.125	0.3899	128	33	0.0320	0.4297	4.1	28.226
5	1.25	0.4333	133	34	0.0346	0.4821	4.1	29.331
5.5	1.375	0.4766	138	36	0.0397	0.5743	4.4	31.092
6	1.5	0.5199	146	38	0.0448	0.6860	4.4	32.989
6.5	1.625	0.5633	158	40	0.0500	0.8271	4.2	35.112
7	1.75	0.6066	163	43	0.0577	0.9845	4.6	37.211
7.5	1.875	0.6499	175	46	0.0653	1.1978	4.5	39.725
8	2	0.6932	183	49	0.0730	1.3999	4.6	41.844
8.5	2.125	0.7366	191	52	0.0807	1.6148	4.6	43.884
9	2.25	0.7799	215	63	0.1089	2.4522	4.9	50.442
9.5	2.375	0.8232	227	67	0.1191	2.8327	4.9	52.926

Table A-3.4

SYSTEM: Polyethylene ($dp = 2205\mu\text{m}$, density = 897Kg/m^3)

Water (density 996kg/m^3)

D = 4in. (6.54cm)

T = 11.5 in. (29.12cm)

Open vessel

Pitched Blade Impeller (downward pumping)

C in.	C/D -	C/T -	Njs rpm	Emf (mV)	Torque (Nm)	Power (watts)	Np -	fi -
2	0.5	0.1733	188	30	0.0244	0.4798	1.4	29.283
2.5	0.625	0.2166	191	29	0.0218	0.4362	1.3	28.368
3	0.75	0.2600	200	30	0.0244	0.5104	1.3	29.893
3.5	0.875	0.3033	226	34	0.0346	0.8193	1.4	35.001
4	1	0.3466	260	38	0.0448	1.2216	1.4	39.986
4.5	1.125	0.3899	272	40	0.0500	1.4239	1.4	42.082
5	1.25	0.4333	286	42	0.0551	1.6507	1.4	44.207
5.5	1.375	0.4766	290	42	0.0551	1.6737	1.4	44.412
6	1.5	0.5199	307	45	0.0628	2.0190	1.4	47.276
6.5	1.625	0.5633	325	47	0.0679	2.3117	1.3	49.459
7	1.75	0.6066	354	51	0.0781	2.8979	1.3	53.329
7.5	1.875	0.6499	385	58	0.0961	3.8747	1.4	14.802
8	2	0.6932	440	65	0.1140	5.2546	1.2	15.519
8.5	2.125	0.7366	470	74	0.1370	6.7478	1.3	17.295
9	2.25	0.7799	457	72	0.1319	6.3159	1.3	19.669
9.5	2.375	0.8232	447	72	0.1319	6.1777	1.4	22.878

Table A-3.5

SYSTEM: Polyethylene ($dp = 2205\mu\text{m}$, density = $897\text{Kg}/\text{m}^3$)

Water (density $996\text{kg}/\text{m}^3$)

$D = 4\text{in.}$ (6.54cm)

$T = 11.5\text{ in.}$ (29.12cm)

Open vessel

Pitched Blade Impeller (upward pumping)

C in.	C/D -	C/T -	Njs rpm	Emf (mV)	Torque (Nm)	Power (watts)	Np -	fi -
2	0.5	0.1733	90	23	0.0064	0.0607	1.7	14.697
2.5	0.625	0.2166	97	23	0.0064	0.0654	1.4	15.068
3	0.75	0.2600	105	23	0.0064	0.0708	1.2	15.472
3.5	0.875	0.3033	115	24	0.0090	0.1084	1.4	17.833
4	1	0.3466	130	25	0.0116	0.1574	1.4	20.195
4.5	1.125	0.3899	149	26	0.0141	0.2203	1.3	22.593
5	1.25	0.4333	169	27	0.0167	0.2953	1.2	24.908
5.5	1.375	0.4766	183	28	0.0192	0.3688	1.2	26.825
6	1.5	0.5199	215	31	0.0269	0.6064	1.2	31.660
6.5	1.625	0.5633	233	34	0.0346	0.8447	1.3	35.359
7	1.75	0.6066	248	35	0.0372	0.9656	1.3	36.971
7.5	1.875	0.6499	257	38	0.0448	1.2075	1.4	39.832
8	2	0.6932	268	50	0.0756	2.1220	2.2	48.067
8.5	2.125	0.7366	280	41	0.0525	1.5409	1.4	43.204
9	2.25	0.7799	280	42	0.0551	1.6160	1.5	43.895
9.5	2.375	0.8232	317	50	0.0756	2.5100	1.6	50.835

Table A-3.6

SYSTEM: Polyethylene (dp = 2205 μ m, density = 897Kg/m³)

Water (density 996kg/m³)

T = 23.5in. (59.69cm)

D = 8in. (20.32cm)

Open vessel

PITCHED BLADE (downward pumping)

C in.	C/D -	C/T -	Njs rpm	Power (watts)	Np -	fi -
3	0.375	0.1304	100	2	1.3	22.967
4	0.5	0.1739	125	4	1.3	28.936
5	0.625	0.2174	126	5	1.6	31.171
6	0.75	0.2609	132	6	1.6	33.124
7	0.875	0.3043	137	6	1.5	33.124
8	1	0.3478	145	7	1.4	34.870
9	1.125	0.3913	155	9	1.5	37.917
10	1.25	0.4348	170	11.5	1.5	41.146
11	1.375	0.4783	179	14	1.5	43.934
12	1.5	0.5217	196	16	1.3	45.934
13	1.625	0.5652	202	18	1.4	47.773
14	1.75	0.6087	195	16	1.4	45.934
15	1.875	0.6522	200	18	1.4	47.773

Table A-3.7

SYSTEM: Polyethylene ($d_p = 2205\mu\text{m}$, density = 897Kg/m^3)

Water (density 996kg/m^3)

T = 23.5in. (59.69cm)

D = 8in. (20.32cm)

Open vessel

Disk Turbine

C in.	C/D -	C/T -	Njs rpm	Power (watts)	Np -	fi -
3	0.375	0.1304	45	0.5	3.4	14.468
4	0.5	0.1739	51	1	4.7	18.229
5	0.625	0.2174	58	1.5	4.8	20.867
6	0.75	0.2609	60	2	5.8	22.967
7	0.875	0.3043	65	2.5	5.7	24.740
8	1	0.3478	70	3	5.5	26.290
9	1.125	0.3913	72	3.5	5.9	27.677
10	1.25	0.4348	75	4	5.9	28.936
11	1.375	0.4783	79	5	6.3	31.171
12	1.5	0.5217	85	6	6.1	33.124
13	1.625	0.5652	90	7	6.0	34.870
14	1.75	0.6087	91	7	5.8	34.870
15	1.875	0.6522	94	8	6.0	36.457

Table A-3.8

SYSTEM: Polyethylene ($dp = 2205\mu\text{m}$, density = 897Kg/m^3)
 Water (density 996kg/m^3)
 T = 23.5in. (59.69cm)
 D = 8in. (20.32cm)

Open vessel

Flat Blade Turbine

C in.	C/D -	C/T -	Njs rpm	Power (watts)	Np -	fi -
3	0.375	0.13043	54	0.6	2.4	15.3747
4	0.5	0.17391	60	1	2.9	18.2287
5	0.625	0.21739	73	1.2	1.9	19.3709
6	0.75	0.26086	83	2	2.2	22.9667
7	0.875	0.30434	96	3	2.1	26.2904
8	1	0.34782	118	6.5	2.5	34.0195
9	1.125	0.39130	128	11	3.3	40.5403
10	1.25	0.43478	134	12.5	3.3	42.3051
11	1.375	0.47826	138	13.5	3.2	43.4045
12	1.5	0.52173	141	14	3.1	43.9338
13	1.625	0.56521	156	15	2.5	44.9559
14	1.75	0.60869	177	21.5	2.4	50.6877
15	1.875	0.65217	191	25	2.2	53.3011

Table A-3.9

SYSTEM: Polyethylene ($d_p = 2205\mu\text{m}$, density = 897Kg/m^3)

Water (density 996kg/m^3)

$D = 4\text{in. (6.54cm)}$

$T = 11.5\text{in. (29.12cm)}$

Closed vessel

Flat Blade Turbine

C in.	C/D -	C/T -	Njs rpm	Emf (mV)	Torque (Nm)	Power (watts)	Np -	fi -
2.5	0.625	0.216	166	33	0.0320	0.5572	2.4	30.781
3	0.75	0.259	167	33	0.0320	0.5589	2.4	30.812
4	1	0.346	194	37	0.0423	0.8594	2.4	35.564
5	1.25	0.433	212	40	0.0500	1.1109	2.3	38.740
6	1.5	0.519	230	43.5	0.0589	1.4200	2.3	42.044
7	1.75	0.606	255	49	0.0730	1.9522	2.4	46.749
8	2	0.693	294	58	0.0961	2.9539	2.3	53.670
9	2.25	0.779	319	66	0.1166	3.8891	2.4	58.824
10	2.5	0.866	343	72	0.1319	4.7404	2.4	62.836

Table A-3.10

SYSTEM: Polyethylene ($d_p = 2205\mu\text{m}$, density = 897Kg/m^3)

Water (density 996kg/m^3)

D = 4in. (6.54cm)

T = 11.5in. (29.12cm)

Closed vessel

Disk Turbine

C in.	C/D -	C/T -	Njs rpm		Torque (Nm)	Power (watts)	Np -	fi -
2.5	0.625	0.216	110	34	0.0346	0.3988	6.0	27.532
3	0.75	0.259	113	35	0.0372	0.4384	6.2	28.416
4	1	0.346	127	37	0.0423	0.5604	5.5	30.839
5	1.25	0.433	141	40	0.0500	0.7376	5.3	33.797
6	1.5	0.519	166	48	0.0705	1.2275	5.3	40.051
7	1.75	0.606	178	55	0.0884	1.6491	5.8	44.193
8	2	0.693	195	57	0.0935	1.9053	5.2	46.372
9	2.25	0.779	220	68	0.1217	2.8057	5.3	52.757
10	2.5	0.866	257	84	0.1627	4.3742	5.2	61.174

Table A-3.11

SYSTEM: Polyethylene ($d_p = 2205\mu\text{m}$, density = $897\text{Kg}/\text{m}^3$)

Water (density $996\text{kg}/\text{m}^3$)

D = 4in. (6.54cm)

T = 11.5in. (29.12cm)

Closed vessel

Pitched Blade Turbine (DP)

C in.	C/D -	C/T -	Njs rpm		Torque (Nm)	Power (watts)	Np -	fi -
2.5	0.625	0.216	170	28	0.0192	0.3416	1.4	26.148
3	0.75	0.259	194	30	0.0244	0.4946	1.4	29.581
4	1	0.346	239	36	0.0397	0.9938	1.5	37.328
5	1.25	0.433	275	39	0.0474	1.3633	1.3	41.477
6	1.5	0.519	334	48	0.0705	2.4654	1.3	50.532
7	1.75	0.606	390	58	0.0961	3.9251	1.3	59.004
8	2	0.693	509	82	0.1575	8.4002	1.3	76.038
9	2.25	0.779	554	97	0.1959	11.3724	1.3	84.117
10	2.5	0.866	520	91	0.1806	9.8374	1.4	80.148

Table A-3.12

SYSTEM: Polyethylene ($d_p = 2205\mu\text{m}$, density = 897Kg/m^3)

Water (density 996kg/m^3)

D = 4in. (6.54cm)

T = 11.5in. (29.12cm)

Closed vessel

Pitched Blade Turbine (UP)

C in.	C/D -	C/T -	Njs rpm		Torque (Nm)	Power (watts)	Np -	fi -
2.5	0.625	0.216	93	23	0.0064	0.0627	1.6	14.858
3	0.75	0.259	100	23	0.0064	0.0674	1.4	15.222
4	1	0.346	110	23.5	0.0077	0.0889	1.3	16.694
5	1.25	0.433	155	27	0.0167	0.2708	1.5	24.200
6	1.5	0.519	210	33	0.0320	0.7049	1.5	33.291
7	1.75	0.606	244	37	0.0423	1.0809	1.5	38.389
8	2	0.693	301	46	0.0653	2.0603	1.5	47.597
9	2.25	0.779	357	55	0.0884	3.3056	1.5	55.721
10	2.5	0.866	369	57	0.0935	3.6147	1.4	57.406

Table A-3.13

SYSTEM: Polyethylene ($d_p = 2205\mu\text{m}$, density = $897\text{Kg}/\text{m}^3$)

Water (density $996\text{kg}/\text{m}^3$)

D = 4in. (6.54cm)

T = 11.5in. (29.12cm)

Open tank

Disk Turbine

C in.	C/D -	C/T -	Njs rpm	Emf (mV)	Torque (Nm)	Power (watts)	Np -	fi -
2.5	0.625	0.216	116	29	0.0218	0.2649	3.4	24.023
3	0.75	0.259	116	30	0.0244	0.2960	3.8	24.930
4	1	0.346	126	33	0.0320	0.4230	4.2	28.078
5	1.25	0.433	135	34	0.0346	0.4894	4.0	29.477
6	1.5	0.519	158	42	0.0551	0.9119	4.6	36.273
7	1.75	0.606	169	46	0.0653	1.1568	4.8	39.266
8	2	0.693	186	49	0.0730	1.4228	4.4	42.071
9	2.25	0.779	215	63	0.1089	2.4522	4.9	50.442

Table A-3.14

THE EFFECT OF LIQUID DRAW-OFF IN A VESSEL

SYSTEM: HD polyethylene (897kg/m³, dp = 2205μm)
Water (996kg/m³)

D = 4in. (6.54cm)
T = 11.5in. (29.12cm)
Disk Turbine
C = 1/2T

H in	Njs rpm	Emf mV	LOG(H)	LOG(Njs)
9	84	27	2.197	4.4308
9.5	100	29	2.251	4.6051
10	134	36	2.302	4.8978
10.5	140	39	2.351	4.9416
11	140	40	2.397	4.9416
11.5	140	40	2.442	4.9416
12	140	40	2.484	4.9416
12.5	140	40	2.525	4.9416
13	150	41	2.564	5.0106
13.25	150	41	2.583	5.0106

Table A-3.31

THE EFFECT OF LIQUID DRAW-OFF IN A VESSEL

SYSTEM: HD polyethylene(897kg/m³, dp = 2205μm)
 Water (996kg/m³)

D = 4in.(6.54cm)

T = 11.5in. (29.12cm)

PITCHED BLADE TURBINE (UP) C 1/2T

H in	Njs rpm	Emf mV	LOG(H)	LOG(Njs)
9.5	94	24	2.251	4.5432
10	101	24	2.302	4.6151
10.5	110	24	2.351	4.7004
11	122	25	2.397	4.8040
11.5	130	25	2.442	4.8675
12	133	25.5	2.484	4.8903
12.5	166	28	2.525	5.1119
13	182	29	2.564	5.2040
13.25	197	31	2.583	5.2832

Table A-3.32

THE EFFECT OF LIQUID DRAW-OFF IN A VESSEL

SYSTEM: HD polyethylene (897kg/m³, dp = 2205μm)
 Water (996kg/m³)

D = 4in. (6.54cm)

T = 11.5in. (29.12cm)

PITCHED BLADE TURBINE (DP)

H in	Njs rpm	Emf mV	LOG(H)	LOG(Njs)
9.5	195	30	2.251	5.2729
10	218	33	2.302	5.3844
10.5	218	33	2.351	5.3844
11	245	37	2.397	5.5012
11.5	272	40	2.442	5.6058
12	297	42	2.484	5.6937
12.5	314	45	2.525	5.7493
13	350	48	2.564	5.8579
13.25	365	51	2.583	5.8998

Table A-3.33

SYSTEM: Polyethylene ($d_p = 2205\mu\text{m}$, density = 897Kg/m^3)

Water (density 996kg/m^3)

D = 4in. (6.54cm)

T = 11.5in. (29.12cm)

Open tank

Pitched Blade Turbine (downward pumping)

C in.	C/D -	C/T -	Njs rpm	Emf (mV)	Torque (Nm)	Power (watts)	Np -	fi -
2.5	0.625	0.216	191	29	0.0218	0.4362	1.3	28.368
3	0.75	0.259	200	30	0.0244	0.5104	1.3	29.893
4	1	0.346	260	38	0.0448	1.2216	1.4	39.986
5	1.25	0.433	286	42	0.0551	1.6507	1.4	44.207
6	1.5	0.519	322	47	0.0679	2.2904	1.4	49.307
7	1.75	0.606	384	59	0.0986	3.9677	1.4	59.217
8	2	0.693	489	82	0.1575	8.0701	1.4	75.029
9	2.25	0.779	540	95	0.1908	10.7952	1.4	82.670

Table A-3.15

SYSTEM: Polyethylene (dp = 2205 μ m, density = 897Kg/m³)

Water (density 996kg/m³)

D = 4in. (6.54cm)

T = 11.5in. (29.12cm)

Open tank

Pitched Blade Turbine (upward pumping)

C in.	C/D -	C/T -	Njs rpm	Emf (mV)	Torque (Nm)	Power (watts)	Np -	fi -
2.5	0.625	0.216	97	23	0.0064	0.0654	1.3	14.581
3	0.75	0.259	105	25	0.0116	0.1271	2.2	18.807
4	1	0.346	130	26	0.0141	0.1922	1.2	19.027
5	1.25	0.433	169	28	0.0192	0.3406	1.4	26.123
6	1.5	0.519	215	32	0.0295	0.6640	1.3	32.634
7	1.75	0.606	248	36	0.0397	1.0321	1.4	37.802
8	2	0.693	287	40	0.0500	1.5024	1.3	42.842
9	2.25	0.779	335	49	0.0730	2.5626	1.4	51.187

Table A-3.16

DIFFERENT BAFFLING SYSTEMS

Open vessel T = 11.5in. (29.12cm)

D = 4in (6.54cm)

SYSTEM: LD Polyethylene (840kg/m^3 , $dp=2200\mu\text{m}$) / Water
(996kg/m^3)

IMPELLER: Disk Turbine

4 full baffles

C in.	C/D -	Njs rpm	Emf mV	Torque N.m	Power watts
2	0.5	120	34	0.034604	0.435021
4	1	140	38	0.044848	0.657770
6	1.5	159	44	0.060214	1.002993
8	2	194	55	0.088385	1.796319

Table A-3.17

3 full baffles

C in.	C/D -	Njs rpm	Emf mV	Torque N.m	Power watts
2	0.5	134	35	0.037165	0.521725
4	1	155	42	0.055092	0.894589
6	1.5	174	47	0.067897	1.237665
8	2	207	55	0.088385	1.916691

Table A-3.18

DIFFERENT BAFFLING SYSTEMS

Open vessel T = 11.5in. (29.12cm)

D = 4in (6.54cm)

SYSTEM: LD Polyethylene (840kg/m^3 , $d_p=2200\mu\text{m}$) /
Water (996kg/m^3)

IMPELLER: Disk Turbine

2 full baffles

C in.	C/D -	Njs rpm	Emf mV	Torque N.m	Power watts
2	0.5	125	32	0.029482	0.386073
4	1	145	37	0.042287	0.642359
6	1.5	175	45	0.062775	1.150875
8	2	200	53	0.083263	1.744558

Table A-3.19

1 full baffle

C in.	C/D -	Njs rpm	Emf mV	Torque N.m	Power watts
2	0.5	130	30	0.02436	0.33176
4	1	145	33	0.032043	0.486748
6	1.5	172	37	0.042287	0.761971
8	2	190	43	0.057653	1.147569

Table A-3.20

DIFFERENT BAFFLING SYSTEMS

Open vessel T = 11.5in. (29.12cm)

D = 4in (6.54cm)

SYSTEM: LD Polyethylene (840kg/m^3 , $d_p=2200\mu\text{m}$) /
Water (996kg/m^3)

IMPELLER: Disk Turbine

2 full baffles & 2 2/3 baffles

C in.	C/D -	Njs rpm	Emf mV	Torque N.m	Power watts
2	0.5	125	32	0.029482	0.386073
4	1	164	44	0.060214	1.034533
6	1.5	177	48	0.070458	1.306492
8	2	231	70	0.1268	3.06856

Table A-3.21

DIFFERENT BAFFLING SYSTEMS

Open vessel T = 11.5in. (29.12cm)

D = 4in (6.54cm)

SYSTEM: LD Polyethylene (840kg/m^3 , $d_p=2200\mu\text{m}$) /
Water (996kg/m^3)

IMPELLER: Disk Turbine

2 2/3H down & 2 1/2H up alternate baffles

C in.	C/D -	Njs rpm	Emf mV	Torque N.m	Power watts
2	0.5	103	28	0.019238	0.207587
4	1	150	40	0.04997	0.785242
6	1.5	165	43	0.057653	0.996573
8	2	188	49	0.073019	1.438126

Table A-3.22

4 2/3H baffles

C in.	C/D -	Njs rpm	Emf mV	Torque N.m	Power watts
2	0.5	130	34	0.034604	0.471273
4	1	193	50	0.07558	1.528155
6	1.5	260	80	0.15241	4.151358
8	2	310	100	0.20363	6.613126

Table A-3.23

DIFFERENT BAFFLING SYSTEMS

Open vessel T = 11.5in. (29.12cm)

D = 4in (6.54cm)

SYSTEM: LD Polyethylene (840kg/m^3 , $d_p=2200\mu\text{m}$) /
Water (996kg/m^3)

IMPELLER: Disk Turbine

3 2/3H baffles an 1 full baffle

C in.	C/D -	Njs rpm	Emf mV	Torque N.m	Power watts
2	0.5	130	34	0.034604	0.471273
4	1	178	45	0.062775	1.170604
6	1.5	208	76	0.142166	3.097864
8	2	260	80	0.15241	4.151358

Table A-3.24

DENSITY DIFFERENCE EFFECTS

SYSTEM: HD polyethylene ($d_p=2205\mu\text{m}$)

Aqueous zinc chloride soln. (0-14%w/w)

Disk turbine, $C/D = 1$

r_s kg/m ³	r_l kg/m ³	$(r_l-r_s)/r_l$ -	N_{js} rpm	Emf mV	f_i -
0.8969	0.996	0.099	125	35	44.59
0.8969	1.072	0.163	146	42	42.17
0.8969	1.114	0.195	165	45	44.50
0.8969	1.146	0.217	186	52	48.14
0.8969	1.176	0.238	194	54	48.66

Table A-3.25

Disk turbine $C = 1/2T$

r_s kg/m ³	r_l kg/m ³	$(r_l-r_s)/r_l$ -	N_{js} rpm	Emf mV	f_i -
0.8969	0.996	0.099	176	47	62.78
0.8969	1.072	0.163	234	67	67.59
0.8969	1.114	0.195	247	84	66.61
0.8969	1.146	0.217	262	86	67.82
0.8969	1.176	0.238	297	104	74.50

Table A-3.26

DENSITY DIFFERENCE EFFECTS

SYSTEM: HD polyethylene (dp=2205 μ m)

Aqueous zinc chloride soln. (0-14%w/w)

C/D =1

D = 4"

Pitched blade turbine (UP)

r_s kg/m ³	r_l kg/m ³	$(r_l-r_s)/r_l$ -	N_{js} rpm	Emf mV	f_i -
0.8969	0.996	0.099497	130	25	46.37
0.8969	1.072	0.163339	157	26	45.35
0.8969	1.114	0.194649	160	26	43.15
0.8969	1.146	0.217457	165	27	42.71
0.8969	1.176	0.237677	212	32	53.18

Table A-3.27

Pitched blade turbine (UP), C = 1/2T

r_s kg/m ³	r_l kg/m ³	$(r_l-r_s)/r_l$ -	N_{js} rpm	Emf mV	f_i -
0.8969	0.996	0.099	176	32	62.78
0.8969	1.072	0.163	295	40	85.21
0.8969	1.114	0.195	315	46	84.95
0.8969	1.146	0.217	335	50	86.72
0.8969	1.176	0.238	391	63	98.09

Table A-3.28

DENSITY DIFFERENCE EFFECTS

SYSTEM: HD polyethylene ($d_p=2205\mu\text{m}$)

Aqueous zinc chloride soln. (0-14%w/w)

C/D = 1

D = 4"

Pitched blade turbine (DP) C/D = 1

r_s kg/m ³	r_l kg/m ³	$(r_l-r_s)/r_l$ -	N_{js} rpm	Emf mV	f_i -
0.8969	0.996	0.099	251	37	89.54
0.8969	1.072	0.163	308	45	88.97
0.8969	1.114	0.195	340	50	91.70
0.8969	1.146	0.217	356	54	92.15
0.8969	1.176	0.238	404	65	101.32

Table A-3.29

Pitched blade turbine, C=1/2T

r_s kg/m ³	r_l kg/m ³	$(r_l-r_s)/r_l$ -	N_{js} rpm	Emf mV	f_i -
0.8969	0.996	0.099	320	62	114.16
0.8969	1.072	0.163	460	74	132.87
0.8969	1.113	0.195	485	90	130.81
0.8969	1.146	0.217	565	104	146.26
0.8969	1.176	0.237	633	130	158.80

Table A-3.30

APPENDIX A-4**TORQUE CALIBRATION****TORQUE-EMF RELATIONSHIP FOR THE COLE PALMER MOTOR**

Experiments done on the Chemineer motor for which the torque exerted on the shaft is measured directly by the turning moment on a dynamometer fixed on the motor.

The experiments are repeated on the Cole Palmer motor at the same speeds, this time measuring the back-emf impressed on the motor shaft due to fluid resistance.

The emf recorded then corresponds to the torque, provided that the same conditions exist.

Impeller type I : Disk turbine

Open vessel, T = 11.5in.

D = 4in., C/D = 1

Speed N (rpm)	Chemineer		Cole Palmer Emf (mV)
	Force F (Lbf)	Torque M (N.m)	
124	0.06	0.034696	34.9
142	0.08	0.046261	38.5
161	0.1	0.057826	43.5
172	0.12	0.069392	46
189	0.14	0.080957	51.5
202	0.16	0.092522	56
216	0.18	0.104088	61.8
224	0.2	0.115653	64
233	0.22	0.127219	68
244	0.24	0.138784	72
266	0.28	0.161915	82
270	0.3	0.173480	84.5
283	0.32	0.185045	92.5
296	0.34	0.196611	98
306	0.37	0.213959	100
320	0.4	0.231307	103.5
329	0.42	0.242872	116
336	0.45	0.260220	120
352	0.49	0.283351	131
361	0.52	0.300699	137

Table A-2.1 Data for disk turbine

Impeller type II : Pitched blade turbine

Open vessel, T = 11.5in.

D = 4in., C/D = 1

Speed N (rpm)	Chemineer		Cole Palmer
	Force F (Lbf)	Torque M (N.m)	Emf (mV)
145	0.02	0.011565	27
172	0.03	0.017348	29
194	0.04	0.023130	30.8
238	0.06	0.034696	36.3
278	0.08	0.046261	41
302	0.1	0.057826	44.4
373	0.14	0.080957	55
395	0.16	0.092522	60
428	0.2	0.115653	66
450	0.22	0.127219	70.8
475	0.24	0.138784	75
490	0.25	0.144567	81
512	0.28	0.161915	88
530	0.3	0.173480	87.5
606	0.38	0.219742	110
625	0.42	0.242872	116
700	0.52	0.300699	142
803	0.68	0.393222	186

Table A-2.2 Data for pitched blade turbine

Impeller type III : Flat blade turbineOpen vessel, $T = 11.5$ $D = 4\text{in.}$, $C/D = 1$

Speed N (rpm)	Chemineer		Cole Palmer Emf (mV)
	Force F (Lbf)	Torque M (N.m)	
134	0.04	0.023130	30
187	0.08	0.046261	38
216	0.1	0.057826	43
240	0.12	0.069392	38
259	0.14	0.080957	54
279	0.16	0.092522	64
288	0.18	0.104088	61
300	0.2	0.115653	64
326	0.22	0.127219	71
346	0.25	0.144567	76.5
379	0.3	0.173480	88
428	0.38	0.219742	105
500	0.52	0.300699	138
600	0.76	0.439484	190
700	1.02	0.589834	200

Table A-2.3 Data for flat blade turbine

The Calibration Curve

Table A-2.4 shows the linear regression analysis which was carried out to determine the value of the torque from emf measurements.

The predicted relationship between torque and emf is

$$\text{Torque} = \text{coeff1} * \text{Emf} + \text{constant.}$$

Impeller	coeff1	const.	corr. %
Disk Turbine	0.002600	-0.05225	99.6
Pitched Blade	0.002454	-0.05112	99.7
Flat Blade	0.002522	-0.06122	97.9
combined data	0.002561	-0.05247	99.1

Table A-2.4 Coefficients for correlation

Impellers: Disk turbine, pitched blade turbine and

Flat blade turbine

D = 4in., C/D = 1, T = 11.5in.

Chemineer Emf (mV)	Cole Palmer Torque M (N.m)
27	0.011565
29	0.017348
30	0.023130
30.8	0.023130
34.9	0.034696
36.3	0.034696
38	0.046261
38	0.069392
38.5	0.046261
41	0.046261
43	0.057826
43.5	0.057826
44.4	0.057826
46	0.069392
51.5	0.080957
54	0.080957
55	0.080957
56	0.092522
60	0.092522
61	0.104088
61.8	0.104088
64	0.115653
64	0.115653
64	0.092522
66	0.115653
68	0.127219
70.8	0.127219
71	0.127219
72	0.138784
75	0.138784
76.5	0.144567
81	0.144567
82	0.161915
84.5	0.173480
87.5	0.173480
88	0.173480
88	0.161915
92.5	0.185045

Table A-2.5 Data for all Impellers

Table A-2.5 Continued

Chemineer Emf (mV)	Cole Palmer Torque M (N.m)
98	0.196611
100	0.213959
103.5	0.231307
105	0.219742
110	0.219742
116	0.242872
116	0.242872
120	0.260220
131	0.283351
137	0.300699
138	0.300699
142	0.300699
186	0.393222
190	0.439484
200	0.589834

Thus the following relationship is used to convert emf recorded on the recorder and the corresponding torque

$$\text{Torque} = (\text{Emf} * 0.254 - 5.2) * 10^{-3} \quad \text{N.m}$$

emf in milli-volts

Figure A-1 shows the calibration chart.

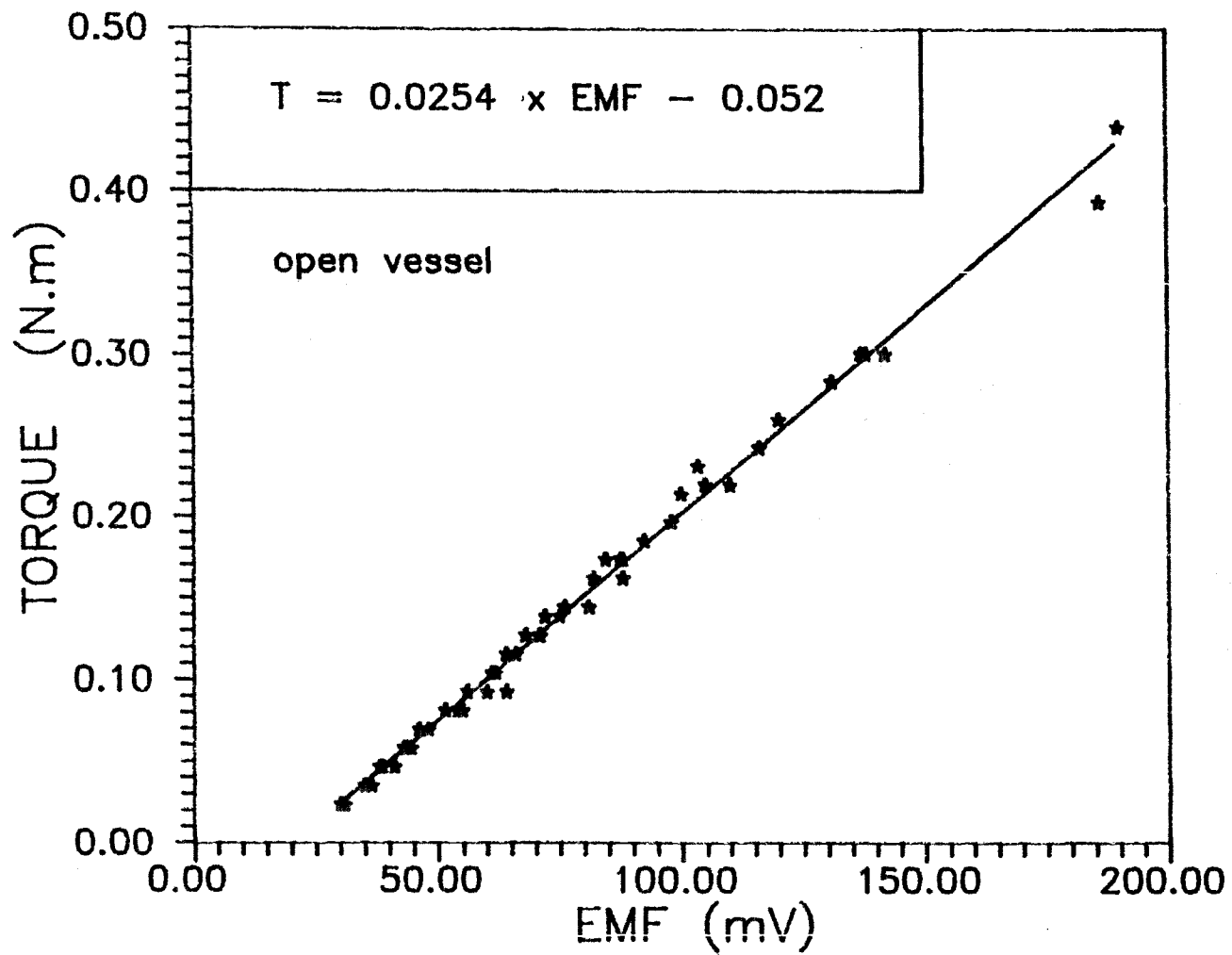


Figure A-1 EMF - TORQUE calibration for Cole Palmer Motor

REFERENCES

1. Th. N. Zwietering, "Suspending of Solid Particles in Liquids by Agitators ", Chemical Engineering Science. **8** , (1958) 244-253
2. Alvin W. Nienow, "Dispersion of Solids in Liquids ", Mixing of Liquids by Mechanical Agitation. **8**, 273-305
3. James Y. Oldshue, "Fluid Mixing Technology", McGraw-Hill Publications Co. New York, N.Y. (1983)
4. M. F. Edwards, D. I. Ellis, " The Drawdown of Floating Solids into Mechanically Agitated Vessels", Mixing Symposium Series. (**89**), 1984. 1-14
5. W. J. Bruining, J. J. Frijlink, "Draw-down of Floating Solids ", Mixing XI Conference, (1987).
6. Kolmogoroff, A. N., C. R. Academic Science U.S.S.R., (1941), 30:301, 31:538, 32:16
7. G. E. H. Joosten, J. G. M. Schilder & A. M. Broere, " The Suspension of Floating Solids in Stirred Vessels ", Trans IChemE. **55** , (1977)
220-223
8. Baldi, G., Conti, R., Alaria E., "Complete Suspension of Particles in Mechanically Agitater Vessels", Chemical Engineering Science, **33** (1978)
9. V. Kolar, "Suspending Solid Particles in Liquids by means of Mechanical Agitation", Collection Czechoslovakia Chemical Communications, **26** (1961)
613-627

10. J. H. Rushton, E.W. Costich and H. J. Everett, " Power Characteristics of Mixing Impellers ", Chemical Engineering Progress . 46, (1950)
395-404
11. Lewis E. Gates, Jerry R. Morton and Phillip L. Fondy, "Selecting Agitator Systems to Suspend Solids in Liquids" ,Chemical Engineering. 5, (1976)
145-150
12. Robert S. Brodkey, "Turbulence in Mixing operations", Academic press, Inc., N.Y. (1975)
13. J. T. Davies, "Turbulence Phenomena", Academic Press. New York , (1972)
14. James Y. Oldshue, "Fluid Mixing in 1989", Chemical Engineering Progress, 85/5, (1989)
33-42
15. Richard V. Calabrese and Carl M. Stoots, "Flow in the Impeller Region of a Stirred Tank", Chemical Engineering Progress, 85/5, (1998)
43-50
16. O. Molerus, W. Latzel, "Suspension of Particles in Agitated Vessels", Chemical Engineering science, 42, (1987), 1423-1430
17. D. Fajner, F. Magelli, M. Nocentini, G. Pasquali "Solids Concentration in a Mechanically Stirred and Staged Column Slurry Reactor", Chemical Engineering Research and design, 63, (1985) 235-240
18. P. Ayazi Shamlou, E. Koutsakos, "Solids Suspension and

Distribution in Liquids under Turbulent Agitation",
Chemical Engineering Science, 44/3, (1989)

529-542

19. Arthur W. Etchells, "Contunuous Slurrying of Solids into Viscous Liquids", AICHE Annual 72nd meeting, San Francisco, (1979)
20. S. Narayanan, V. K. Bhatia, D. K. Guha & M. N. Rao, "Suspension of Solids By Mechanical Agitation", Chemical Engineering Science. 24 (1969)
223-230
21. A. W. Etchells III, "Solid Suspension in Agitated Vessels - An Overview", AICHE Jersey Meeting, Newark, Delaware (1989)
22. D. L. Smith, R.R Hemrajani, R.M. Koros, and L. Tarmy, "Suspending Floating Solids in Stirred Tanks - Mixer Design , Scale up and Optimization" , 6th European Conference on Mixing, Pavia, Italy (1988)
23. Jessyca Susanto, "Multiphase Solid-Liquid and Solid-Liquid-Gas Mixing", Masters Thesis, NJIT, (1989)